Tunisia-Italy Power Interconnector Project

Environmental and Social Impact Assessment (ESIA)

Section 5 - Environmental baseline – Marine domain

Draft for Consultations

JV HPC – IDEACONSULT – PROGER – ELARD - PLEXUS

03	2023-02-02	Draft emission for consultations	HPC (L.Rufini) ELARD (M.Nader)	HPC (R.Andrighetto)	HPC (A.Cappellini)
02	2023-01-23	Revision after WB's comments			
01	2022-11-30	Revision after Elmed's comments			
00	2022-11-08	First emission			
Rev.	Date	Description	Prepared by	Checked by	Approved by

ELMED

Revision Approved	**Approval Date**	**Approved by**

TABLE OF CONTENTS

LIST OF DRAWINGS

1. INTRODUCTION

This section presents the baseline information on the existing physical and biological environment which may potentially be affected by the marine components of the Project.

Environmental data have been collected by means of desktop review of available official data and by primary data from site surveys commissioned by the Client to third parties (in particular to Rina-Comete Joint Venture). Details on data source are provided hereinafter in the characterization, as appropriate.

The present environmental baseline characterization for the marine domain analyzed the following environmental components:

- Meteorology and Physical Oceanography
- Seabed Geology and geomorphology;
- Underwater noise;
- Marine Biodiversity.

1.1 Project area of influence

Existing environmental conditions for the environmental components taken into account in the assessment have been characterized over the Project Area of Influence (referred to as AoI hereinafter), intended as the area potentially affected by the Project (relatively to its marine section).

Table 1.1: Project area of influence definition and baseline characterization

Environmental component	Project Area of Interest (AoI) intended as the area potentially affected by the project	Baseline characterization
Meteorology and Physical Oceanography	Regional area	Secondary data available at regional level
Geology and geomorphology	Coincident to Project footprint	Secondary data available at regional level + primary data from marine survey
Underwater noise	Up to 2 km from the Project elements	Secondary data
Biodiversity	Up to 2 km from the Project elements	Secondary data available at regional level + primary data from marine survey

1.2 Marine survey

A reconnaissance survey focused on defining the marine cable route was carried out between October and December 2021 by the Joint Venture formed by the companies RINA Consulting S.p.A and COMETE Engineering. The scope of work for the survey and assignment to the Joint Venture were defined by Elmed. Following a preliminary feasibility study conducted by ELMED, n° 3 Routes Options were identified for the connection and used as the reference routes to be analyzed through a Desk Top Study. Following the reconnaissance survey results, two survey routes were identified for the ROV detailed survey phase. The two routes resulted to be coincident up to KP 184.963, where they split depending on the Tunisian shore approach.

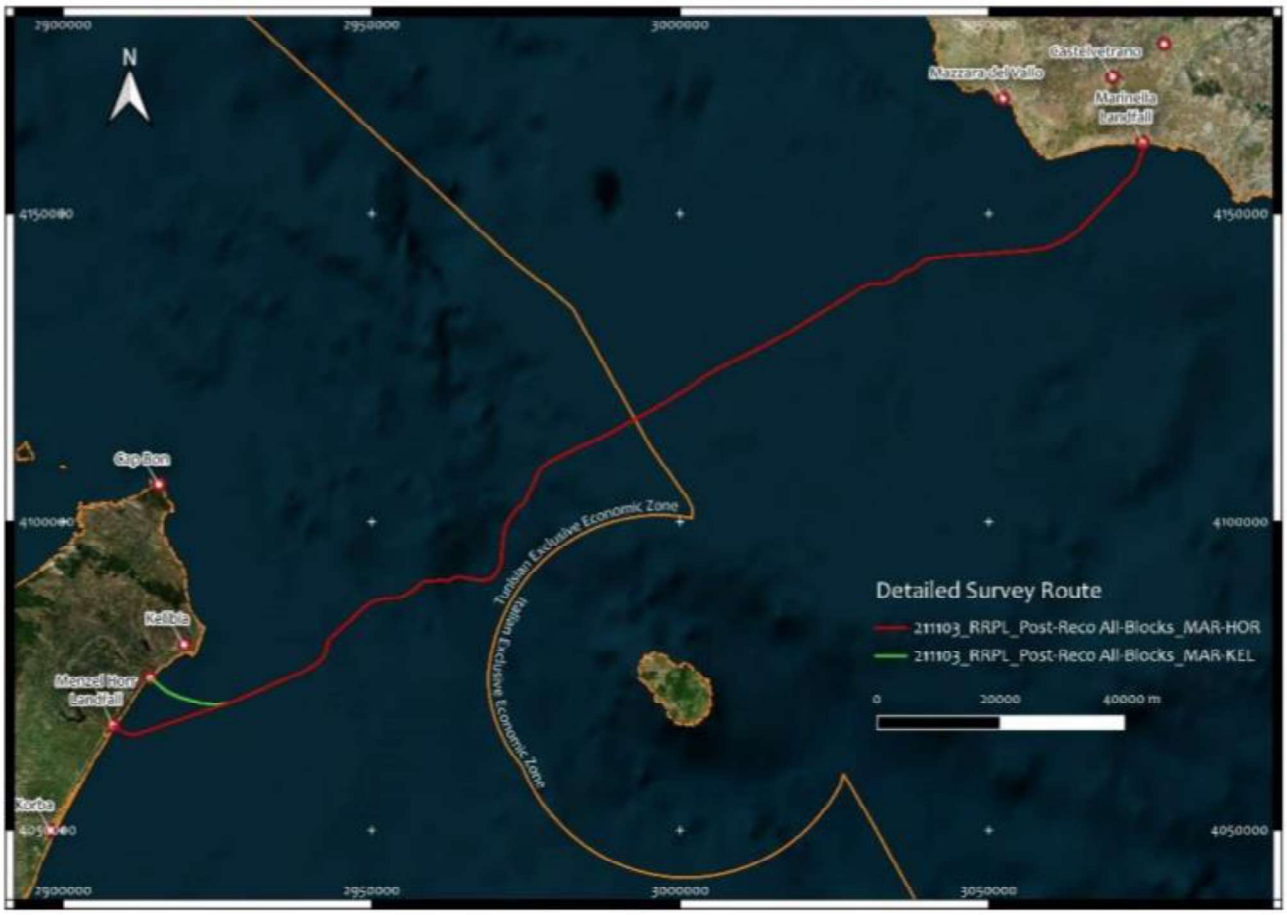

Figure 1.1: detailed survey routes

The survey comprised two separate activities:

- nearshore survey: this is related to the area from the shoreline to 40 m water depth;
- offshore survey: this is related to the offshore area with water depth greater than 40 m.

1.2.1 Offshore survey

The Offshore Survey was divided in two phases:

- Reconnaissance survey: bathymetric and morphological survey by means of MBES, installed on the offshore vessel along 3 km wide corridor from 40 m water depth at Italian side to 40 m water depth at Tunisian side. This activity was aimed to acquire bathymetry and morphology information of the study's corridor. During this phase there was a continuous and online assessment of the data to define the best RPL and then the relative corridor for the second phase.
- Detailed survey: bathymetric, morphological, and geophysical survey by MBES, SSS, SBP installed on ROV, along 500m wide corridor centered on the route selected after the reconnaissance survey. During this survey, a target visual analysis was also carried out in order to identify UXO's and archaeological targets.

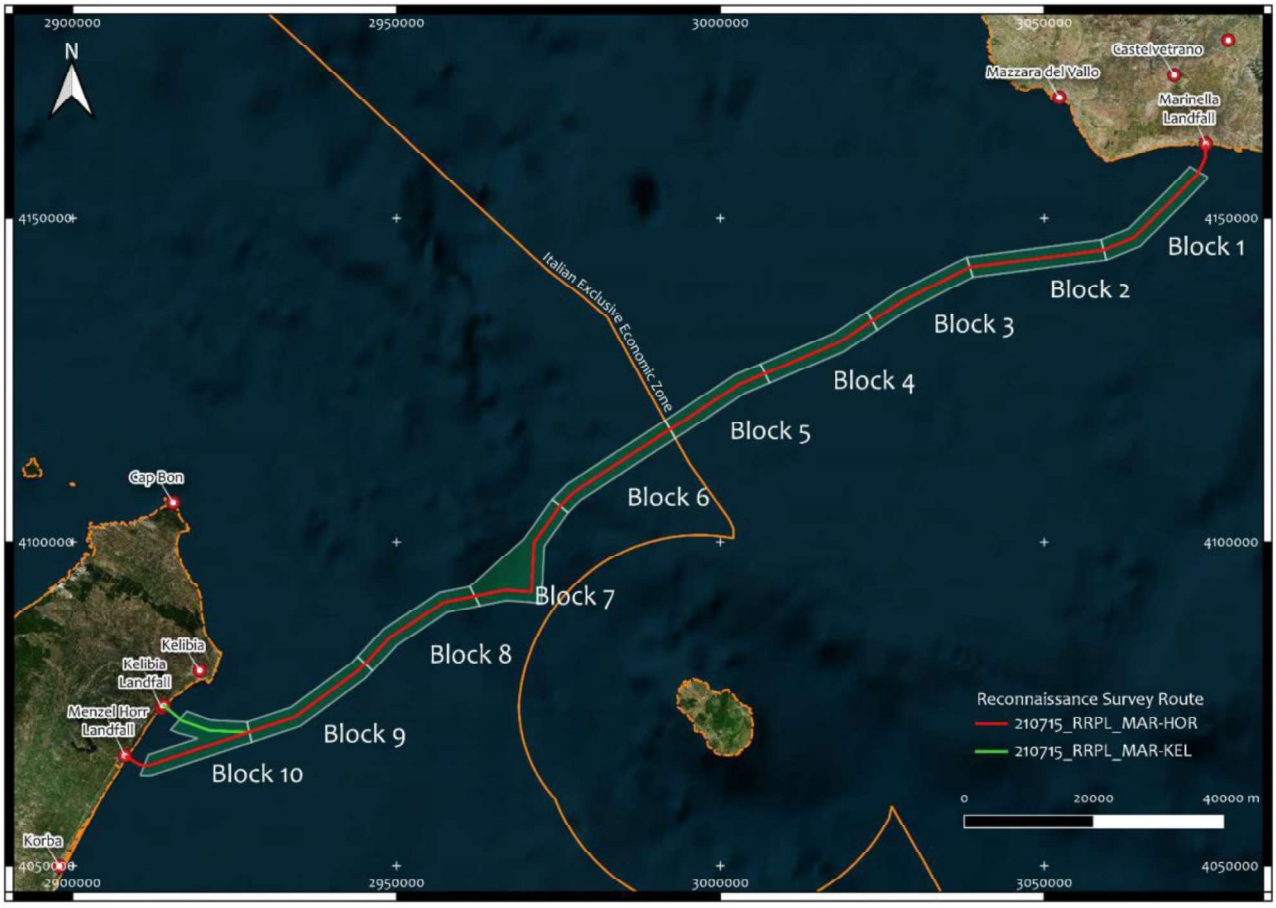

Figure 1.2: Reconnaissance survey plan

The offshore survey (geophysical and ROV survey) was executed by the OSV Artabro.

Figure 1.3: OSV Artabro

1.2.1.1 Geophysical survey methodology

1.2.1.1.1 Multi Beam Echo Sounder

The reconnaissance bathymetric survey was conducted with the pole mounted MBES Reson Seabat 7160 @44kHz to produce a digital terrain model (DTM) with a 5X5m cell size and 10m up to 400 m WD and 10x10m cell size up to 800m WD. On the other hand, the detailed survey was performed with a ROV mounted dual head MBES system, the array was
composed by two WBMS Norbit to produce a preliminary digital terrain model (DTM) with a 0.5x0.5 cell size. The DTM for
final report is produced with a 0.25x0.25 cell size.

1.2.1.1.2 Side scan sonar

The Side Scan Sonar (SSS) EdgeTech 2050 sensors mounted on ROV (Triple Frequency 230/540/850 kHz) was used to
determine the seabed sediment texture and morphological features (outcropping rock, ripples, scars, etc), sonar contacts
and possible risks or obstructions. Survey lines were run, parallel between them and in opposite direction with the ROV,
the range was set at 150m, assuring an overlap of 100% between the lines.

1.2.1.1.3 Sub Bottom Profiler

The Sub Bottom Profiler (SBP) EdgeTech 2050 sensors mounted on ROV (Frequency Band 2-16 kHz) was used for the
acquisition of seismic data. The system ensures a penetration deeper than 10 m in sandy and clayey sediments.

1.2.1.1.4 ROV Visual Inspection

This phase consists of a visual inspection on the targets selected by the board technicians with the ROV equipped with HD Camera, green laser system, avoiding object sonar and an underwater positioning system. In the following figure the ROV deployment operation before to start the visual inspection phase.

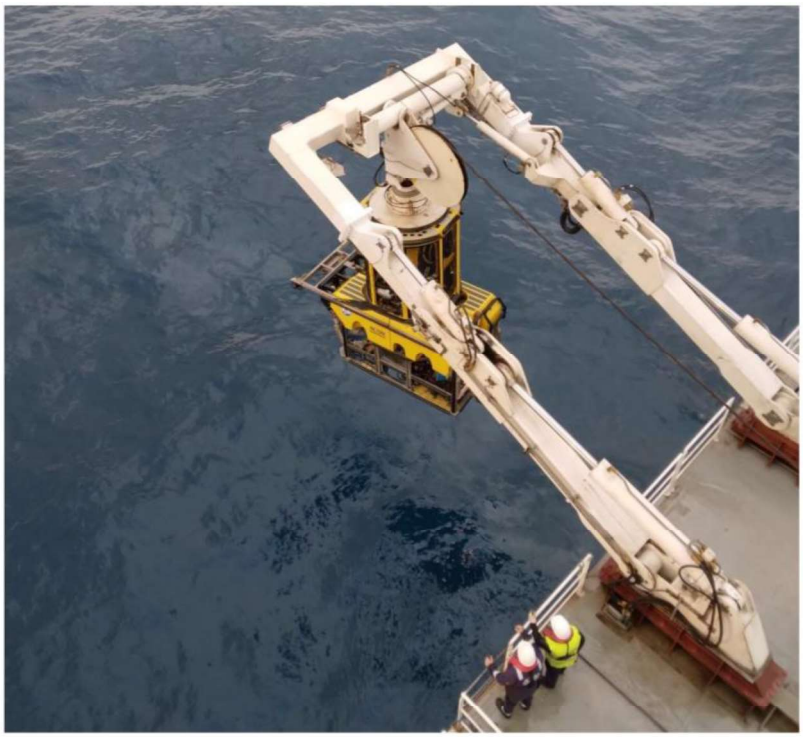

Figure 1.4: ROV Triton XLX 35

1.2.1.1.5 Processing parameters

The following table details processing parameters during the survey.

Table 1.2: Equipment parameters during the survey

Equipment Parameters	Value
MBES	
Grid cell size	**Reconnaissance Survey** • 5m up to 400m WD, • 10m from 400m up to 800m WD **Detailed Survey** • 0.25m whole corridor
Contour parameters	Minor 1 m, Major 5m (up to 200m WD) Minor 5m, Major 50m (up to 800m WD)
Grid nodes sign convention	Positive below datum
Accepted soundings sign convention	Positive below datum
SBP Parameters	
Digitize reflectors	Yes
Interpretation of horizons	Yes
Sediment depth of interest	Upper 5 m and rock basement
SSS Parameters	
Mosaic resolution	0.2m
Size of contacts to detect	≥0.2 m on minimum one dimension
Classification of seabed surface sediments	Yes
Classification of contacts	Boulders <0.5 m Boulders 0.5 – 2 m Boulders >2 m
	Wire Fishing Net Soft Rope Anchor Metallic Cable Pipeline Non-Metallic Wreck Debris Potential Archaeological Interest Other Unknown
Linear features	Digitize trawl marks or polygons of trawl marks
	Digitize cables and pipelines
Classification of ripples and sand waves	Ripples: Length <5m, Height 0.01-0.1m
	Large Ripples: Length 5-15 m, Height 0.1-1m
	Mega Ripples: Length 15-50 m, Height 1-3m
	Sand Waves: Length 50-200 m, Height 3-5m

1.2.2 Nearshore survey

This activity allows to characterize the seabed in front of the landing points and it was performed along the routes at both N° 2 Tunisian landing options.

Nearshore survey was performed with the following equipment installed on vessel:

✓ Multi Beam Echo Sounder (MBES).

✓ Side Scan Sonar (SSS).

✓ Sub Bottom Profiler (SBP).

Nearshore survey included the investigation of:

✓ the pole cable corridors

✓ the electrode cable corridors

✓ the electrode positioning areas

After the geophysical survey a detailed ROV visual inspection was also performed to identify:
✓ Posidonia oceanica or Cymodocea nodosa lower limit (along the whole corridor).
✓ Posidonia oceanica or Cymodocea nodosa upper limit (along the whole corridor).
✓ Sonar target deemed of interest (in particular UXOs and archaeological)

The near shore survey vessel mobilized for the geophysical and ROV surveys from 3 m to 40 m water depth is the LINO VICCICA.

Figure 1.5: M/B LINO VICCICA - Nearshore Vessel

1.2.2.1 Investigated areas

Two alternative landing options were investigated: Kelibia and Menzel-Horr.

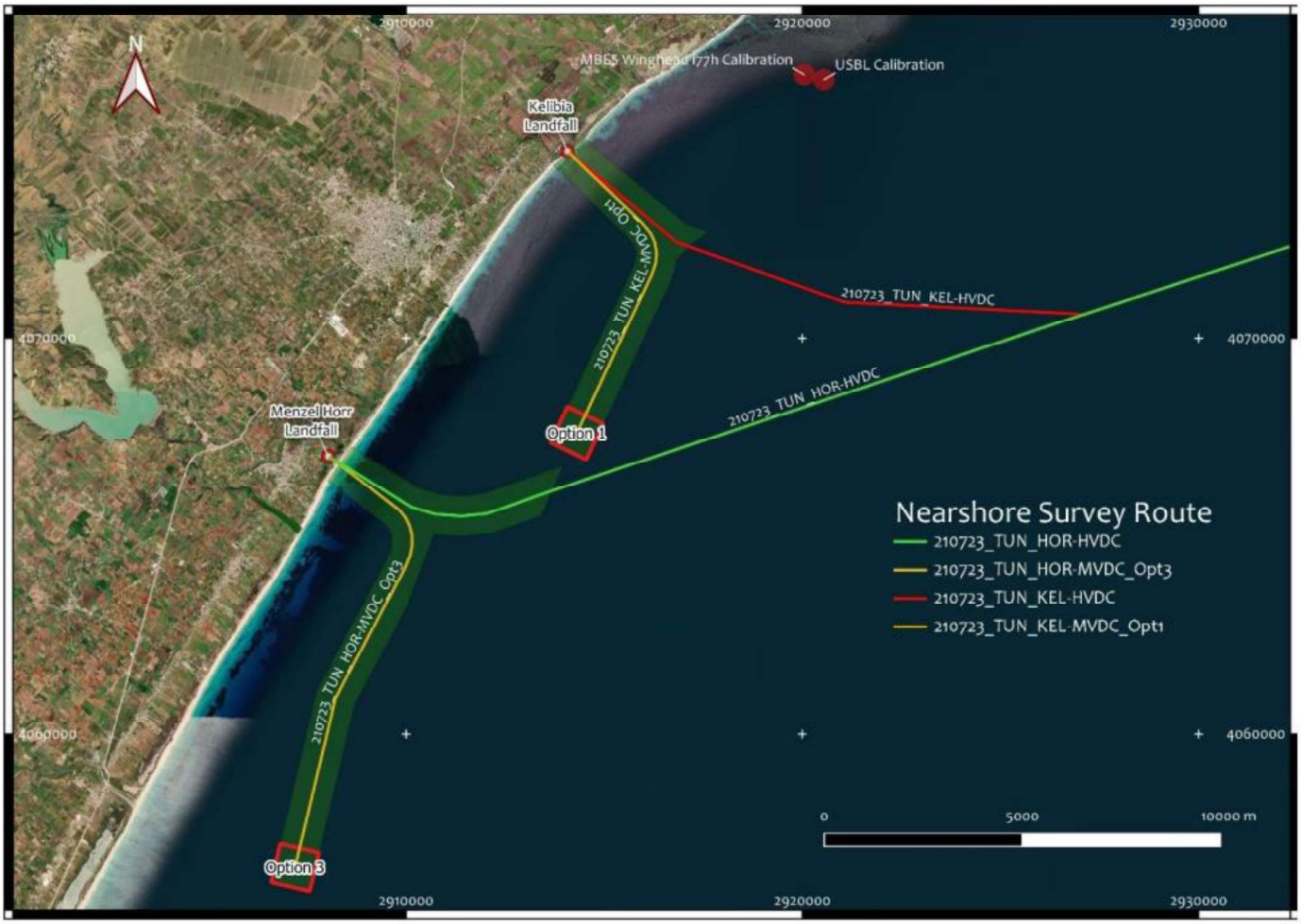

Figure 1.6: Alternative landing options investigated by the survey

1.2.2.1.1 Kelibia landing point

Kelibia nearshore work area consists of a pole cable corridor SE-NW oriented, 1000 m wide and approximately 3800 m long.
Kelibia electrode cable corridor investigated extends from Kelibia Landfall for approximately 8500m and is 1000 m wide.

Figure 1.7: Kelibia nearshore survey area

Figure 1.8: Kelibia electrode survey area

1.2.2.1.2 Menzel Horr landing point

Menzel Horr nearshore work area consists of a pole cable corridor E-W oriented, 1000 m wide and approximately 6000 m long.
The corresponding electrode cable corridor investigated extends from the Landfall for approximately 12000m and is 1000 m wide.

Figure 1.9:Menzel-Horr nearshore survey area

Figure 1.10: Menzel-Horr electrode survey area

1.2.2.2 Geophysical survey methodology

1.2.2.2.1 Multi Beam Echo Sounder

A high resolution MBES system, NORBIT Winghead i77h, was pole-mounted on the M/B LINO VICCICA to produce a
digital terrain model (DTM), with a 0.25m (up to 40m WD).

1.2.2.2.2 Side scan sonar

The Side Scan Sonar (SSS) Edgetech 4200 (Dual Frequency 230-560kHz) was used to determine the seabed sediment
texture and morphological features (outcropping rock, ripples, scars, etc), sonar contacts and possible risks or obstructions.
Survey lines were run from the M/B LINO VICCICA, parallel between them and in opposite direction with the towed SSS;
the range was set at 50m, assuring an overlap of 100% between the lines.

1.2.2.2.3 Sub Bottom Profiler

Sub-bottom Profiler Geo Pulse Compact (single frequency, 5-18 kHz) was used for the acquisition of seismic data. The
SBP system was pole-mounted on the M/B LINO VICCICA. The survey area seafloor is characterized by outcropping

rocks, presence of Posidonia and sandy sediment, the system ensures a penetration deeper than 3 m in sediment soil.

1.2.2.2.4 ROV Visual Inspection

This phase consisted of a visual inspection with ROV equipped with a HD Camera and an underwater positioning system.
The ROV visual inspection can be summarized with the following points:

✓ Investigation of Posidonia oceanica limit;

✓ Visual inspection along the infield selected route (IFSR)

✓ Visual inspection on the targets selected by the board technicians and archaeologist.

1.2.3 Archaeological and Historical finds

During the Offshore Survey one Archaeological and Historical target and two Historical targets have been identified. The post-survey route has been engineered keeping into account the survey data available in the surveyed corridor in order maximize as much as possible the distance from such targets (distance of the route from all of them is currently approx. 200m).
The Archaeological and Historical target Wreck "OSH_B7_ID0001" has been found in a fine sand sediment and classified as "Wreck", with height of 0.54 m, length 34.50 m and width 8.09 m, a burial percentage of 30%, and material classified as "Metal – undefined". For this target potential risk was classified as "Low".

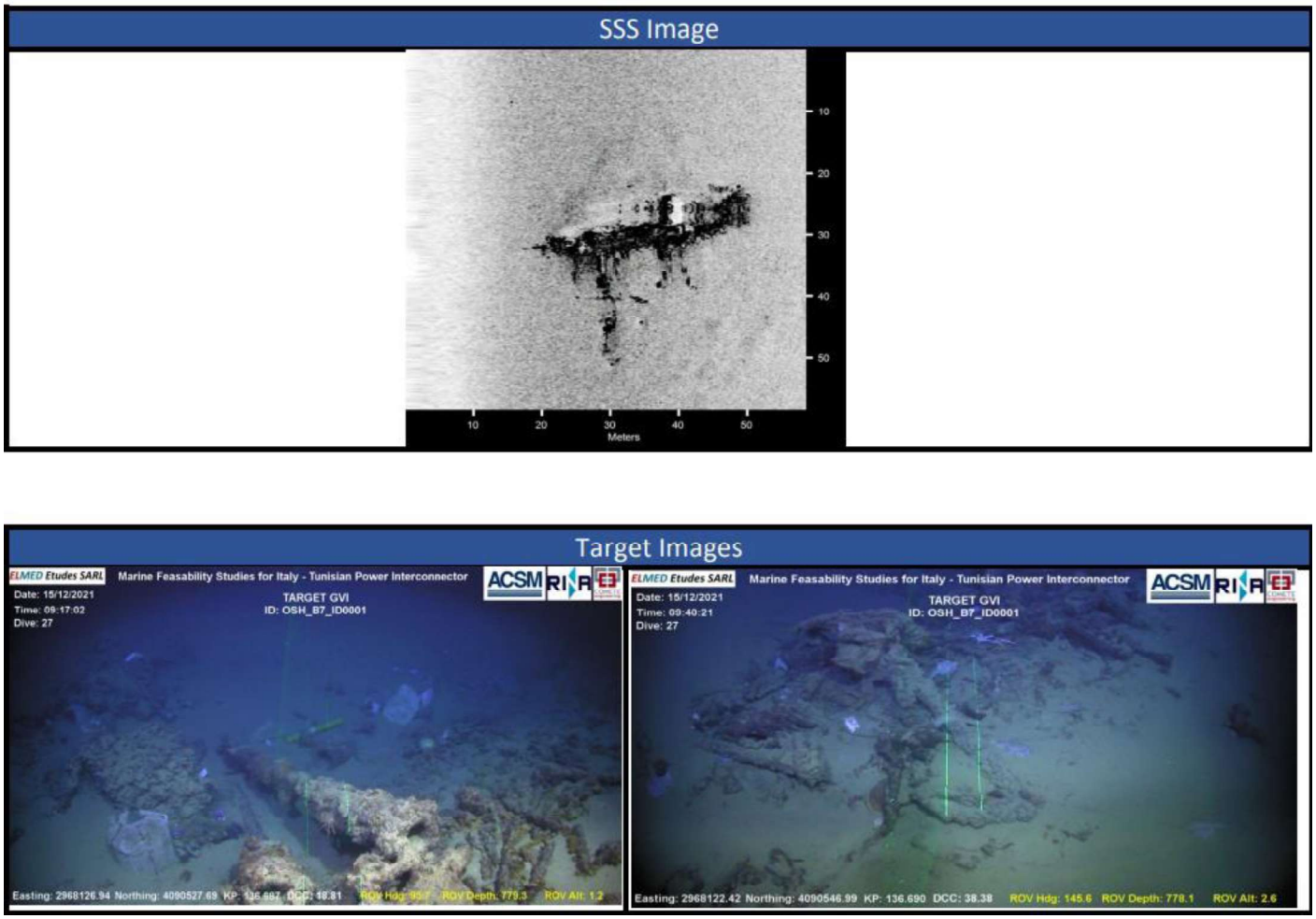

Figure 1.11: Sonar and ROV images of Archaeological and Historical target "Wreck OSH_B7_ID0001"

The Historical targets Metal Debris Area “OSH_B7_ID0002” and Engine “OSH_B7_ID0003” have been found in a fine sand sediment. The first one, “OSH_B7_ID0002”, was classified as “Metal Debris Area”, with length of 120.82 m and width of 91.07 m, with a low potential risk.
The second target, “OSH_B7_ID0003”, was classified as “Engine”, with a length of 2.75 m, height 0.70 m, and width 2.53 m, with a low potential risk.
Both Historical targets had a burial percentage of 0%.

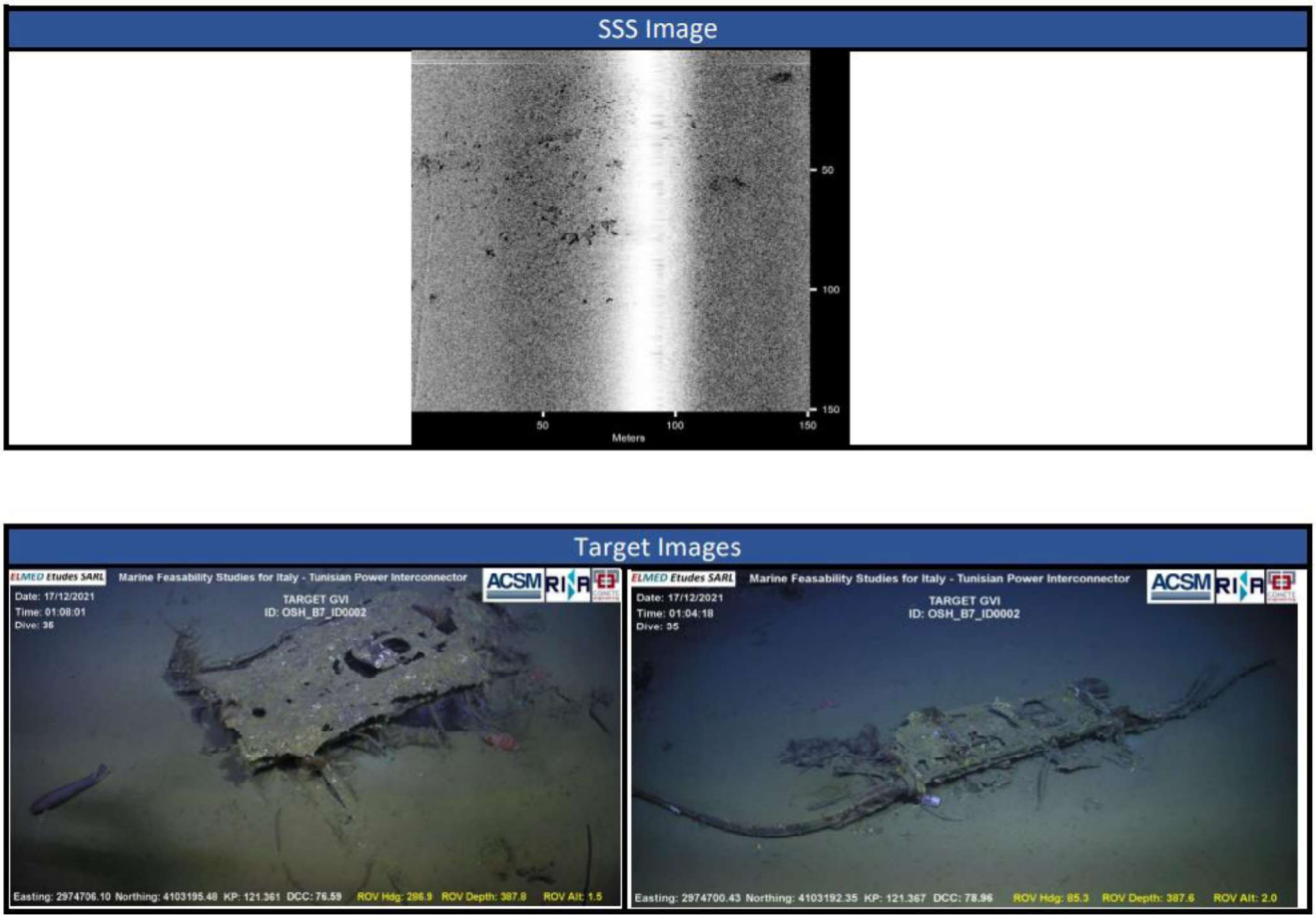

Figure 1.12: Sonar and ROV images of Historical target “Metal Debris Area OSH_B7_ID0002”

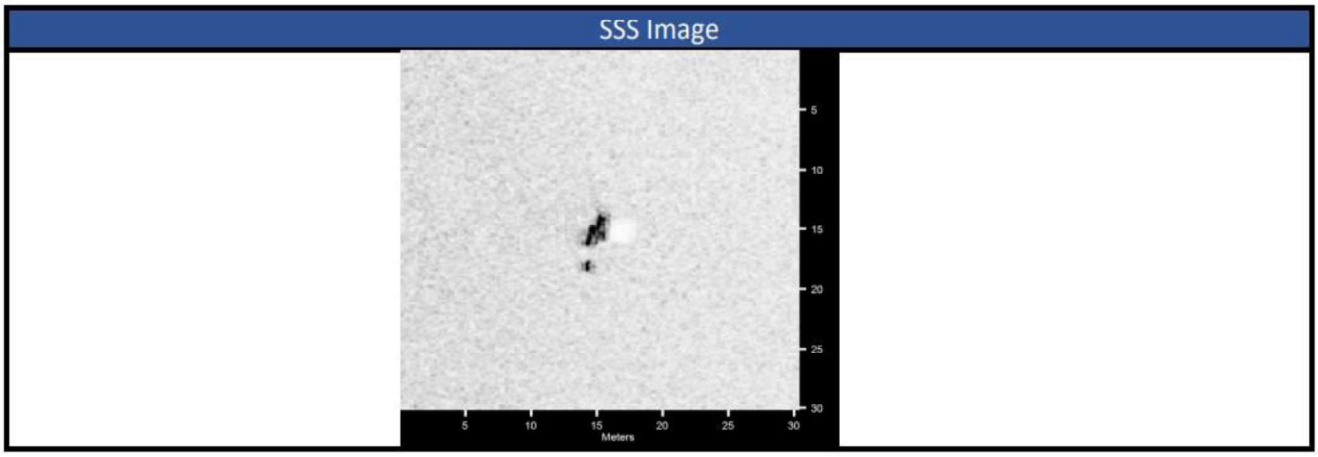

Figure 1.13: Sonar and ROV images of Historical target "Engine OSH_B7_ID0001"

2. METEREOLOGY AND PHYSICAL OCEANOGRAPHY

The content of this chapter derives from the study "RVFR18400A00012, revision 05, 29/09/2021, Marine Feasibility Studies for Tunisia-Italy Power Interconnector " by Rina-Comete.

2.1 Tunisian nearshore section

The general characteristics of the offshore wind regime extracted from hindcasted data are reported for the Tunisian nearshore section as annual and monthly distributions and extreme values.

The general characteristics of the wave climate analytically propagated to the nearshore area are reported for the nearshore area of interest as annual and monthly distributions and extreme values.

Note that in the frequency distribution table the thresholds must be considered upper thresholds (winds speed lower or equal to 2 m/s, 4 m/s, waves lower or equal to 0.5 m, 1.0 m, …).

2.1.1 Winds

The typical regime of winds and extreme values are here reported for the Tunisian nearshore section.

2.1.1.1 Typical Regime

The annual distribution of wind speed vs. incoming direction is shown in Table 2.1 and in Figure 2.1 (wind rose). The typical wind regime is characterized by about 44% events from NW (300-0°N) and about 28% from SE (120-180°N). The wind intensity is characterized by about 91% of events with speeds less than 10 m/s. The maximum speed is less than 22 m/s. Monthly wind roses show that the main incoming wind directions remains the NW and SW sectors, with mild conditions during summer.

Table 2.1: Annual Frequency (%) Distribution of Wind Speed vs Incoming Direction – Tunisian Nearshore Section

Dir (°N)	Wind(m/s) 1hour - Annual Tunisian Offshore												
	2	4	6	8	10	12	14	16	18	20	22	>22.00	TOT.
0	0.73	2.74	3.4	2.27	0.96	0.29	0.13	0.04	0.01				10.59
30	0.65	2.25	1.97	0.68	0.19	0.09	0.01	0.01					5.86
60	0.74	1.71	0.8	0.24	0.1	0.06	0.01						3.66
90	0.82	1.94	0.93	0.35	0.22	0.09	0.04	0.01	0.01				4.41
120	0.69	2.45	2.31	1.23	0.69	0.28	0.11	0.05	0.01				7.81
150	0.68	2.65	3.33	2.31	1.04	0.29	0.06	0.01					10.37
180	2	2.13	2.38	1.77	0.87	0.26	0.04	0.01					9.46
210	0.62	1.44	1.17	0.72	0.39	0.14	0.03	0.01					4.53
240	0.55	1.2	0.81	0.42	0.16	0.04	0.02	0.01					3.2
270	0.68	1.72	1.53	1.31	1.02	0.59	0.22	0.08	0.02				7.17
300	0.69	2.25	3.08	3.47	3.3	2.17	1.02	0.45	0.14	0.01			16.57
330	0.66	2.83	3.9	3.87	2.9	1.39	0.52	0.23	0.07	0.01			16.37
TOT.	9.53	25.29	25.59	18.63	11.85	5.68	2.22	0.91	0.26	0.03	0.01		100

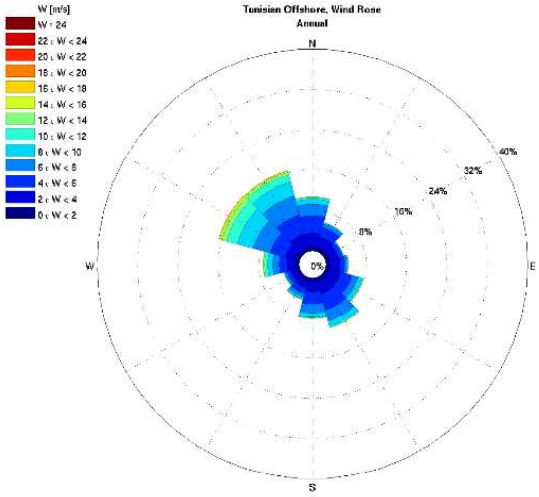

Figure 2.1: Annual Wind Rose – Tunisian Nearshore Section

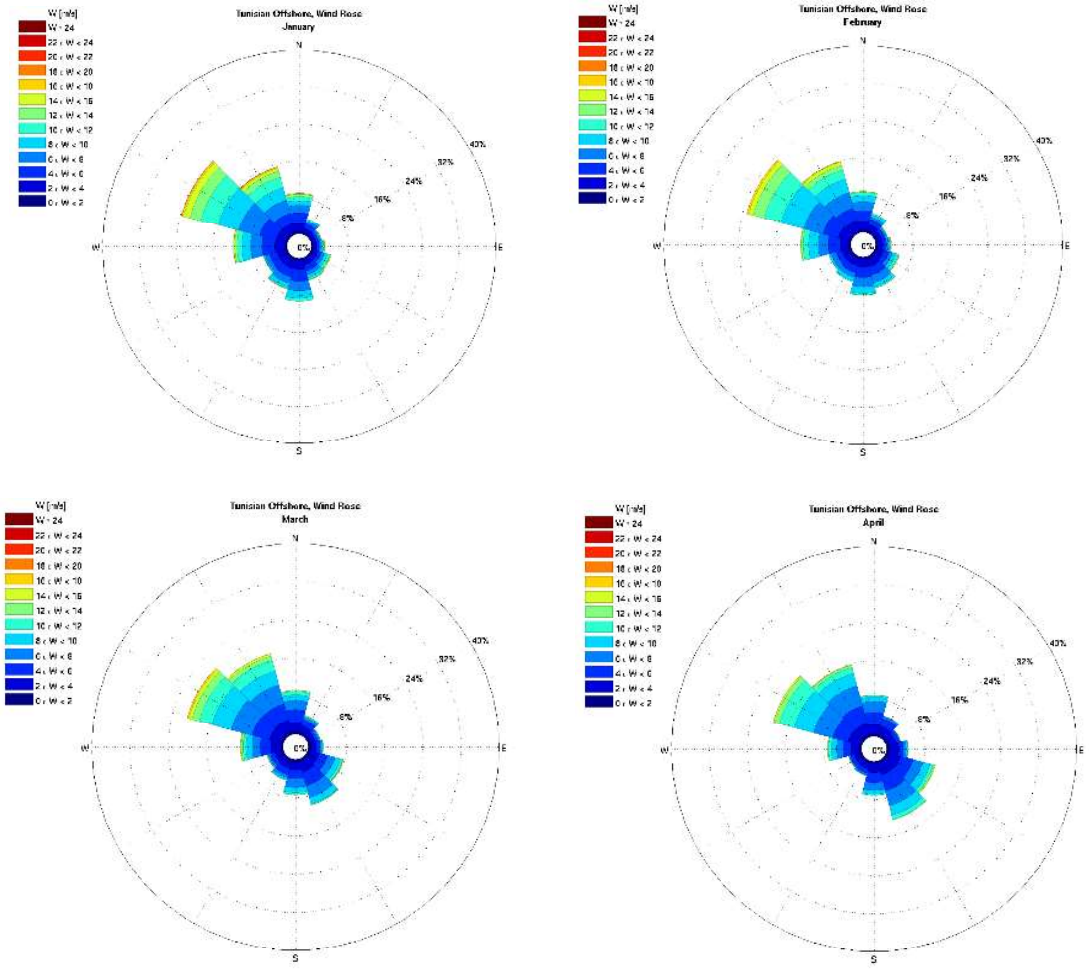

Figure 2.2: Wind Rose – January, February, March, April - Tunisian Nearshore Section

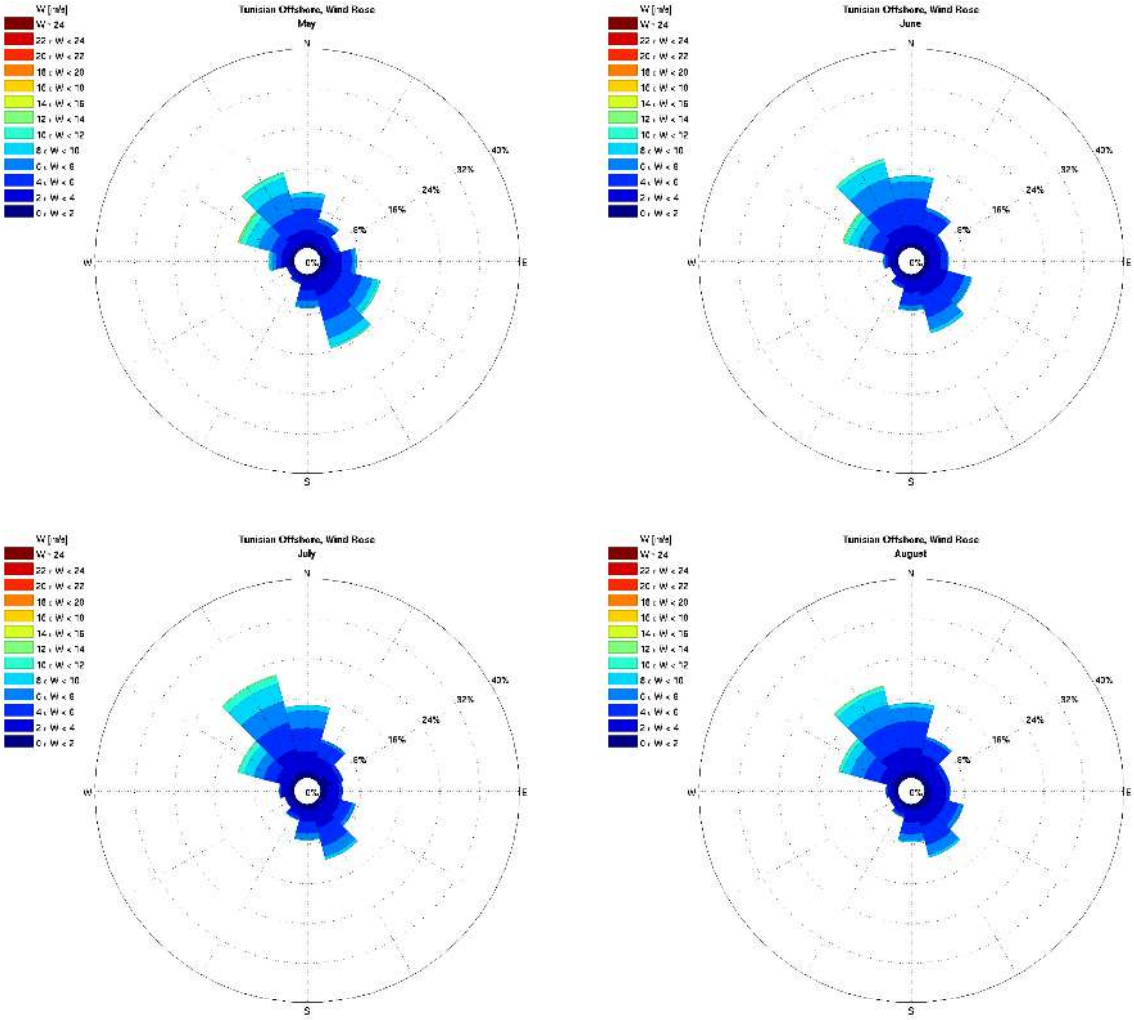

Figure 2.3: Wind Rose – May, June, July, August - Tunisian Nearshore Section

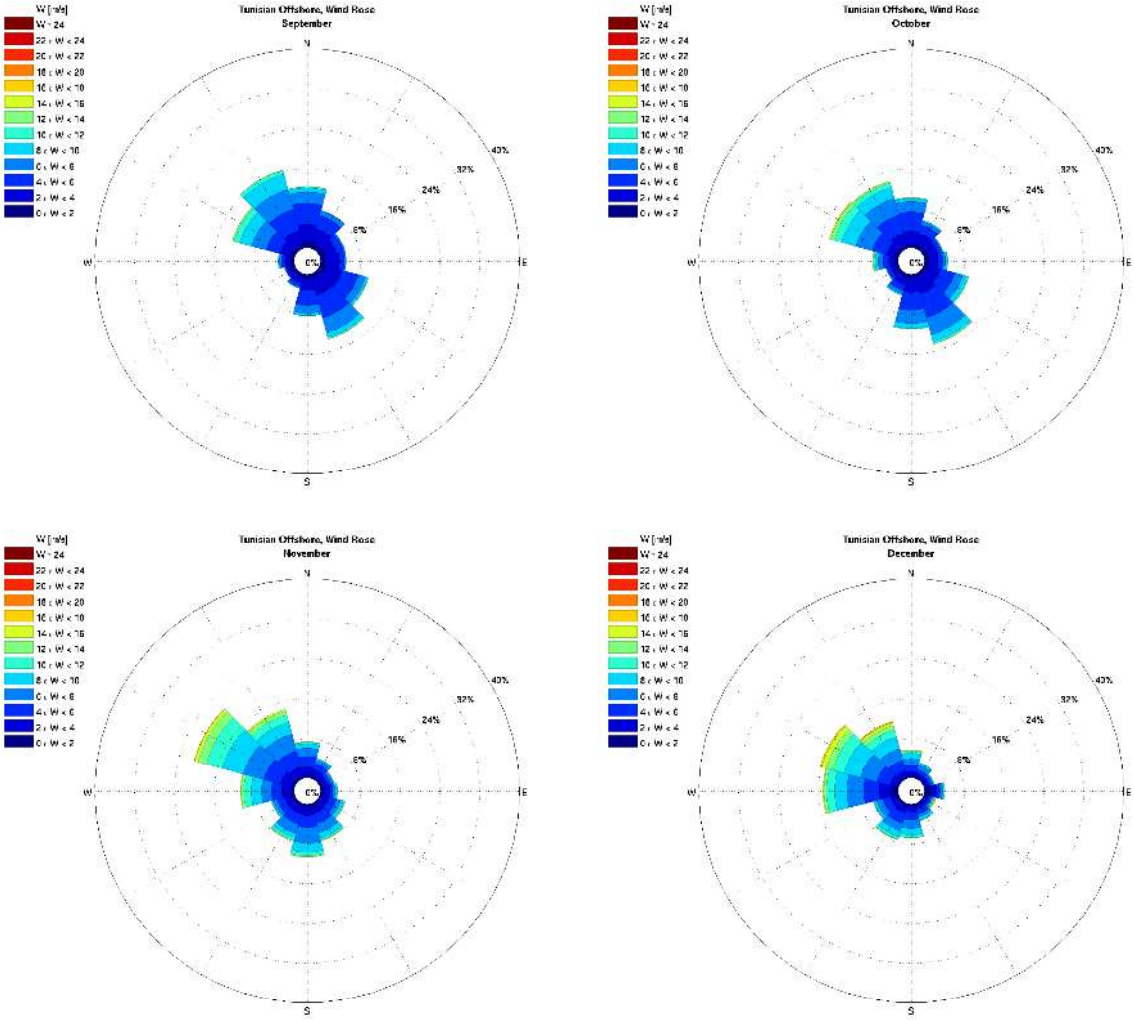

Figure 2.4: Wind Rose – September, October, November, December - Tunisian Nearshore Section

2.1.1.2 Extreme Values

Estimated omnidirectional, directional and monthly extreme wind speeds, referred to hourly data, are shown in Table 2.2 for different return periods (i.e. 1, 10, 50 and 100 years) , using the Weibull distribution function (Figure 2.5).

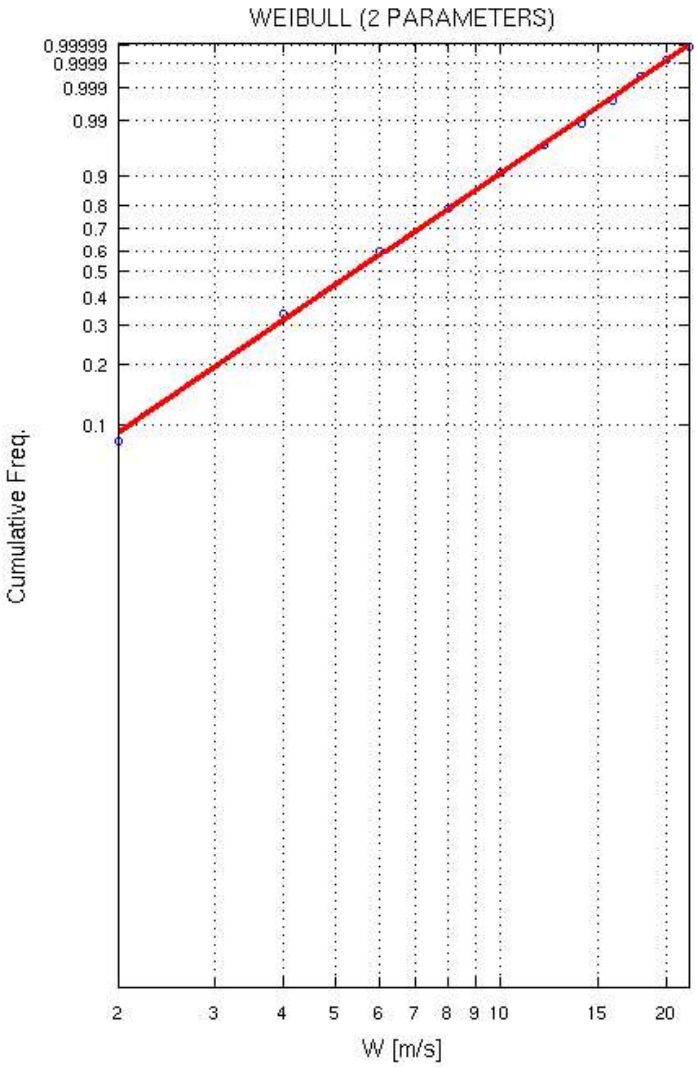

Figure 2.5: Omnidirectional Wind Fitting Distribution – Tunisian Nearshore Section

Table 2.2: Extreme Hourly Winds– Tunisian Nearshore Section

	Return Period (year)			
	1	10	50	100
Dir (°N)	**W_1h (m/s)**	**W_1h (m/s)**	**W_1h (m/s)**	**W_1h (m/s)**
OMNI	19.6	21.9	23.4	24.0
0	16.3	19.4	21.4	22.3
30	13.8	17.1	19.2	20.1
60	12.3	15.1	16.8	17.5
90	15.8	20.3	23.3	24.0
120	15.3	17.8	19.3	20.0
150	14.4	16.4	17.6	18.1
180	14.3	16.4	17.7	18.3
210	14.5	17.2	19.0	19.7
240	13.5	16.5	18.4	19.2
270	17.1	20.0	21.8	22.5
300	19.6	21.9	23.4	24.0
330	18.4	20.8	22.2	22.8
Month	**W_1h (m/s)**	**W_1h (m/s)**	**W_1h (m/s)**	**W_1h (m/s)**
Jan	19.6	21.9	23.4	24.0
Feb	18.0	20.7	22.4	23.1
Mar	17.5	20.1	21.8	22.5
Apr	16.4	18.9	20.4	21.0
May	14.7	17.1	18.5	19.1
Jun	14.1	16.5	18.0	18.7
Jul	13.3	15.5	16.8	17.3
Aug	12.5	14.4	15.5	16.0
Sept	13.7	15.8	17.1	17.6
Oct	15.8	18.3	19.9	20.5
Nov	17.6	20.3	22.0	22.7
Dec	18.3	21.2	22.9	23.7

2.1.2 Waves

The wave climate from Tunisian Offshore Point has been analytically propagated towards the Tunisian Kelibia landfall, taking into account the exposition and coastal orientation of the site. The nearshore climate is referred to about 20 m of W.D.

2.1.2.1 Wave Climate

The annual distribution of the wave height vs. incoming direction is shown in Table 3.14 and in Figure 3.27 (wave rose). The wave climate is characterized by about 45% of calm events. Kelibia landfall is exposed to wave coming from 60°N to 210°N.

Most of the waves come from 90-150°N (about 49% of the total events) the sectors characterized by longest fetch. The wave climate is characterized by about 53% of events with height less than 2 m with maximum observed Hs less than 6 m, coming from Southeast.

Monthly wave roses show that the main incoming wave directions remains the same along the year, with mild conditions during summer (with maximum wave height less than 2.5 m).

Table 2.3: Annual Frequency (%) Distribution of Wave Height vs Incoming Direction – Tunisian Nearshore Section

Dir (°N)	Hs (m)- Annual Tunisian Nearshore														
	0.5	1	1.5	2	2.5	3	3.5	4	4.5	5	5.5	6	6.5	> 6.50	TOT.
0															
30															
60	0.77	0.32	0.07	0.02	0.01										1.19
90	3.18	2.76	0.76	0.21	0.07	0.03	0.01	0.00		0.00					7.04
120	4.32	8.08	3.89	1.67	0.79	0.29	0.13	0.06	0.02	0.01	0.00	0.00			19.26
150	6.81	10.84	3.78	0.93	0.26	0.06	0.01	0.01	0.00						22.70
180	1.61	1.45	0.66	0.21	0.04	0.01									3.99
210	0.29	0.20	0.04	0.00											0.52
240															
270															
300															
330															
TOT.	16.99	23.64	9.20	3.05	1.16	0.38	0.15	0.07	0.02	0.01	0.00	0.00			54.69

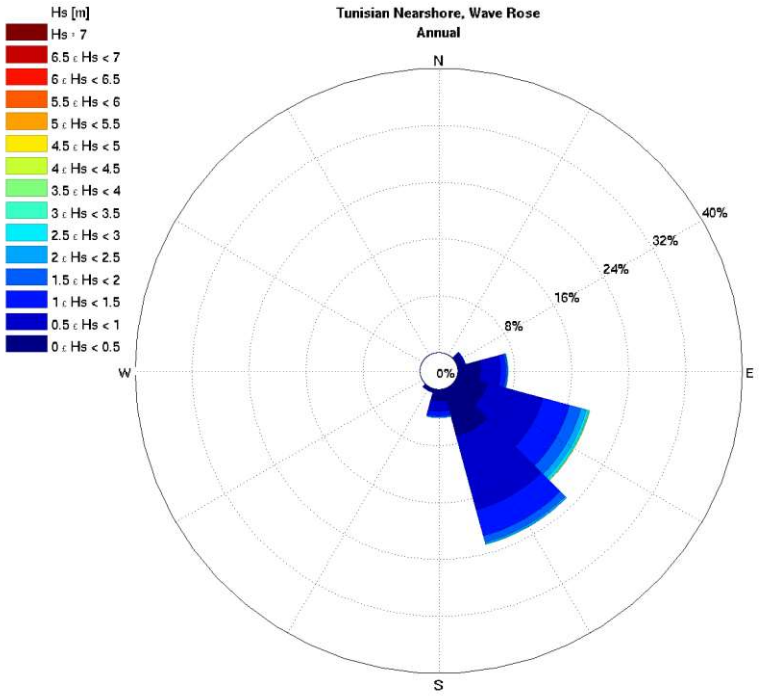

Figure 2.6: Annual Wave Rose – Tunisian Nearshore Section

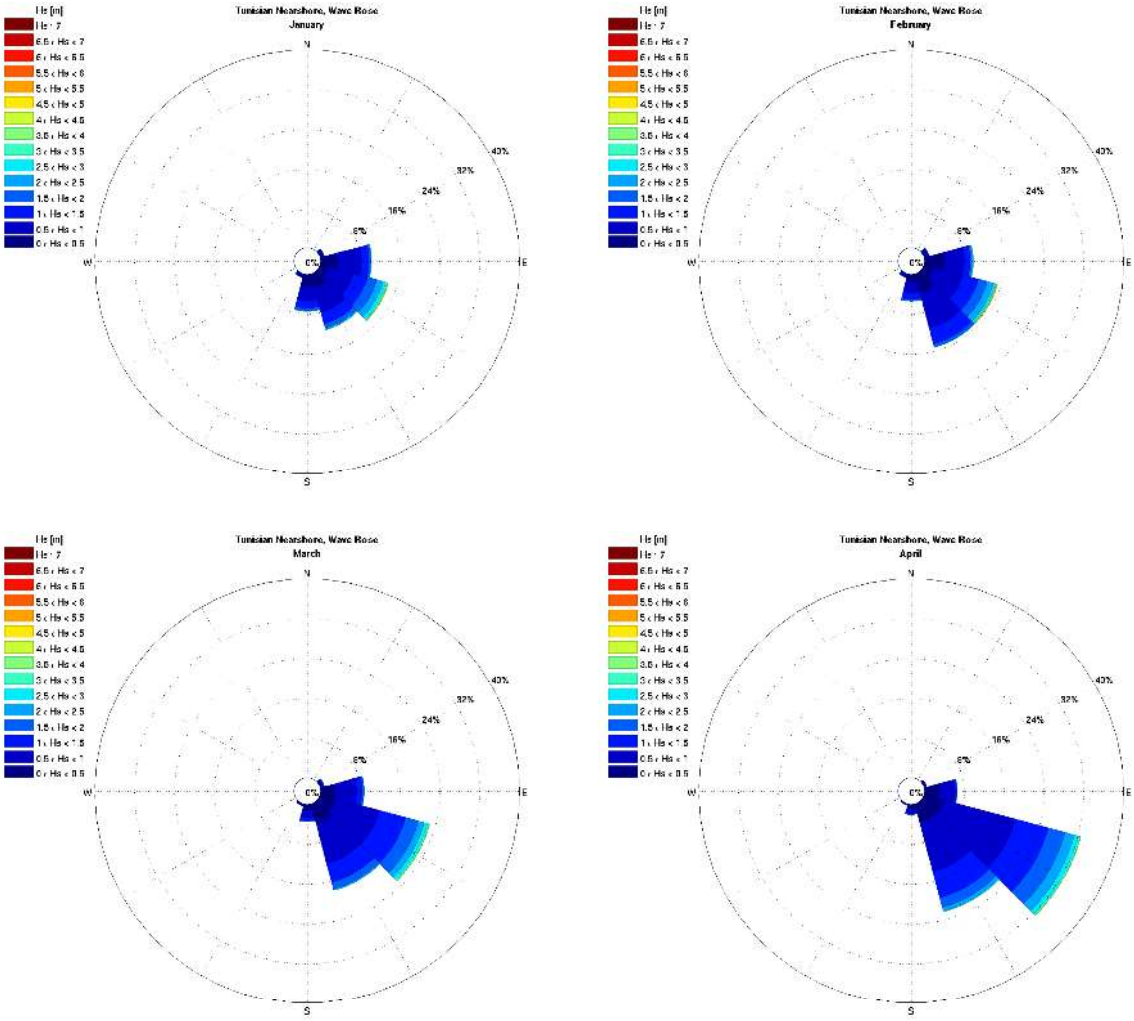

Figure 2.7: Wave Rose – January, February, March, April - Tunisian Nearshore Section

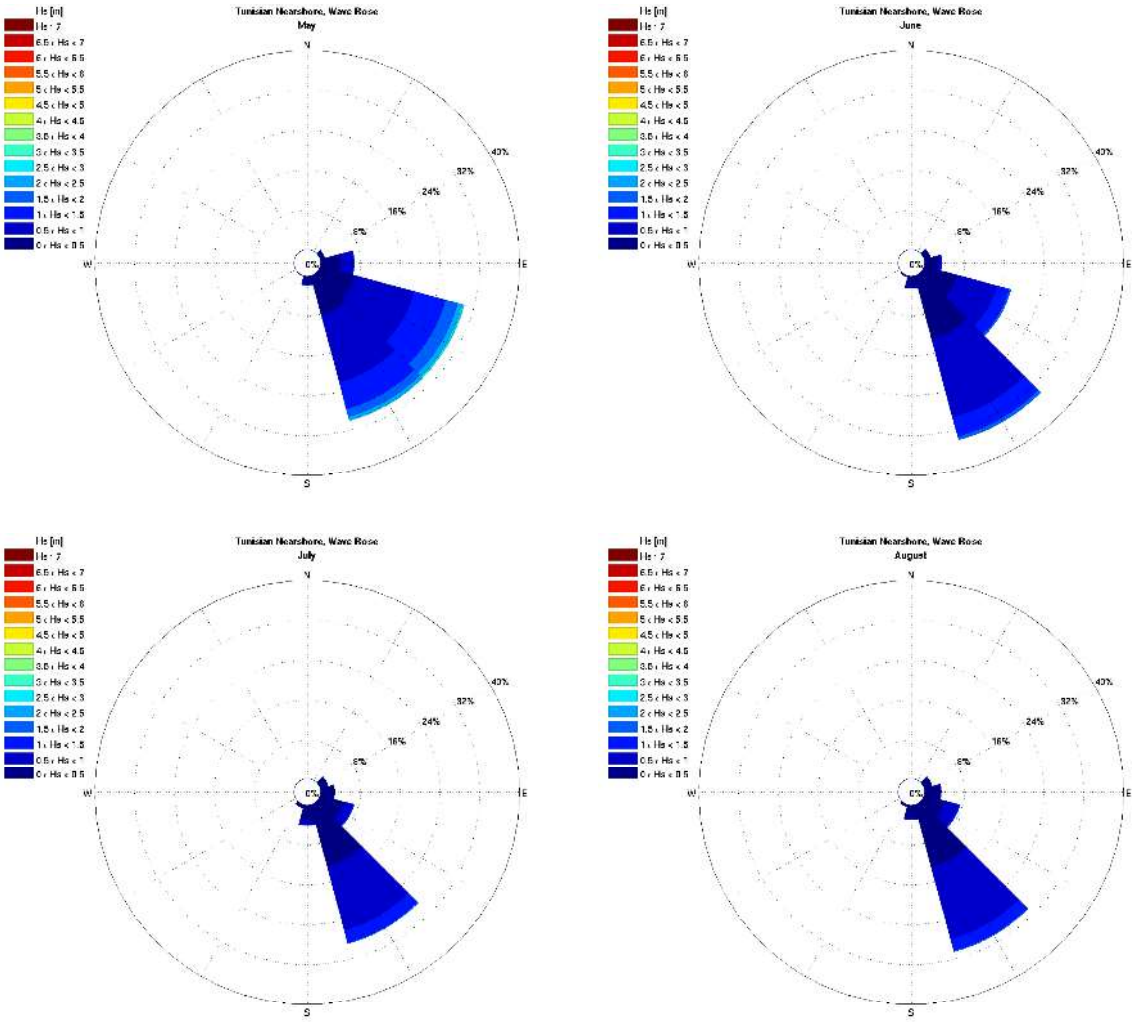

Figure 2.8: Wave Rose – September, October, November, December - Tunisian Nearshore Section

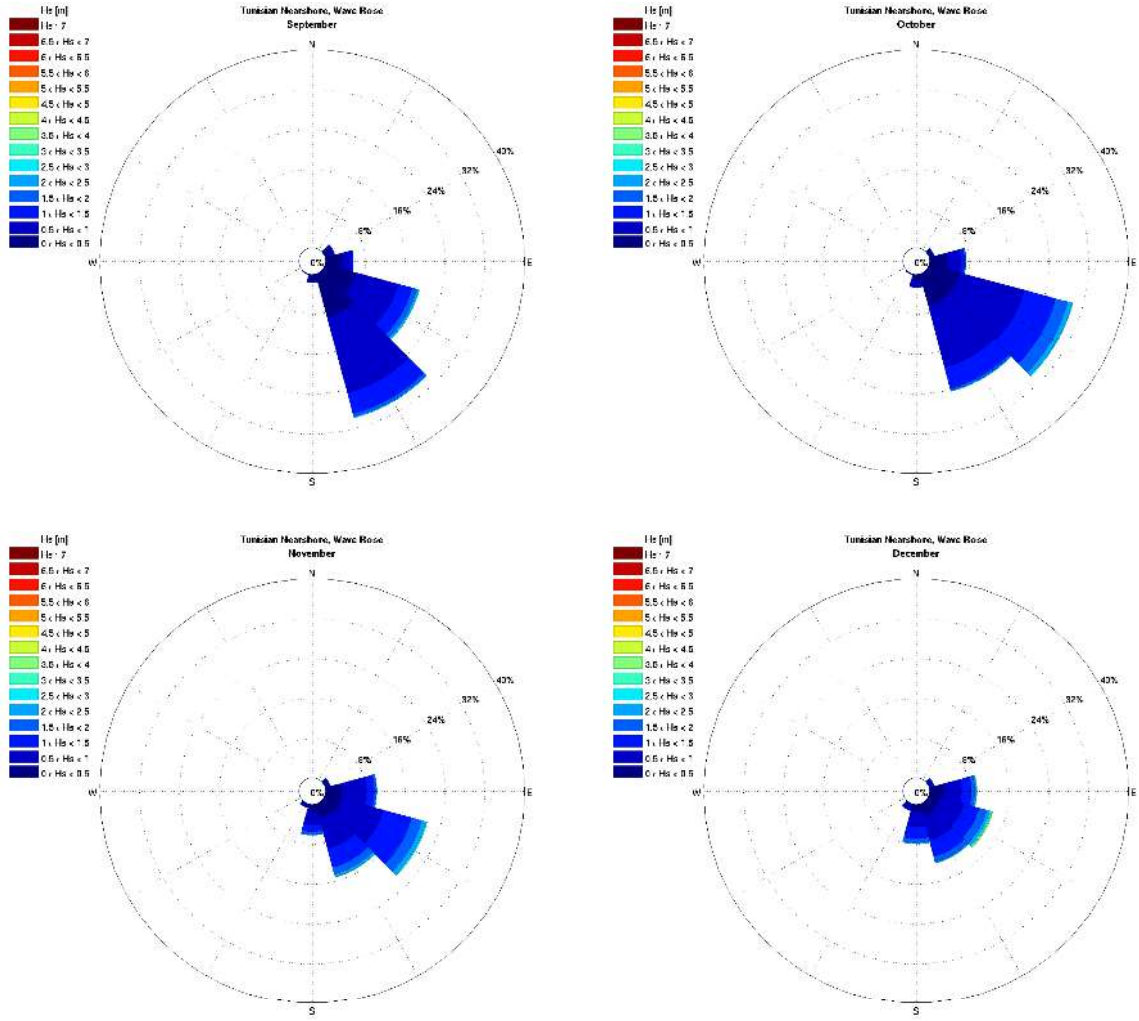

Figure 2.9: Wave Rose – May, June, July, August - Tunisian Nearshore Section

2.1.2.2 Hs-Tp Relationship

The annual distribution of total wave height vs. peak period is shown in Table 2.4: the table shows that about 98% of the storms are characterized by wave with peak period less than 9 s, with maximum wave peak period of 13 s.

To determine H-T relations, the H_s-T_p scatter is analyzed. Figure 3.31 shows the relations between H_s and T_p that can be used:

$$H_s=0.055*T_p^2$$

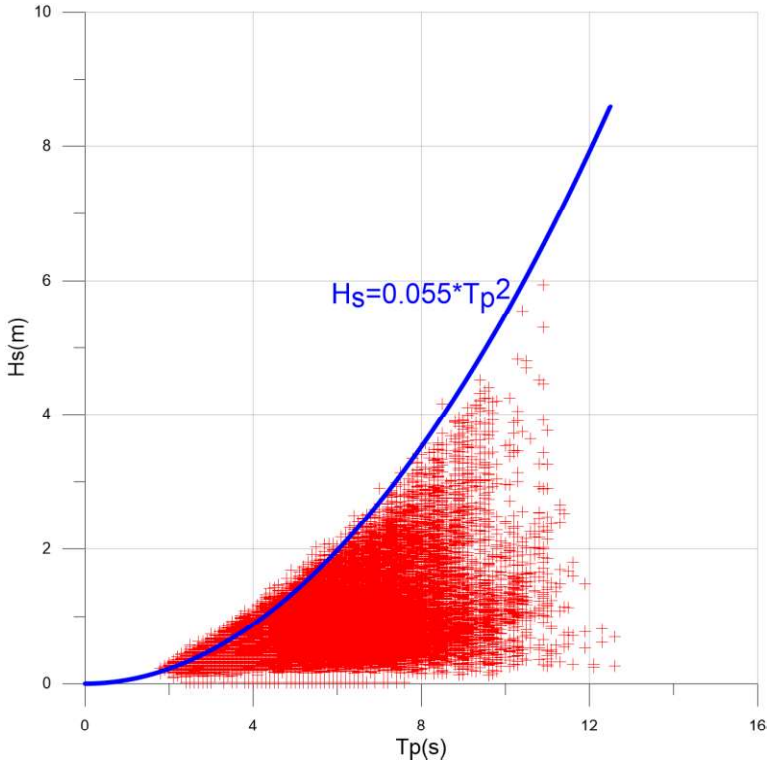

Figure 2.10: Omnidirectional Scatter Diagram of Wave Height VS Peak Period – Tunisian Nearshore Section

Table 2.4: Omnidirectional Frequency (%) Distribution of Wave Height vs Peak Period – Tunisian Nearshore Section

Tp(s)	Hs (m)- OMNI Tunisian Nearshore														
	0.5	1	1.5	2	2.5	3	3.5	4	4.5	5	5.5	6	6.5	> 6.50	TOT.
1															
2	0.07														0.07
3	4.44	0.31													4.75
4	4.00	4.33	0.02												8.35
5	3.31	6.16	1.59	0.01											11.07
6	2.53	5.37	2.93	0.67	0.01										11.49
7	1.53	3.83	2.36	1.09	0.26	0.01									9.09
8	0.72	2.18	1.36	0.78	0.50	0.15	0.02								5.72
9	0.24	1.07	0.55	0.36	0.28	0.16	0.08	0.03	0.00						2.77
10	0.10	0.32	0.24	0.08	0.07	0.05	0.04	0.03	0.02	0.00					0.95
11	0.03	0.05	0.14	0.06	0.03	0.01	0.01	0.01	0.00	0.01	0.00	0.00			0.35
12	0.01	0.01	0.01	0.00	0.00	0.00									0.04
13	0.00	0.00													0.01
14															
>14.00															
TOT.	16.98	23.64	9.20	3.05	1.16	0.38	0.15	0.07	0.02	0.01	0.00	0.00			54.67

2.1.2.3 Extreme Values

Estimated omnidirectional directional and monthly extreme wave heights, referred to 3-hour wave climate, are shown in Table 2.5 and Table 2.6 for different return periods (i.e. 1, 10,50 and 100 years), using the Weibull distribution function (Figure 2.11).

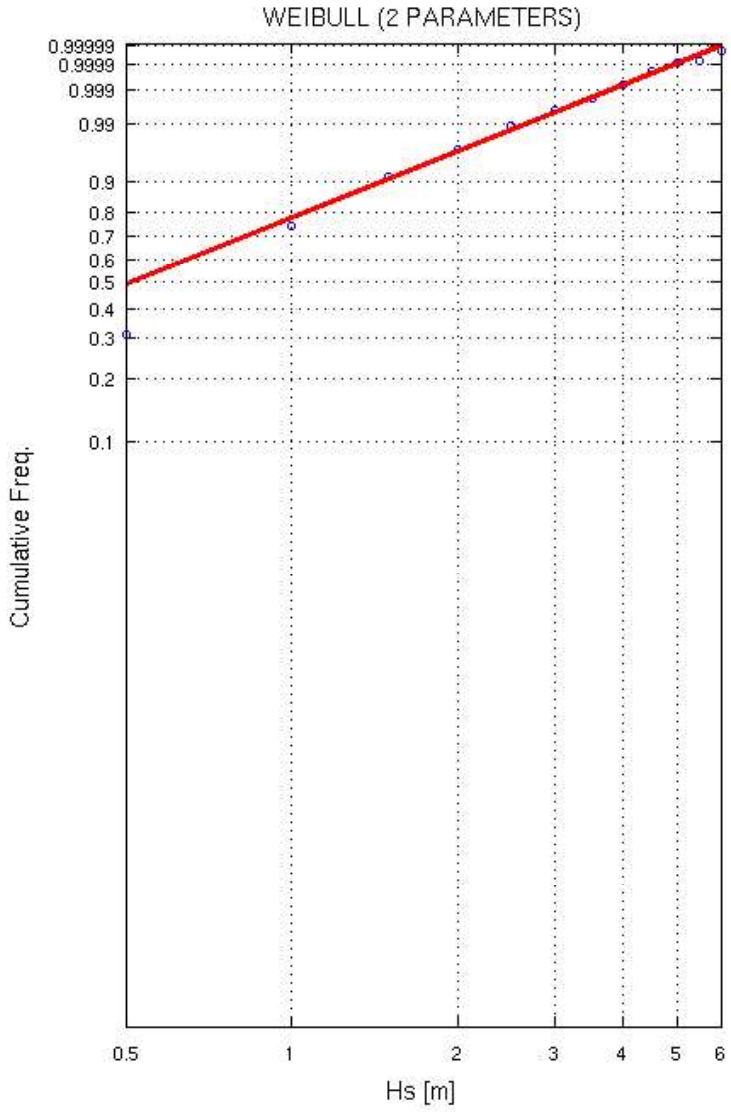

Figure 2.11: Omnidirectional Total Wave Fitting Distribution – Tunisian Nearshore Section

Table 2.5: Extreme Wave Parameters – Tunisian Nearshore Section - Return Period 1, 10 Years

	Return Period (year)				Return Period (year)			
	1				10			
Dir (°N)	Hs (m)	Tp (s)	Hmax(m)	T_Hmax (s)	Hs (m)	Tp (s)	Hmax(m)	T_Hmax (s)
OMNI	4.37	8.91	7.87	8.87	5.46	9.96	9.83	9.91
60	1.64	5.46	2.95	5.43	2.40	6.61	4.32	6.57
90	3.01	7.40	5.42	7.36	4.18	8.72	7.52	8.67
120	4.37	8.91	7.87	8.87	5.46	9.96	9.83	9.91
150	3.18	7.60	5.72	7.57	3.98	8.51	7.16	8.46
180	2.28	6.44	4.10	6.41	2.88	7.24	5.18	7.20
210	1.14	4.55	2.05	4.53	1.54	5.29	2.77	5.26
Month	**Hs (m)**	**Tp (s)**	**Hmax(m)**	**T_Hmax (s)**	**Hs (m)**	**Tp (s)**	**Hmax(m)**	**T_Hmax (s)**
Jan	3.51	7.99	6.32	7.95	4.54	9.09	8.17	9.04
Feb	4.37	8.91	7.87	8.87	5.46	9.96	9.83	9.91
Mar	3.23	7.66	5.81	7.62	4.04	8.57	7.27	8.53
Apr	3.28	7.72	5.90	7.68	4.04	8.57	7.27	8.53
May	2.89	7.25	5.20	7.21	3.62	8.11	6.52	8.07
Jun	1.86	5.82	3.35	5.79	2.27	6.42	4.09	6.39
Jul	1.53	5.27	2.75	5.25	1.90	5.88	3.42	5.85
Aug	1.53	5.27	2.75	5.25	1.89	5.86	3.40	5.83
Sept	2.43	6.65	4.37	6.61	3.07	7.47	5.53	7.43
Oct	2.60	6.88	4.68	6.84	3.29	7.73	5.92	7.70
Nov	2.90	7.26	5.22	7.22	4.16	8.70	7.49	8.65
Dec	3.35	7.80	6.03	7.77	4.38	8.92	7.88	8.88

Table 2.6: Extreme Wave Parameters – Tunisian Nearshore Section - Return Period 50, 100 Years

	Return Period (year)				Return Period (year)			
	50				100			
Dir (°N)	Hs (m)	Tp (s)	Hmax(m)	T_Hmax (s)	Hs (m)	Tp (s)	Hmax(m)	T_Hmax (s)
OMNI	6.20	10.62	11.16	10.56	6.52	10.89	11.74	10.83
60	2.91	7.27	5.24	7.24	3.13	7.54	5.63	7.51
90	5.01	9.54	9.02	9.50	5.36	9.87	9.65	9.82
120	6.20	10.62	11.16	10.56	6.52	10.89	11.74	10.83
150	4.51	9.06	8.12	9.01	4.74	9.28	8.53	9.24
180	3.25	7.69	5.85	7.65	3.41	7.87	6.14	7.83
210	1.78	5.69	3.20	5.66	1.88	5.85	3.38	5.82
Month	**Hs (m)**	**Tp (s)**	**Hmax(m)**	**T_Hmax (s)**	**Hs (m)**	**Tp (s)**	**Hmax(m)**	**T_Hmax (s)**
Jan	5.21	9.73	9.38	9.68	5.48	9.98	9.86	9.93
Feb	6.20	10.62	11.16	10.56	6.52	10.89	11.74	10.83
Mar	4.56	9.11	8.21	9.06	4.77	9.31	8.59	9.27
Apr	4.53	9.08	8.15	9.03	4.73	9.27	8.51	9.23
May	4.09	8.62	7.36	8.58	4.29	8.83	7.72	8.79
Jun	2.53	6.78	4.55	6.75	2.64	6.93	4.75	6.89
Jul	2.13	6.22	3.83	6.19	2.23	6.37	4.01	6.34
Aug	2.11	6.19	3.80	6.16	2.20	6.32	3.96	6.29
Sept	3.49	7.97	6.28	7.93	3.66	8.16	6.59	8.12
Oct	3.73	8.24	6.71	8.19	3.92	8.44	7.06	8.40
Nov	5.05	9.58	9.09	9.53	5.44	9.95	9.79	9.90
Dec	5.05	9.58	9.09	9.53	5.33	9.84	9.59	9.79

2.1.3 Currents

The typical regime of currents (from HYCOM hindcasted data), the vertical profile and superficial extreme values are here reported for the Tunisian nearshore section.

Please note that the current direction is intended as a propagation direction.

2.1.3.1 Typical Conditions

The annual distribution of current speed vs. propagating direction is shown in Table 2.7 and in Figure 2.12 (current rose).

Table 2.7 shows that offshore current mainly flows toward SE, 150-180°N sectors (about 57% of total events). Most events are less or equal to 0.70 m/s (about 98% of total events), while the most intense current velocities are of about 1.1 m/s associated to 180°N directional sector.

Table 2.7: Annual Frequency (%) Distribution of Surface Current vs Direction of Propagation – Tunisian Nearshore Section

Dir (°N)	V (m/s) - Annual Tunisian Nearshore - depth =sur m																
	0.1	0.2	0.3	0.4	0.5	0.6	0.7	0.8	0.9	1	1.1	1.2	1.3	1.4	1.5	>1.5	TOT.
0	0.82	1.27	0.86	0.27	0.08	0.02											3.32
30	1.20	2.45	2.36	1.64	0.49	0.05	0.02										8.19
60	1.67	3.19	2.62	0.83	0.17	0.06											8.55
90	1.48	2.96	1.31	0.19	0.02												5.94
120	1.81	3.71	1.71	0.44	0.02	0.02											7.70
150	2.06	4.75	4.94	3.41	2.23	0.74	0.31	0.13	0.14	0.03							18.74
180	1.92	6.07	8.35	8.80	5.78	4.35	2.22	0.74	0.35	0.24	0.05						38.86
210	1.26	1.90	1.16	0.50	0.24	0.06	0.03	0.03									5.19
240	0.60	0.33	0.11	0.03													1.07
270	0.31	0.13	0.05														0.49
300	0.41	0.27	0.03	0.03	0.02												0.75
330	0.60	0.39	0.16	0.06													1.21
TOT.	14.11	27.41	23.66	16.20	9.04	5.30	2.58	0.90	0.49	0.27	0.05						100.00

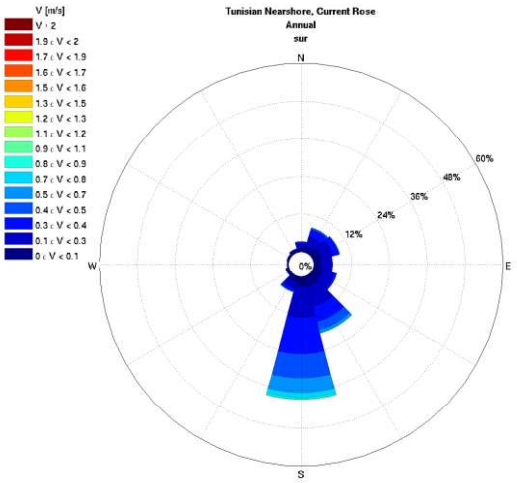

Figure 2.12: Surface Current Rose – Tunisian Nearshore Section

The vertical current profile of Figure 2.13 shows a sharp decrease of current intensity with the increase of depth, characterized by maximum current speed of about 0.9 m/s at 10 m of W.D., and about 0.4 m/s on the sea bottom. The current rose along the vertical profile (Figure 2.14) shows that the current is mainly directed towards South until 80m of W.D, while the last two layers investigated (90 and 100 m of W.D.) show the presence of a countercurrent towards North.

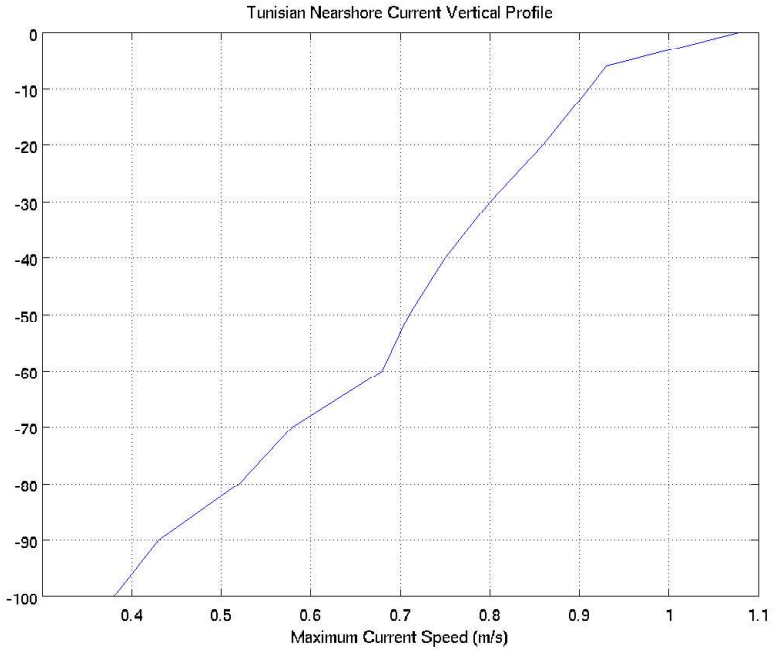

Figure 2.13: Vertical Current Profile – Tunisian Nearshore Section

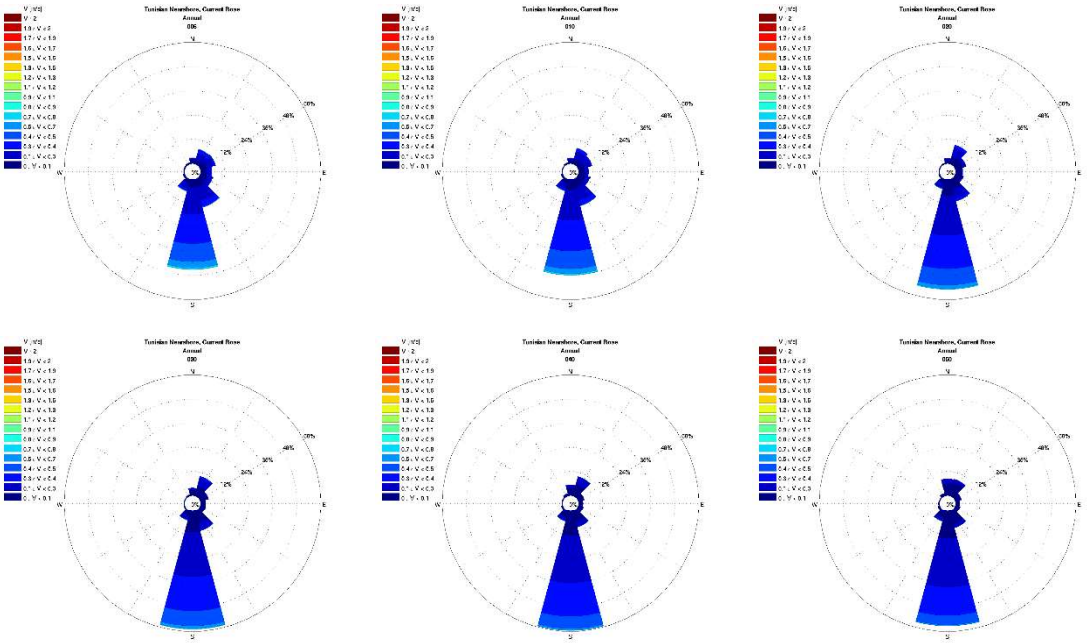

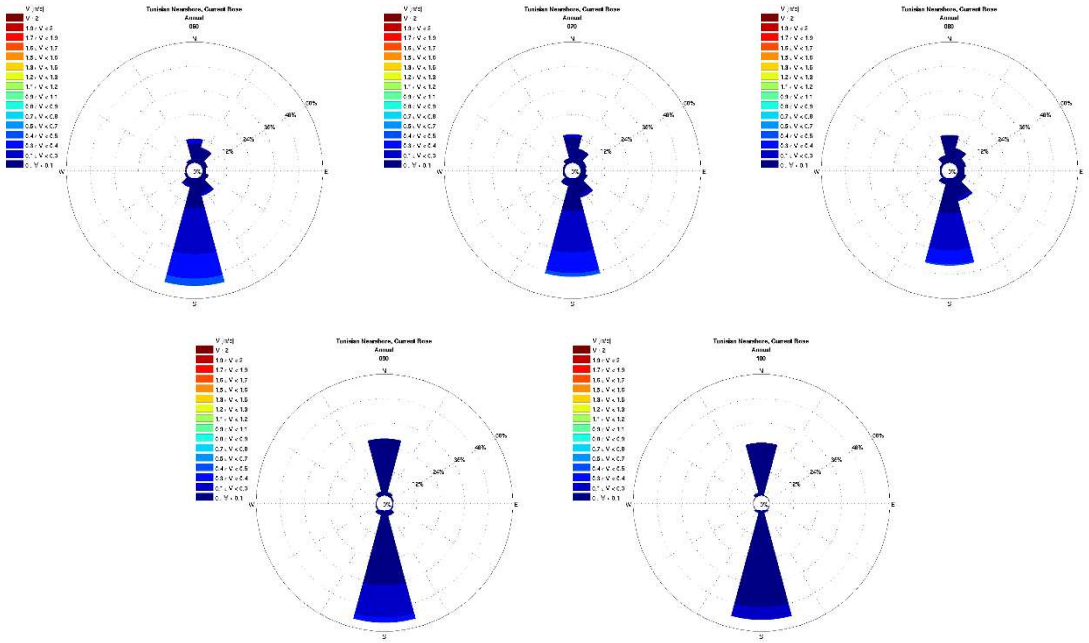

Figure 2.14: Current Rose along the Vertical Profile – Tunisian Nearshore Section

2.1.3.2 Extreme Values

The extreme omnidirectional and directional values of surface total current, reported in Table 3.19, have been assessed using the Weibull distribution function (Figure 2.15) applied to the surface current regime.

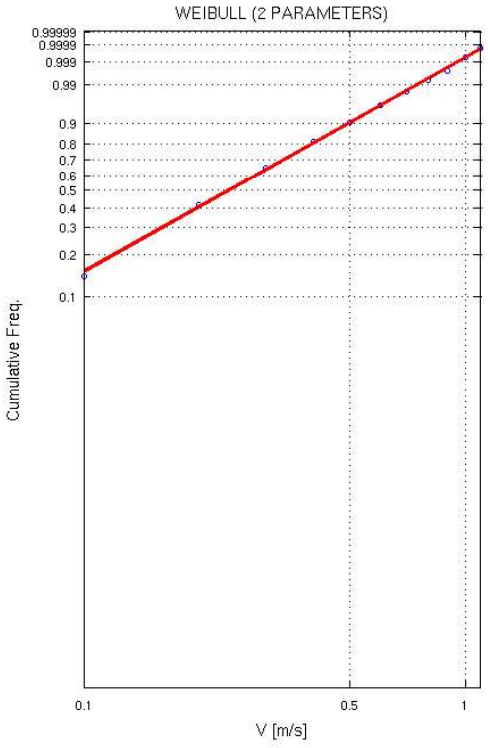

Figure 2.15: Omnidirectional Current Fitting Distribution – Tunisian Nearshore Section

Table 2-8: Extreme Values of Surface Total Current – Tunisian Nearshore Section

	Return Period (year)			
	1	10	50	100
Dir (°N)	V (m/s)	V (m/s)	V (m/s)	V (m/s)
OMNI	0.9	1.1	1.2	1.2
0	0.4	0.5	0.6	0.7
30	0.5	0.6	0.7	0.7
60	0.4	0.5	0.6	0.6
90	0.3	0.4	0.5	0.5
120	0.3	0.4	0.5	0.5
150	0.7	1.0	1.1	1.2
180	0.9	1.0	1.2	1.2
210	0.5	0.7	0.9	0.9
240	0.2	0.4	0.5	0.5
270	0.1	0.3	0.4	0.4
300	0.1	0.4	0.7	0.8
330	0.2	0.4	0.5	0.5

2.1.4 Physical Parameters

In this section, sea water parameters are reported as monthly vertical profile of temperature and salinity.

2.1.4.1 Temperature Profiles

The monthly average depth profile of temperature is reported in graphical form in Figure 2.16. It can be noted that from December to April the vertical profile is well mixed, while from June to October a stable thermocline is formed with a maximum ΔT of about 10°C between surface and deep water.

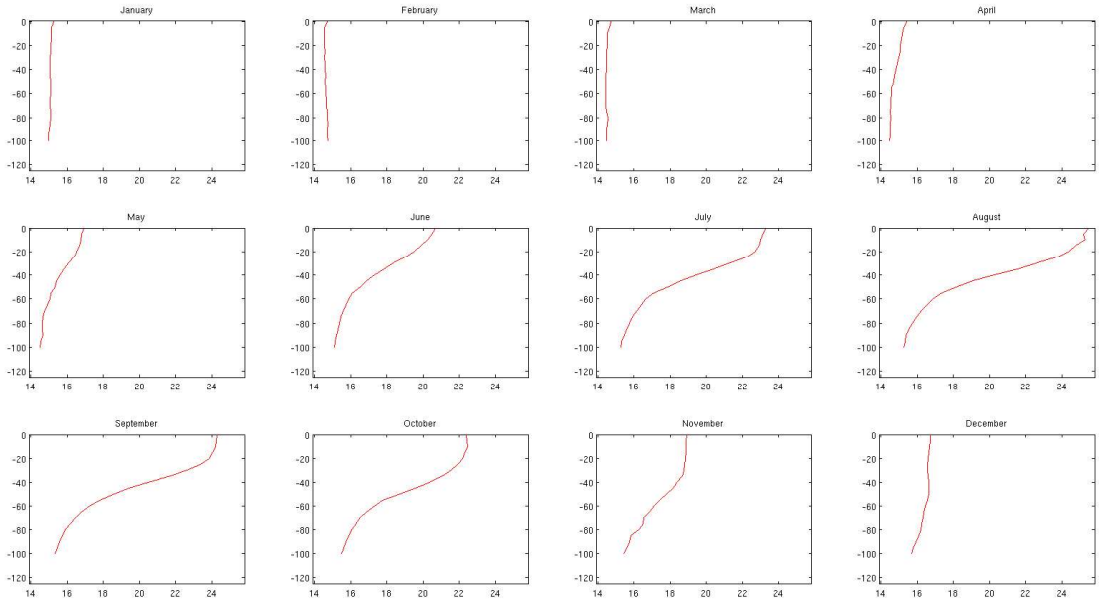

Figure 2.16: Average Monthly Water Temperature Profile – Tunisian Nearshore Section

2.1.4.2 Salinity Profiles

The monthly average depth profile of salinity is reported in graphical form in Figure 2.17.

It can be noted that salinity profile shows a halocline from August to October due to the evaporation during summer of the water with the creation of relatively more saline water in the surface.

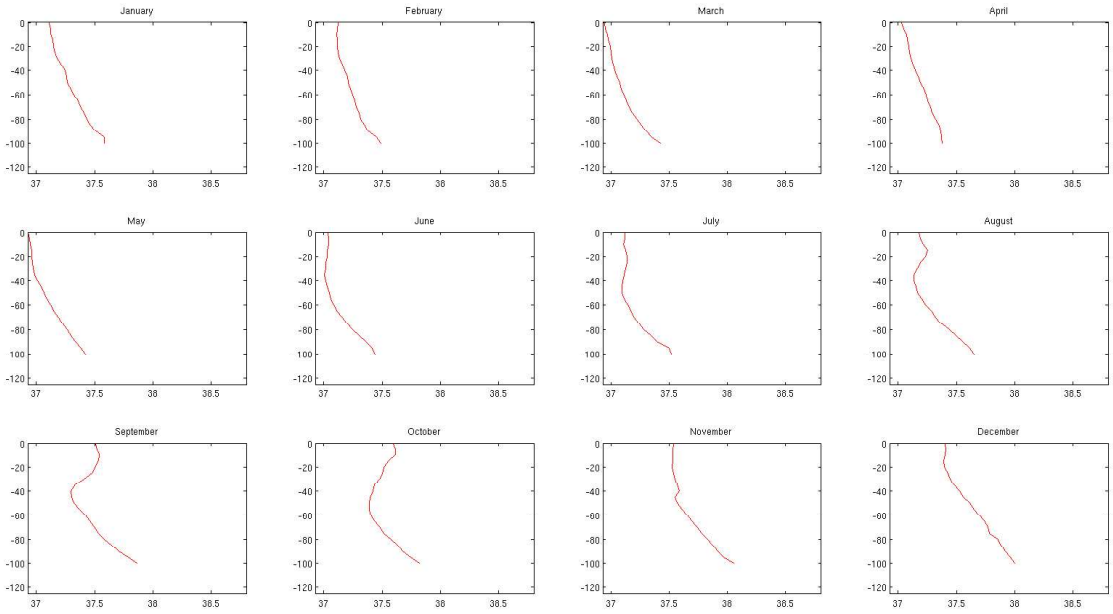

Figure 2.17: Average Monthly Water Salinity Profile – Tunisian Nearshore Section

2.2 Offshore section

The general characteristics of the offshore wind regime extracted from hindcasted data are reported in this Section as annual and monthly distributions and extreme values.

Note that in the frequency distribution table the thresholds must be considered upper thresholds (winds speed lower or equal to 2 m/s, 4 m/s, waves lower or equal to 0.5 m, 1.0 m, …).

2.2.1 Winds

The typical regime of winds and extreme values are here reported for the Offshore section.

2.2.1.1 Typical Regime

The annual distribution of wind speed vs. incoming direction is shown in Table 2. and in Figure 2.18 (wind rose). The typical wind regime is characterized by about 55% events from NW (270-0°N) and about 27% from SE (120-180°N). The wind intensity is characterized by about 88% of events with speeds less than 10 m/s. The maximum speed is less than 22 m/s. Monthly wind roses (Figure 2.19 - Figure 2.21) show that the main incoming wind directions remains the NW and SW sectors, with mild conditions during summer.

Table 2.9: Annual Frequency (%) Distribution of Wind Speed vs Incoming Direction –Offshore Section

Dir (°N)	Wind(m/s) 1hour - Annual Offshore Section												
	2	4	6	8	10	12	14	16	18	20	22	>22.00	TOT.
0	0.71	2.63	3.17	2.23	0.94	0.35	0.16	0.05	0.01				10.27
30	0.67	1.54	1.16	0.59	0.23	0.09	0.03	0.01					4.31
60	0.57	0.94	0.49	0.21	0.08	0.03	0.01						2.35
90	0.69	1.03	0.63	0.37	0.25	0.14	0.07	0.03	0.01				3.23
120	0.64	1.47	1.56	1.37	1.13	0.78	0.36	0.15	0.06				7.54
150	0.66	2.13	3.01	2.64	1.56	0.57	0.15	0.03	0.01				10.76
180	2.02	2.00	2.22	1.47	0.78	0.29	0.05	0.01					8.85
210	0.63	1.52	1.05	0.60	0.35	0.15	0.05	0.01					4.36
240	0.64	1.30	0.82	0.46	0.23	0.11	0.03	0.01					3.61
270	0.69	1.74	1.59	1.38	1.23	0.78	0.36	0.15	0.06	0.01			7.98
300	0.65	2.34	3.37	3.99	3.84	2.66	1.36	0.60	0.24	0.03			19.09
330	0.71	2.75	4.39	4.72	3.04	1.27	0.46	0.23	0.08	0.01			17.65
TOT.	9.29	21.38	23.47	20.03	13.67	7.23	3.08	1.29	0.49	0.05	0.01		100.00

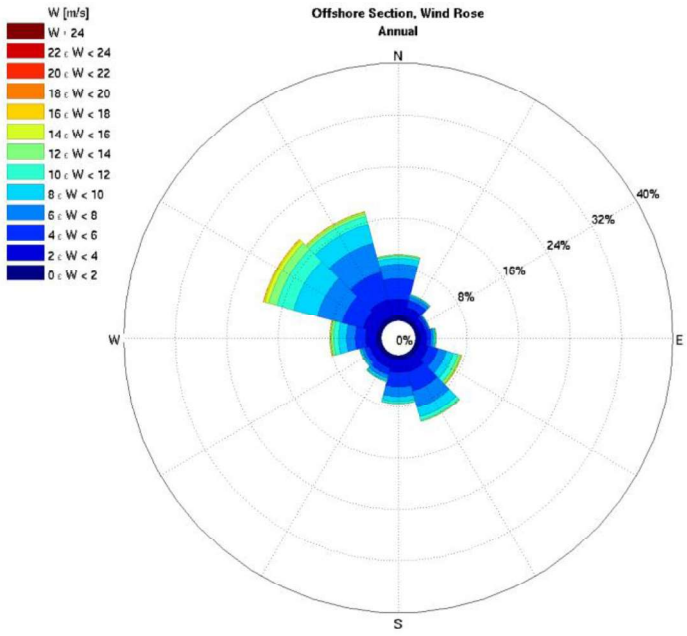

Figure 2.18: Annual Wind Rose – Offshore Section

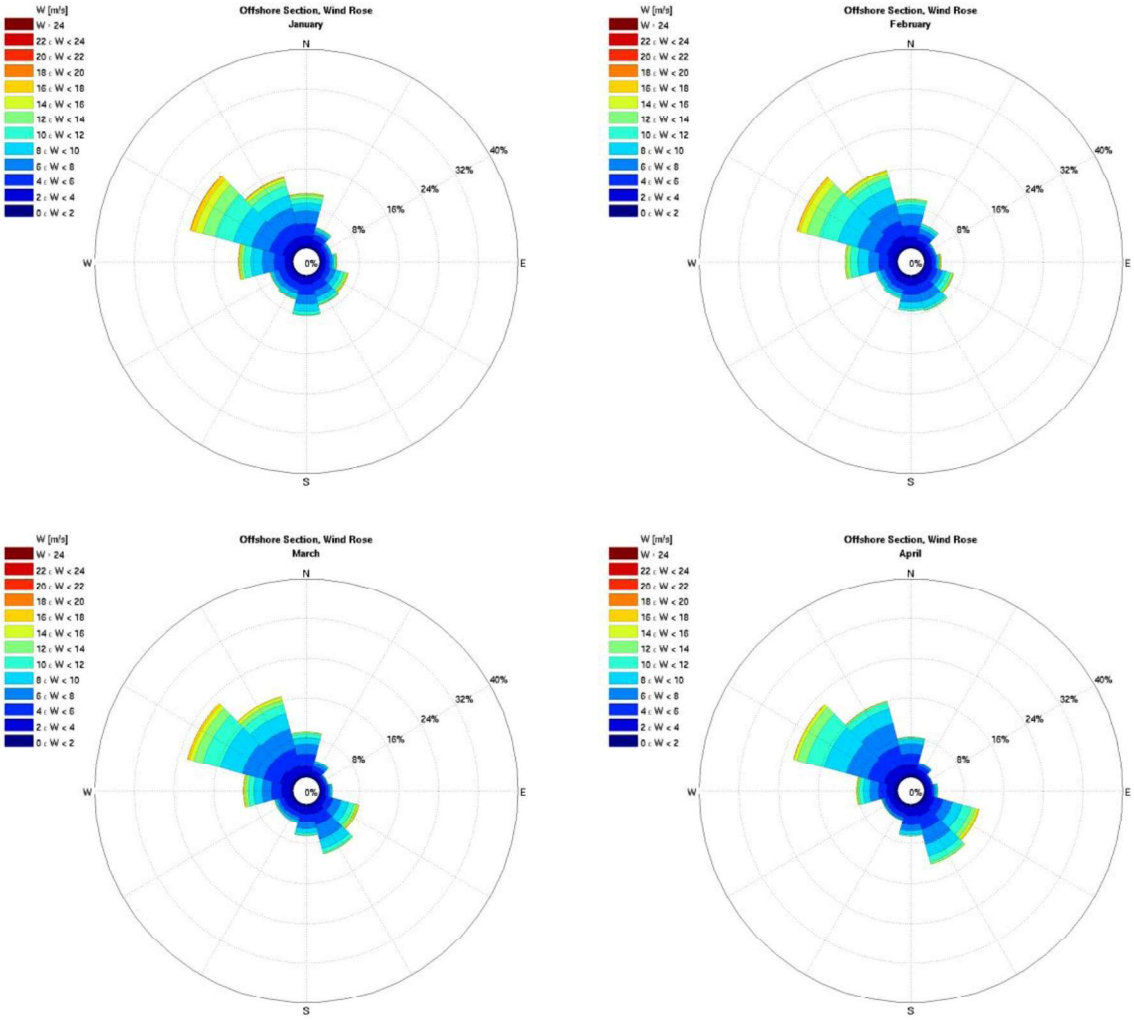

Figure 2.19: Wind Rose – January, February, March, April - Offshore Section

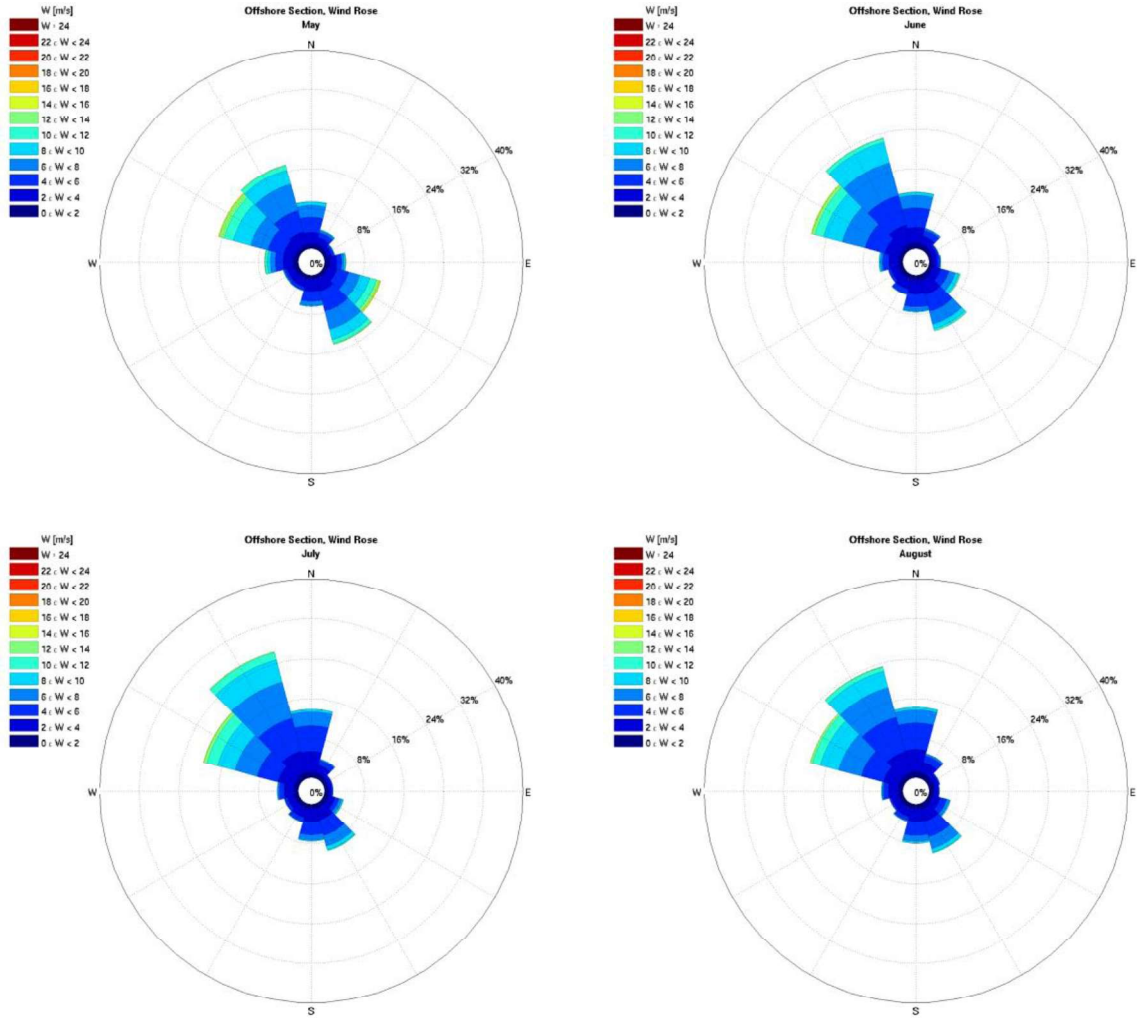

Figure 2.20: Wind Rose – May, June, July, August - Offshore Section

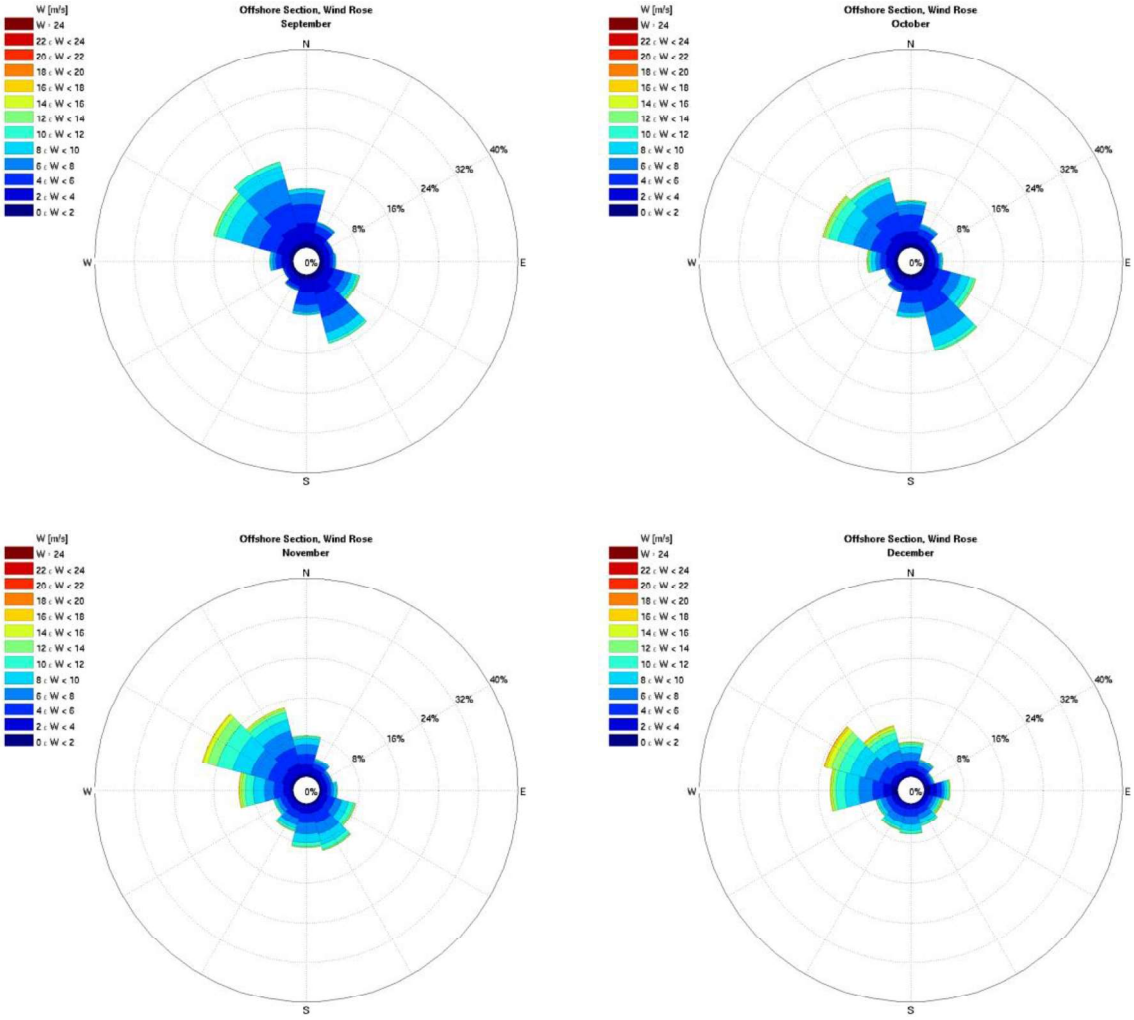

Figure 2.21: Wind Rose – September, October, November, December - Offshore Section

2.2.1.2 Extreme Values

Estimated omnidirectional, directional and monthly extreme wind speeds, referred to hourly data, are shown in Table 2. for different return periods (i.e. 1, 10, 50 and 100 years) , using the Weibull distribution function (Figure 2.22:).

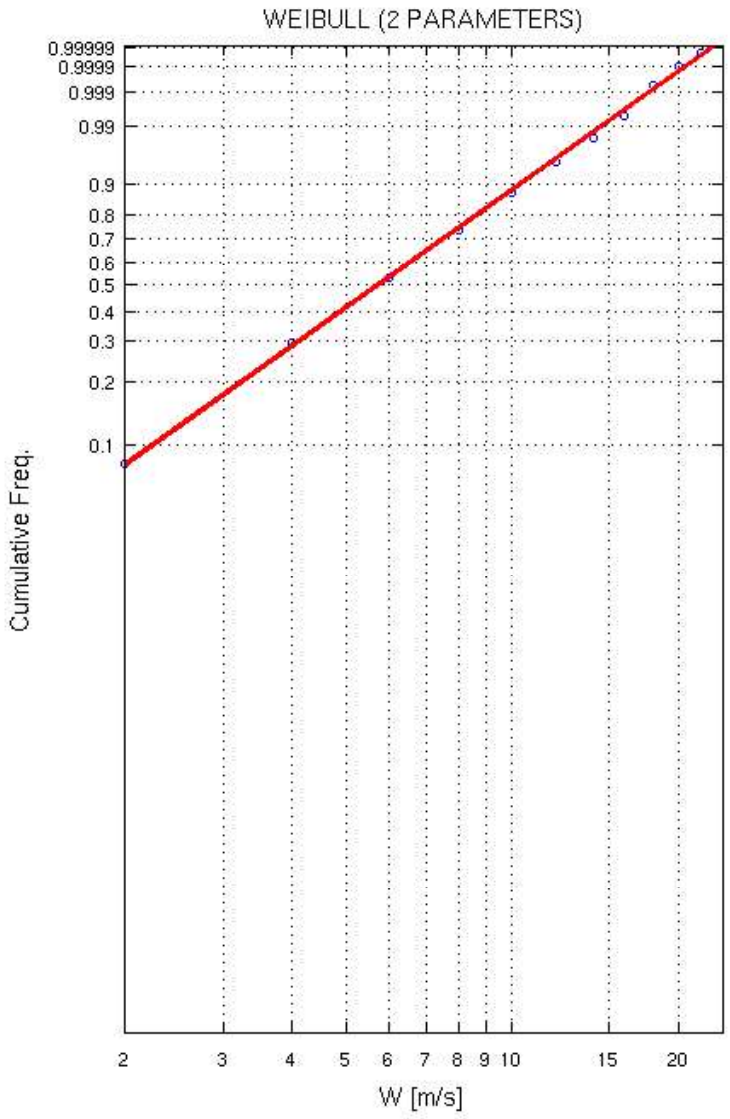

Figure 2.22: Omnidirectional Wind Fitting Distribution – Offshore Section

Table 2.10: Extreme Hourly Winds– Offshore Section

	Return Period (year)			
	1	10	50	100
Dir (°N)	**W_1h (m/s)**	**W_1h (m/s)**	**W_1h (m/s)**	**W_1h (m/s)**
OMNI	21.6	23.9	25.4	26.0
0	18.4	21.2	23.1	23.8
30	15.9	18.9	20.9	21.7
60	14.3	17.7	19.9	20.9
90	17.9	21.3	23.5	24.4
120	18.9	21.2	22.7	23.3
150	16.8	18.8	20.1	20.6
180	15.5	17.5	18.8	19.3
210	15.9	18.6	20.3	21.0
240	15.7	18.7	20.5	21.3
270	19.3	21.8	23.3	23.9
300	21.2	23.5	24.9	25.5
330	19.8	22.1	23.5	24.1
Month	**W_1h (m/s)**	**W_1h (m/s)**	**W_1h (m/s)**	**W_1h (m/s)**
Jan	21.6	23.9	25.4	26.0
Feb	19.3	21.7	23.1	23.7
Mar	19.5	21.9	23.5	24.1
Apr	18.6	21.0	22.5	23.1
May	16.9	19.2	20.6	21.2
Jun	16.1	18.3	19.7	20.3
Jul	14.7	16.5	17.6	18.0
Aug	14.6	16.5	17.7	18.2
Sept	15.7	17.8	19.2	19.7
Oct	18.1	20.6	22.2	22.8
Nov	19.5	22.0	23.6	24.2
Dec	19.8	22.3	23.8	24.4

2.2.2 Waves

The wave climate from the three selected Offshore Point has been considered for the characterization of the Offshore section. The resulting tables are therefore representative of the cumulative condition along the Offshore route.

2.2.2.1 Wave Climate

The annual distribution of the wave height vs. incoming direction is shown in Table 2. and in Figure 2.23 (wave rose). The wave climate reflects the wind regime, and it is characterized by about 56% events from NW (270-0°N) and about 34% from SE (120-180°N). The wave height is characterized by about 87% of events with height less than 2 m, and 99% less than 4 m. The maximum height is less than 8.2 m, coming from 330°N.

Monthly wave roses (Figure 2.24 - Figure 2.26) show that the main incoming wave directions remains the same along the year, with mild conditions during summer (with maximum wave height less than 4.5 m).

Table 2.11: Annual Frequency (%) Distribution of Wave Height vs Incoming Direction –Offshore Section

Dir (°N)	Hs (m) - Annual Offshore Section														
	0.5	1	1.5	2	2.5	3	3.5	4	4.5	5	5.5	6	6.5	> 6.50	TOT.
0	3.17	3.61	1.17	0.48	0.28	0.14	0.09	0.05	0.03	0.01	0.01	0.00	0.00	0.00	9.06
30	0.89	0.51	0.14	0.05	0.03	0.01	0.00	0.00	0.00						1.64
60	0.29	0.14	0.05	0.02	0.01	0.01	0.00	0.00	0.00						0.51
90	0.92	0.99	0.29	0.09	0.03	0.02	0.01	0.00	0.00	0.00	0.00				2.37
120	1.79	3.68	2.37	1.25	0.66	0.34	0.16	0.09	0.05	0.02	0.01	0.00			10.42
150	2.90	6.20	3.45	1.54	0.67	0.27	0.10	0.04	0.02	0.01	0.00				15.21
180	2.57	3.51	1.48	0.45	0.12	0.02	0.01	0.00	0.00						8.17
210	1.04	0.88	0.43	0.18	0.06	0.02	0.01	0.00	0.00						2.62
240	0.46	0.32	0.17	0.06	0.02	0.01	0.00	0.00	0.00						1.05
270	0.63	0.74	0.47	0.21	0.09	0.04	0.02	0.01	0.00	0.00	0.00	0.00			2.21
300	2.68	7.83	7.04	5.03	3.08	1.88	1.08	0.62	0.36	0.22	0.11	0.06	0.02	0.01	30.02
330	3.02	6.16	3.36	1.85	0.99	0.55	0.32	0.20	0.11	0.07	0.04	0.02	0.00	0.00	16.69
TOT.	20.37	34.57	20.44	11.22	6.04	3.30	1.80	1.02	0.59	0.33	0.18	0.08	0.02	0.02	99.96

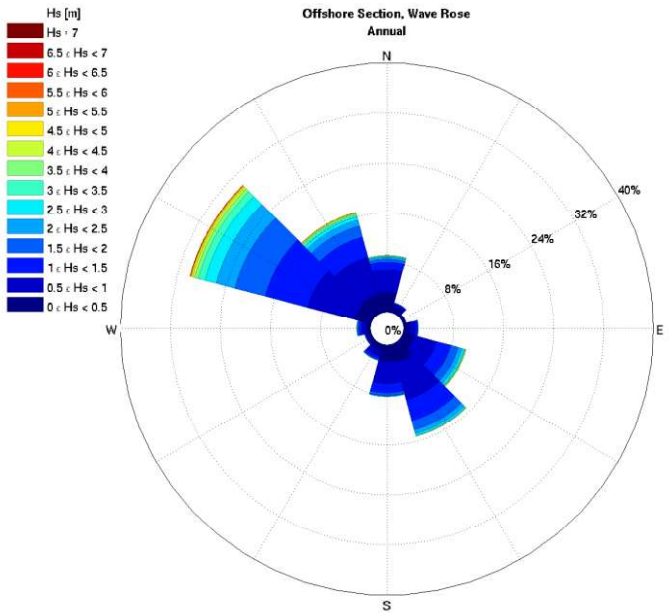

Figure 2.23: Annual Wave Rose – Offshore Section

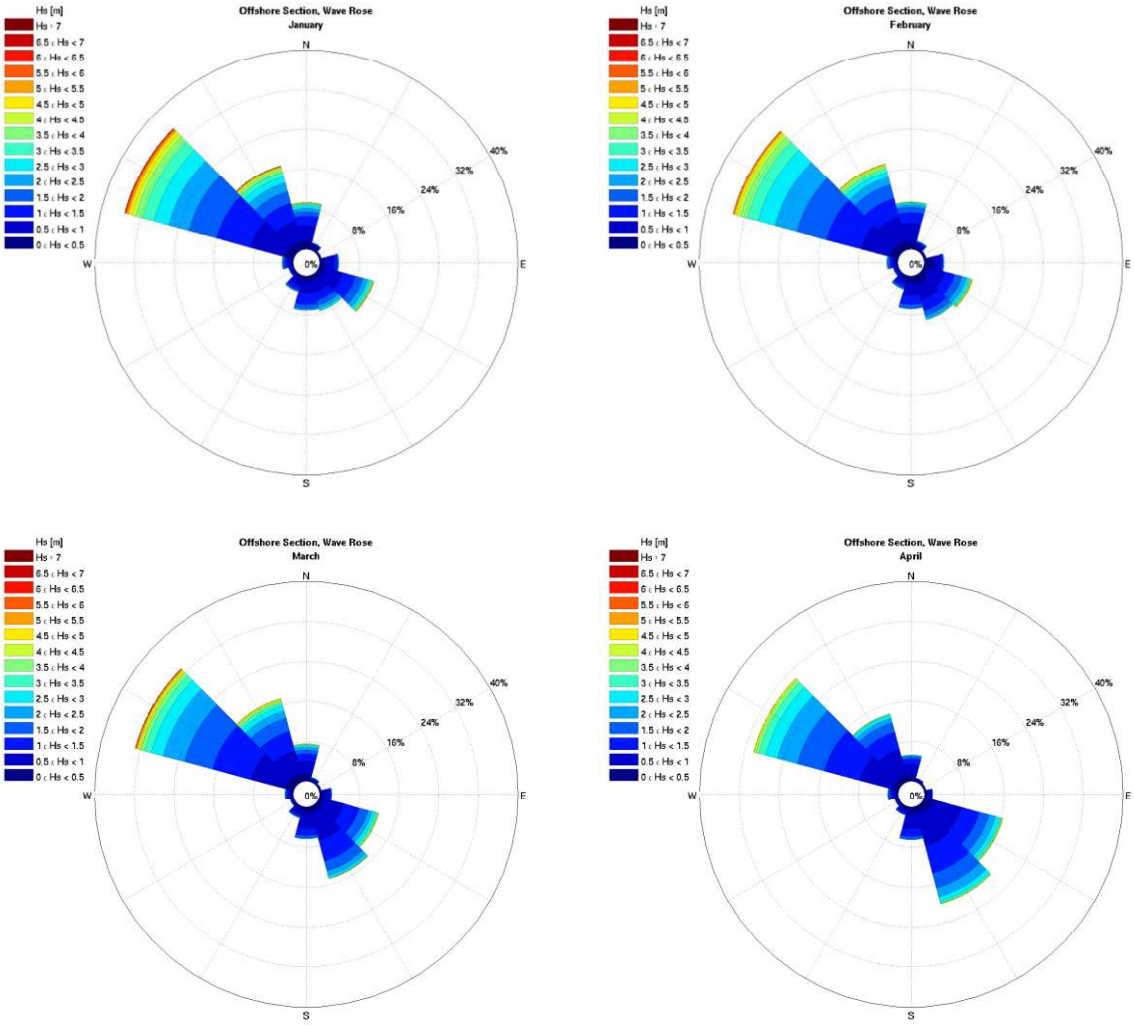

Figure 2.24: Wave Rose – January, February, March, April - Offshore Section

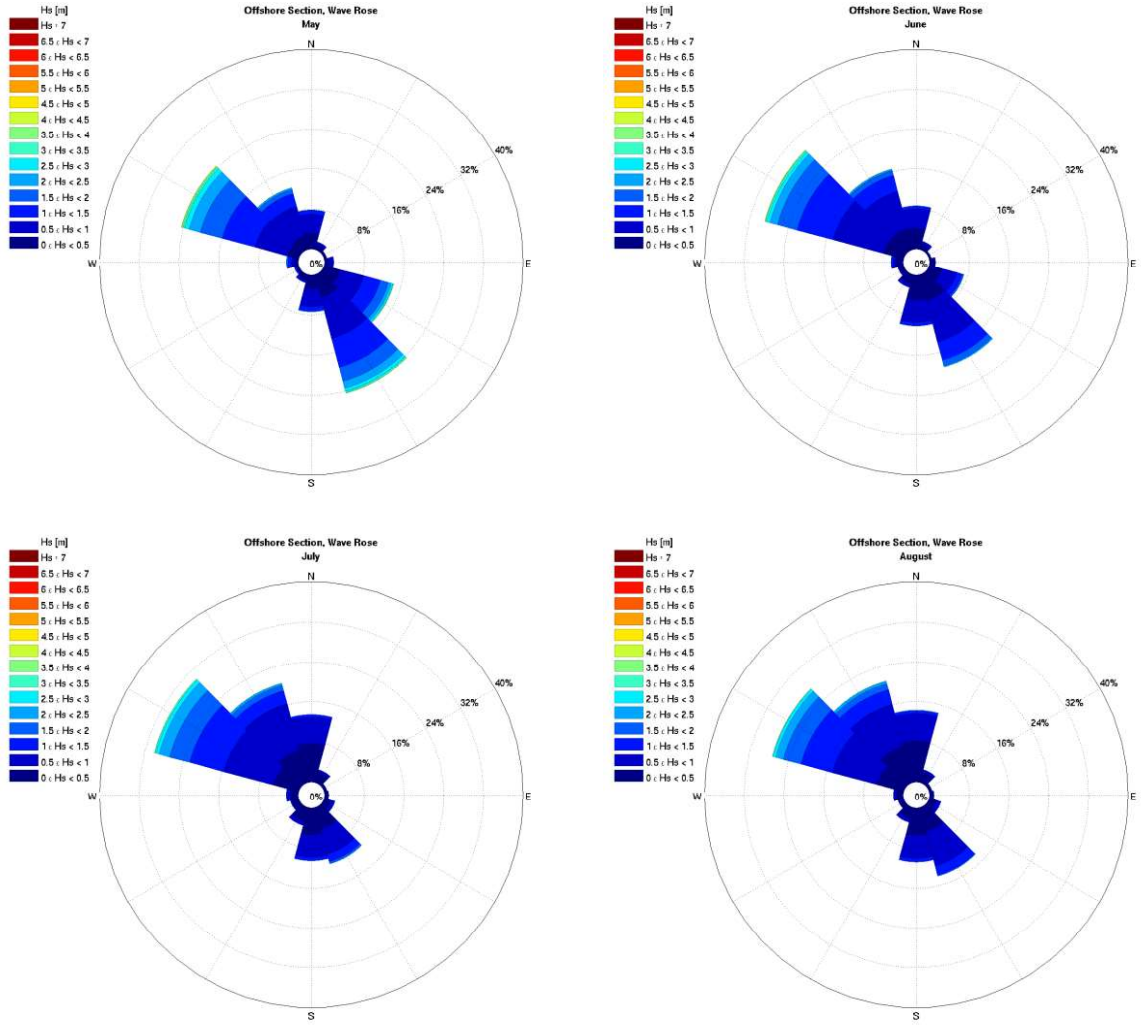

Figure 2.25: Wave Rose – May, June, July, August - Offshore Section

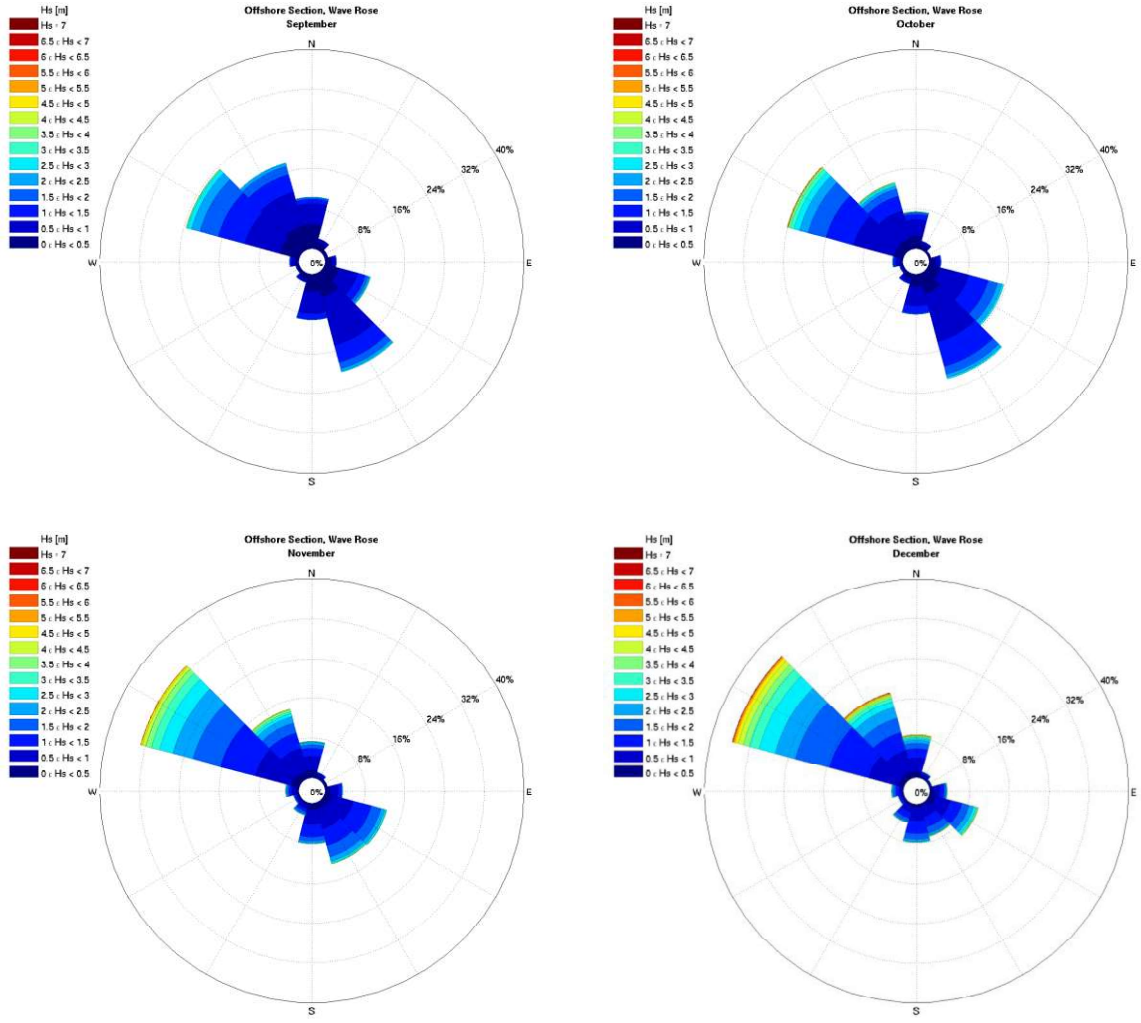

Figure 2.26: Wave Rose – September, October, November, December - Offshore Section

2.2.2.2 Hs-Tp Relationship

The annual distribution of total wave height vs. peak period is shown in Table 2.: the table shows that about 99% of the storms are characterized by wave with peak period less than 10 s, with maximum wave peak period of 14.2 s.

To determine H-T relations, the H_s-T_p scatter is analyzed. Figure 2.27 shows the relations between H_s and T_p that can be used:

$$H_s=0.055*T_p^2$$

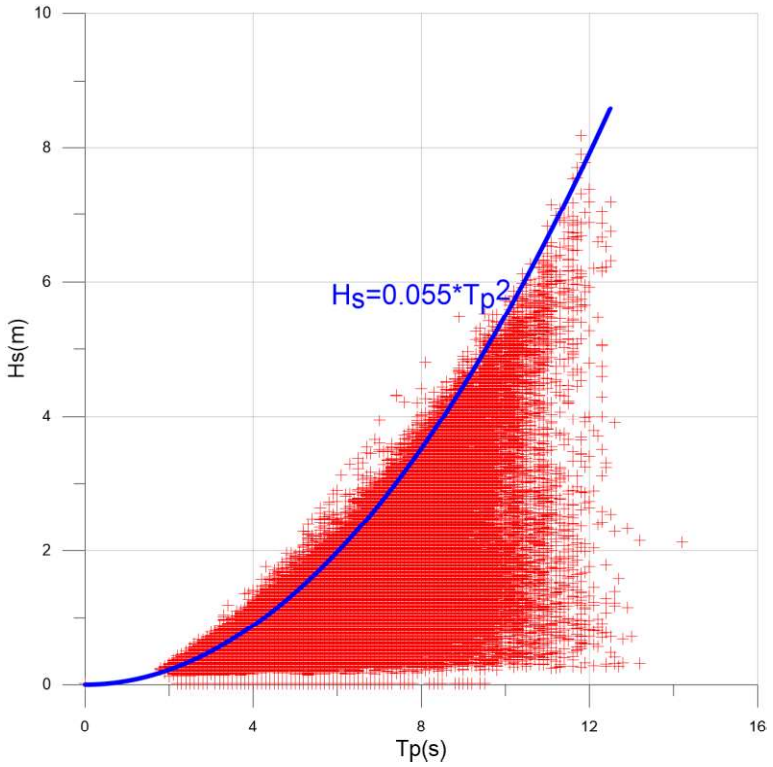

Figure 2.27: Omnidirectional Scatter Diagram of Wave Height VS Peak Period – Offshore Section

Table 2.12: Annual Frequency (%) Distribution of Wave Height vs Peak Period –Offshore Section

Tp(s)	Hs (m)- OMNI Offshore Section														
	0.5	1	1.5	2	2.5	3	3.5	4	4.5	5	5.5	6	6.5	> 6.50	TOT.
1															
2	0.04														0.04
3	6.55	0.50													7.05
4	5.93	8.26	0.12												14.31
5	4.63	9.98	4.28	0.11											18.99
6	1.83	9.04	7.00	2.88	0.17	0.01									20.93
7	0.81	4.06	5.39	4.50	2.25	0.30	0.01	0.00							17.32
8	0.32	1.72	2.28	2.41	2.38	1.67	0.48	0.05	0.00						11.29
9	0.13	0.69	0.91	0.88	0.89	0.97	0.93	0.54	0.16	0.01	0.00				6.12
10	0.07	0.22	0.33	0.31	0.23	0.26	0.31	0.35	0.33	0.18	0.04	0.00			2.63
11	0.04	0.07	0.12	0.10	0.10	0.08	0.07	0.07	0.09	0.13	0.13	0.06	0.01	0.00	1.05
12	0.01	0.03	0.02	0.02	0.01	0.01	0.01	0.01	0.01	0.01	0.01	0.02	0.01	0.01	0.18
13	0.00	0.01	0.00	0.00	0.00	0.00	0.00	0.00	0.00	0.00	0.00		0.00	0.00	0.03
14	0.00				0.00										0.00
>14.00					0.00										0.00
TOT.	20.36	34.57	20.44	11.22	6.04	3.30	1.80	1.02	0.59	0.33	0.18	0.08	0.02	0.02	99.96

2.2.2.3 Extreme Values

Estimated omnidirectional directional and monthly extreme wave heights, referred to 3-hour wave climate, are shown in Table 2. and Table 2. for different return periods (i.e. 1, 10,50 and 100 years) , using the Weibull distribution function (Figure 2.28).

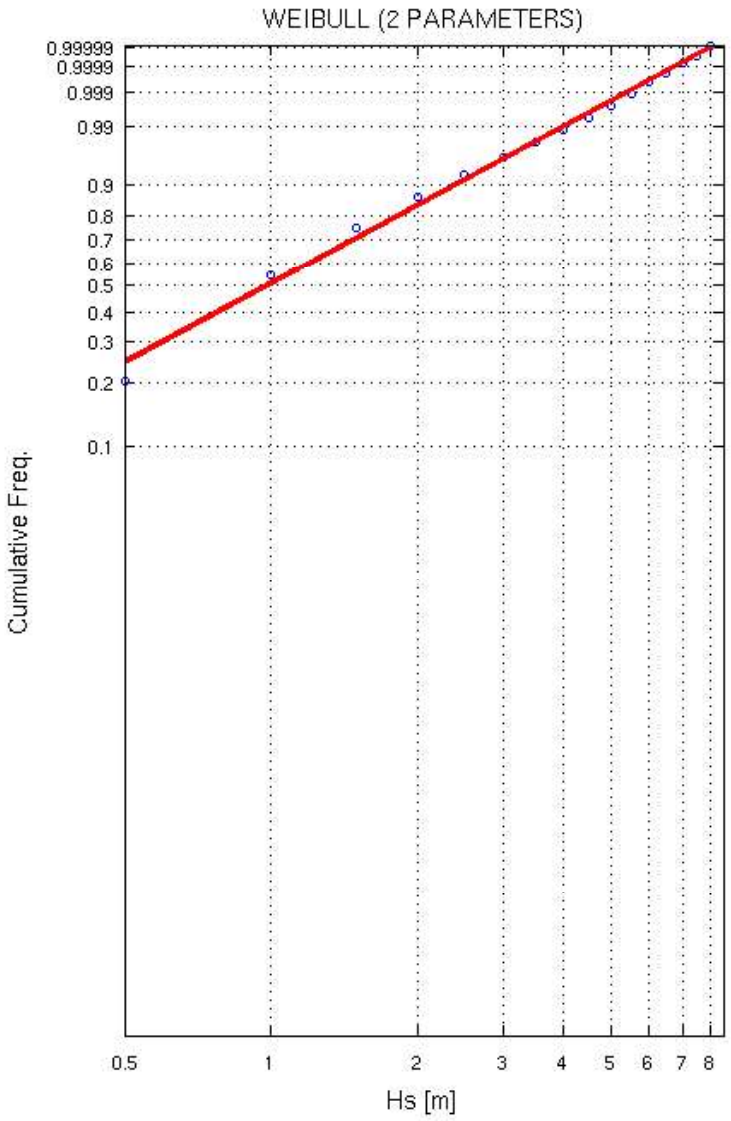

Figure 2.28: Omnidirectional Total Wave Fitting Distribution – Offshore Section

Table 2.13: Extreme Wave Parameters – Offshore Section - Return Period 1, 10 Years

	Return Period (year)				Return Period (year)			
	1				10			
Dir (°N)	Hs (m)	Tp (s)	Hmax(m)	T_Hmax (s)	Hs (m)	Tp (s)	Hmax(m)	T_Hmax (s)
OMNI	6.66	11.00	11.99	10.95	7.88	11.97	14.18	11.91
0	5.15	9.68	9.27	9.63	7.00	11.28	12.60	11.22
30	2.61	6.89	4.70	6.85	3.84	8.36	6.91	8.31
60	2.18	6.30	3.92	6.26	3.55	8.03	6.39	7.99
90	3.18	7.60	5.72	7.57	4.62	9.17	8.32	9.12
120	4.83	9.37	8.69	9.32	5.95	10.40	10.71	10.35
150	4.32	8.86	7.78	8.82	5.28	9.80	9.50	9.75
180	3.17	7.59	5.71	7.55	4.00	8.53	7.20	8.49
210	3.00	7.39	5.40	7.35	3.94	8.46	7.09	8.42
240	2.81	7.15	5.06	7.11	4.02	8.55	7.24	8.51
270	3.65	8.15	6.57	8.11	5.09	9.62	9.16	9.57
300	6.47	10.85	11.65	10.79	7.65	11.79	13.77	11.73
330	6.66	11.00	11.99	10.95	7.88	11.97	14.18	11.91
Month	Hs (m)	Tp (s)	Hmax(m)	T_Hmax (s)	Hs (m)	Tp (s)	Hmax(m)	T_Hmax (s)
Jan	6.66	11.00	11.99	10.95	7.88	11.97	14.18	11.91
Feb	5.02	9.55	9.04	9.51	6.03	10.47	10.85	10.42
Mar	5.53	10.03	9.95	9.98	6.69	11.03	12.04	10.97
Apr	4.51	9.06	8.12	9.01	5.34	9.85	9.61	9.80
May	3.89	8.41	7.00	8.37	4.77	9.31	8.59	9.27
Jun	3.40	7.86	6.12	7.82	4.21	8.75	7.58	8.71
Jul	3.16	7.58	5.69	7.54	3.92	8.44	7.06	8.40
Aug	3.10	7.51	5.58	7.47	3.86	8.38	6.95	8.34
Sept	3.54	8.02	6.37	7.98	4.37	8.91	7.87	8.87
Oct	4.77	9.31	8.59	9.27	6.13	10.56	11.03	10.50
Nov	4.93	9.47	8.87	9.42	5.90	10.36	10.62	10.31
Dec	5.83	10.30	10.49	10.24	6.98	11.27	12.56	11.21

Table 2.14: Extreme Wave Parameters – Offshore Section - Return Period 50, 100 Years

	Return Period (year)				Return Period (year)			
	50				100			
Dir (°N)	Hs (m)	Tp (s)	Hmax(m)	T_Hmax (s)	Hs (m)	Tp (s)	Hmax(m)	T_Hmax (s)
OMNI	8.70	12.58	15.66	12.51	9.04	12.82	16.27	12.76
0	8.30	12.28	14.94	12.22	8.86	12.69	15.95	12.63
30	4.71	9.25	8.48	9.21	5.08	9.61	9.14	9.56
60	4.52	9.07	8.14	9.02	4.94	9.48	8.89	9.43
90	5.64	10.13	10.15	10.08	6.08	10.51	10.94	10.46
120	6.69	11.03	12.04	10.97	6.99	11.27	12.58	11.22
150	5.92	10.37	10.66	10.32	6.18	10.60	11.12	10.55
180	4.55	9.10	8.19	9.05	4.78	9.32	8.60	9.28
210	4.56	9.11	8.21	9.06	4.81	9.35	8.66	9.30
240	4.84	9.38	8.71	9.33	5.19	9.71	9.34	9.67
270	6.07	10.51	10.93	10.45	6.49	10.86	11.68	10.81
300	8.43	12.38	15.17	12.32	8.75	12.61	15.75	12.55
330	8.70	12.58	15.66	12.51	9.04	12.82	16.27	12.76
Month	Hs (m)	Tp (s)	Hmax(m)	T_Hmax (s)	Hs (m)	Tp (s)	Hmax(m)	T_Hmax (s)
Jan	8.70	12.58	15.66	12.51	9.04	12.82	16.27	12.76
Feb	6.68	11.02	12.02	10.97	6.94	11.23	12.49	11.18
Mar	7.43	11.62	13.37	11.56	7.74	11.86	13.93	11.80
Apr	5.87	10.33	10.57	10.28	6.08	10.51	10.94	10.46
May	5.35	9.86	9.63	9.81	5.59	10.08	10.06	10.03
Jun	4.73	9.27	8.51	9.23	4.95	9.49	8.91	9.44
Jul	4.42	8.96	7.96	8.92	4.63	9.18	8.33	9.13
Aug	4.36	8.90	7.85	8.86	4.57	9.12	8.23	9.07
Sept	4.91	9.45	8.84	9.40	5.13	9.66	9.23	9.61
Oct	7.04	11.31	12.67	11.26	7.43	11.62	13.37	11.56
Nov	6.53	10.90	11.75	10.84	6.79	11.11	12.22	11.06
Dec	7.71	11.84	13.88	11.78	8.02	12.08	14.44	12.01

2.2.3 Sea level

In Table 2., the expected tidal water levels are reported for Valletta tidal station.The standard levels considered are the following (Admiralty tide tables 2012)

- ✓ HAT (Highest Astronomical Tide): the elevation of the highest predicted astronomical tide expected to occur at a specific tide station above chart datum;
- ✓ MHWS (Mean High Water Spring): the average height of the high waters of spring tide above LAT;
- ✓ MHWN (Mean High Water Neap): the average height of the high waters of neap tide above LAT;
- ✓ MSL (Mean Sea Level): average level of the sea surface over a long period, normally 19 years, or the average level which would exist in the absence of tides above chart datum;
- ✓ MLWN (Mean Low Water Neap): the average height of the low waters of neap tide above LAT;
- ✓ MLWS (Mean Low Water Spring): the average height of the low waters of spring tide above LAT.

Table 2.15: Tidal Water Level at Valletta Tidal Station

	N(°,')		E (°,')		MHWS	MHWN	MLWN	MLWS	MSL	HAT
Valletta	35	53	14	31	0.8	0.7	0.6	0.4	0.63	1.1

2.2.4 Currents

The general circulation of the water masses in the Mediterranean is mainly determined by exchange of heat and salt/thermohaline circulation and by earth rotation effect (Coriolis force). As a result, circulation roughly runs counterclockwise along the continental slopes, but dynamical activity at mesoscale is superimposed nearly everywhere in the Mediterranean, modifying locally and episodically this mean path.

Mesoscale phenomena are typically upwellings, fronts, meanders and eddies. Locally and episodically (up to several months, (Millot ,1999)), they can strongly perturb the general circulation. The main water masses of the Mediterranean Sea are:

- ✓ the Modified Atlantic Water (MAW) in the upper layer;
- ✓ the Levantine Intermediate Water (LIW) below;
- ✓ the Mediterranean Deep Water (MDW) down to the bottom.

Figure 2.29 shows the MAW circulation scheme.

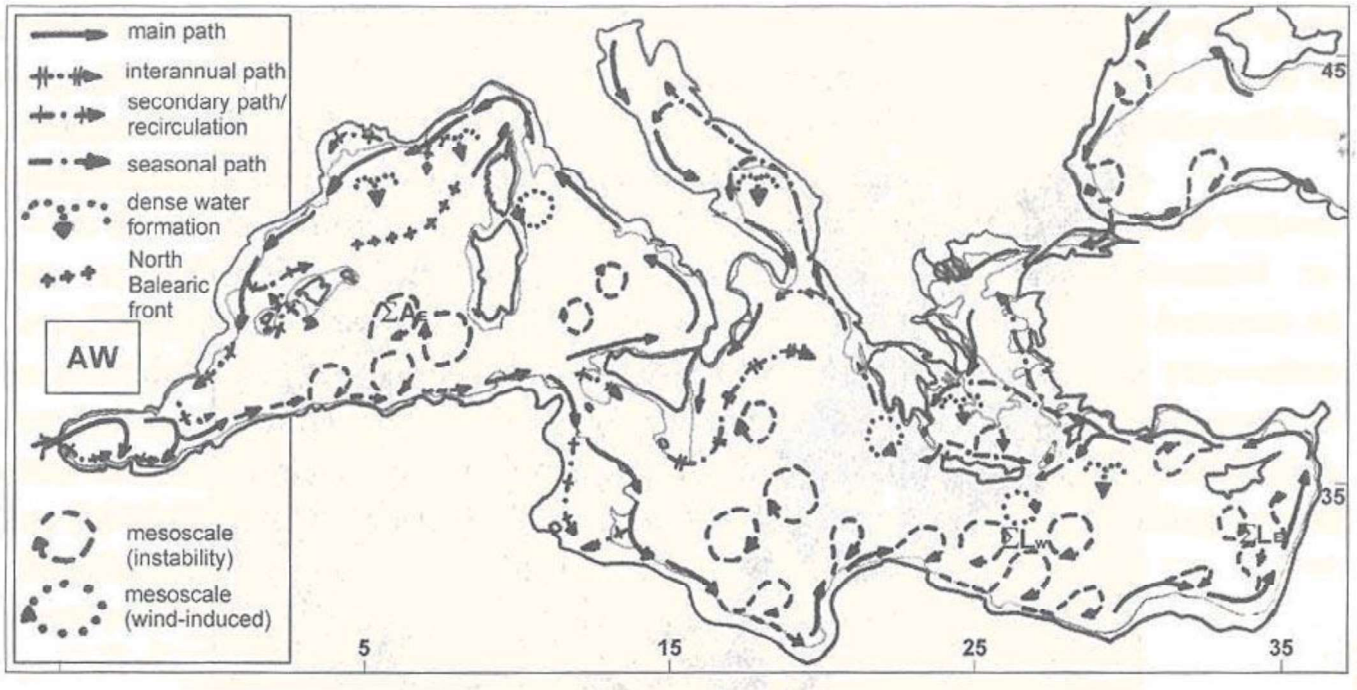

Figure 2.29: MAW Circulation Scheme (Millot, 1999)

The intermediate and deep waters circulations in the south of the Eastern Basin are still debated: Figure 2.30 shows the LIW circulation scheme, according to some authors.

LIW formed in the northern part of the Levantine Basin, along the southern continental slope of the Cretan Arc island, from Rhodes and to the Peloponnese. This warm and salty water flows along the Sicilian slope and then skirts Sicily. Then LIW mainly circulates around the Tyrrhenian at 200-600 m.

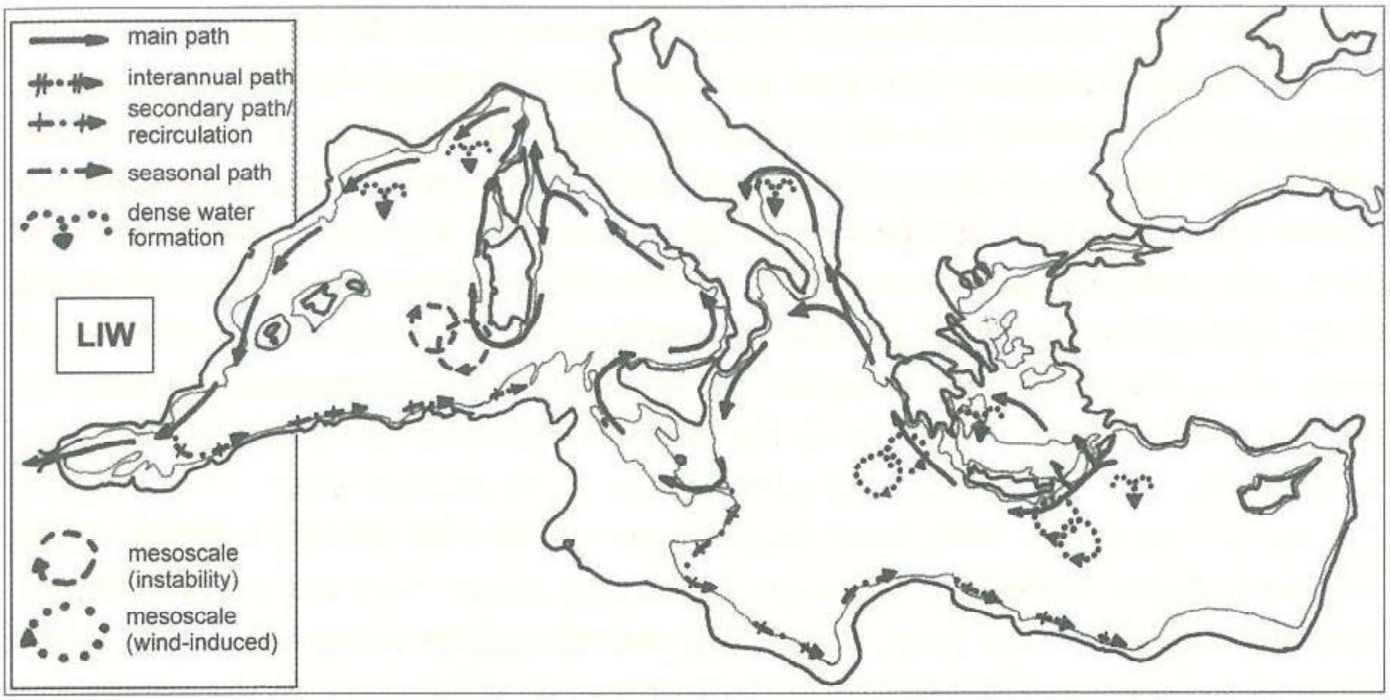

Figure 2.30: LIW Circulation Scheme

The typical regime of currents (from HYCOM hindcasted data), the vertical profile and superficial extreme values are here reported for the Offshore section. To better characterize the characteristics of the offshore section two points of HYCOM database were extracted, respectively located at 11.44°E 36.88°N and 11.60°E 36.96°N. The first Offshore point (hereinafter named Off_1) is located in correspondence of the center of the jet current entering in the Sicily Channel (that affects the surface water) at about 200 m of WD. The second Offshore point (hereinafter named Off_2) has been chosen at about 500m of WD, located in correspondence of the maximum water depth of the Sicily Channel and shows the presence of deep water current flowing on the bottom with opposite direction respect to the surface current. The Hycom data extracted from Off_1 and Off_2 confirms the large scale circulation reported in literature.

Please note that the current direction is intended as a propagation direction.

2.2.4.1 Typical Conditions

The annual distribution of current speed vs. propagating direction of point Off_1 is shown in Table 2. and in Figure 2.31 (current rose).

Table 2. shows that offshore current mainly flows toward SE, 150-180°N sectors (about 59% of total events). Most events are less or equal to 0.60 m/s (about 93% of total events), while the most intense current velocities are of about 1.3 m/s associated to 180°N directional sector.

Table 2.16: Annual Frequency (%) Distribution of Surface Current vs Direction of Propagation – Offshore Section_ Point HYCOM_Off1

Dir (°N)	V (m/s) - Annual Offshore 1 - depth =sur m																
	0.1	0.2	0.3	0.4	0.5	0.6	0.7	0.8	0.9	1	1.1	1.2	1.3	1.4	1.5	>1.5	TOT.
0	0.72	1.37	0.83	0.19	0.03												3.14
30	0.82	2.11	1.29	0.46	0.08												4.75
60	1.02	1.98	1.21	0.57	0.05												4.83
90	1.34	2.28	1.13	0.27	0.02	0.02	0.02										5.06
120	1.29	3.17	1.85	0.69	0.17	0.08	0.02	0.02									7.29
150	1.62	4.54	5.63	5.09	3.36	1.81	0.93	0.60	0.39	0.25	0.03	0.03					24.28
180	1.65	4.94	6.74	7.18	5.60	4.20	2.40	1.20	0.58	0.50	0.11	0.02	0.02				35.13
210	1.20	2.37	1.93	1.16	0.52	0.49	0.16	0.02	0.03								7.87
240	0.94	0.88	0.49	0.20	0.03												2.55
270	0.79	0.55	0.16	0.08	0.02												1.59
300	0.72	0.75	0.13	0.06	0.02	0.02											1.70
330	0.57	0.82	0.35	0.06	0.02												1.81
TOT.	12.67	25.76	21.74	16.02	9.90	6.60	3.52	1.82	1.01	0.75	0.14	0.05	0.02				100.00

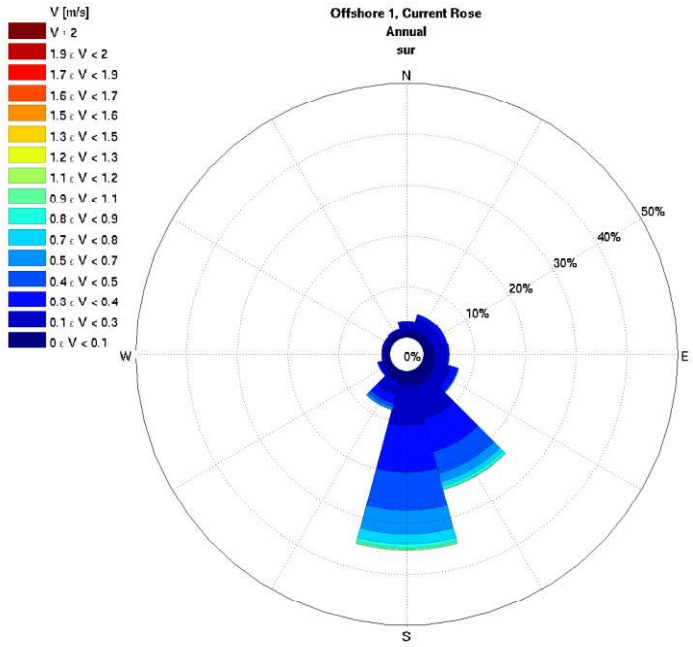

Figure 2.31: Surface Current Rose – Offshore Section – Off_1

The vertical current profile of Figure 2.32 shows a decrease of current intensity with the increase of depth. The vertical profile is characterized for about 70 m of water column by higher currents propagating towards Southeast, with maximum current speed greater than 0.7 m/s. From 70 m of W.D. and the sea floor the current speed decreases slowly, and it reaches about 0.3 m/s on the sea bottom. The current rose along the vertical profile (Figure 2.33) shows that the current is mainly directed towards South until 80m of W.D, where

the presence of a countercurrent begins to reveal, while the last layer investigated (200 m of W.D.) the NW countercurrent prevails.

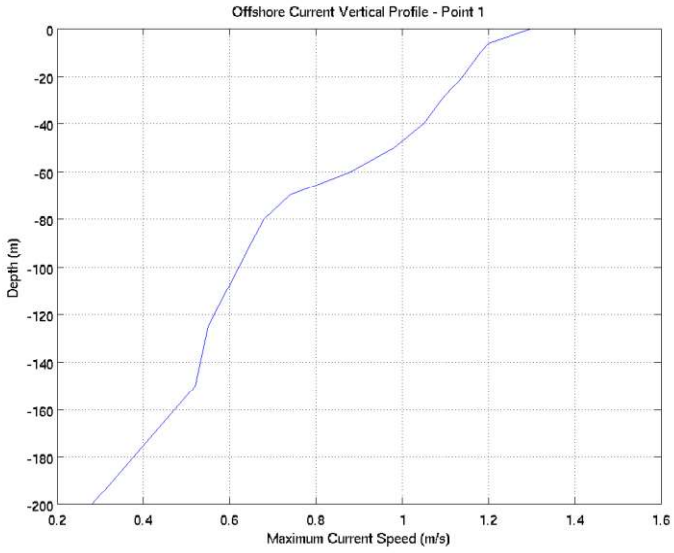

Figure 2.32: Vertical Current Profile – Offshore Section – Off_1

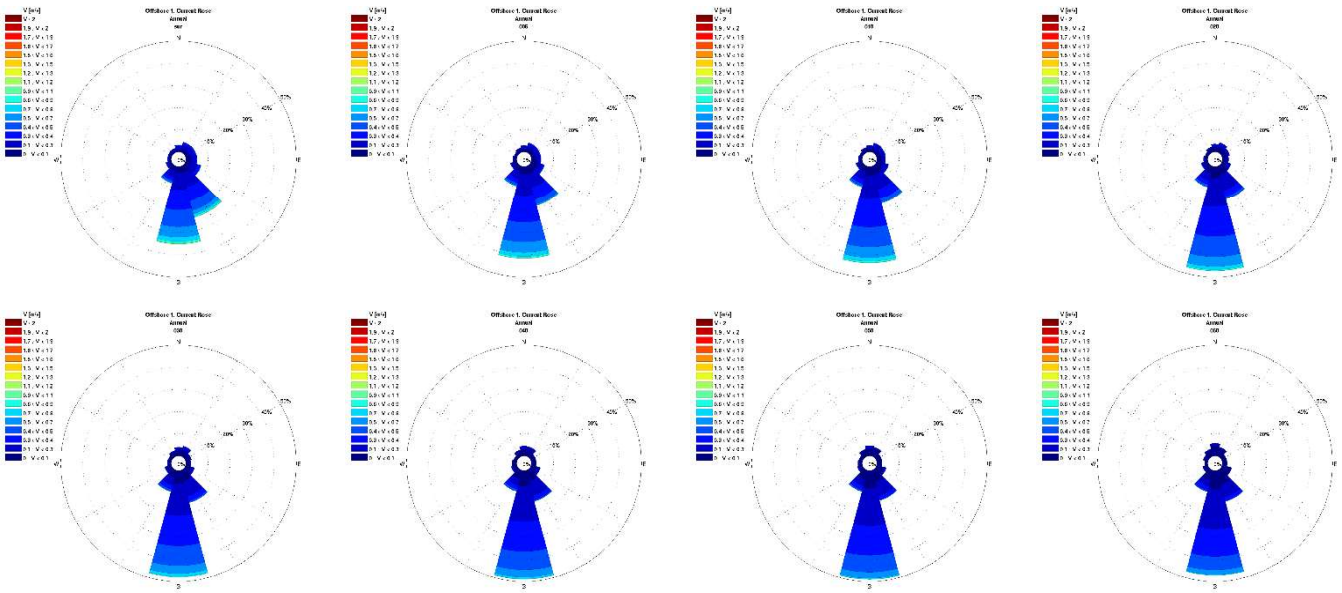

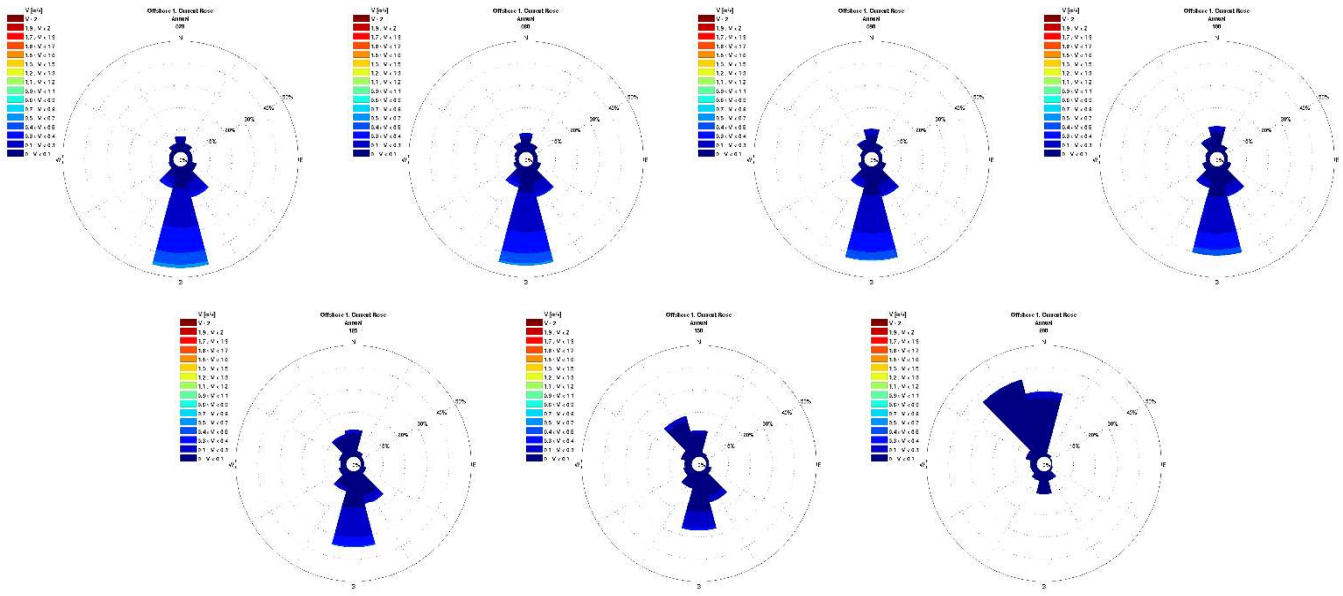

Figure 2.33: Current Rose along the Vertical Profile – Offshore Section – Off1

The annual distribution of current speed vs. propagating direction of point Off_2 is shown in Table 2..

Table 2. shows that offshore current mainly flows toward S, 150-210°N sectors (about 43% of total events). Most events are less or equal to 0.40 m/s (about 93% of total events), while the most intense current velocities are of about 0.9 m/s associated to 150-180°N directional sector.

Table 2.17: Annual Frequency (%) Distribution of Surface Current vs Direction of Propagation – Offshore Section_ Point HYCOM_Off2

Dir (°N)	V (m/s) - Annual Offshore 2 - depth =sur m																
	0.1	0.2	0.3	0.4	0.5	0.6	0.7	0.8	0.9	1	1.1	1.2	1.3	1.4	1.5	>1.5	TOT.
0	2.36	3.10	1.21	0.25	0.02	0.02											6.95
30	1.93	2.55	1.32	0.16	0.02												5.97
60	1.93	2.25	1.02	0.38													5.58
90	1.82	2.56	1.16	0.24		0.02											5.80
120	2.30	3.62	1.78	0.46	0.13	0.03											8.30
150	2.34	3.80	3.46	1.98	0.88	0.44	0.09	0.06	0.02								13.08
180	2.50	4.57	4.24	3.28	1.37	0.79	0.36	0.08	0.02								17.21
210	2.17	3.77	3.27	1.84	0.94	0.53	0.08	0.24									12.84
240	2.22	2.64	1.67	0.94	0.39	0.08	0.02										7.95
270	1.90	2.08	1.01	0.55	0.08												5.61
300	2.26	2.26	0.74	0.17	0.06		0.02										5.52
330	1.85	2.25	0.79	0.25	0.03	0.02											5.19
TOT.	25.59	35.44	21.66	10.50	3.91	1.92	0.57	0.38	0.03								100.00

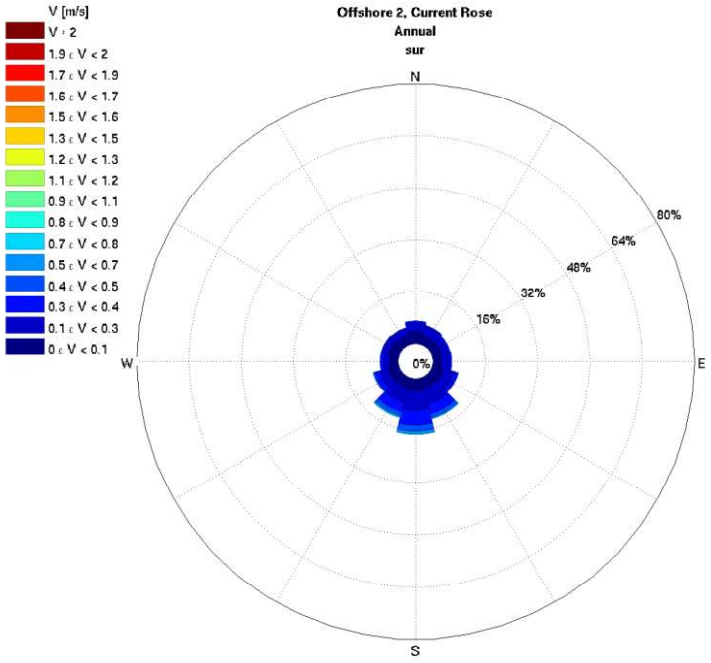

Figure 2.34: Surface Current Rose – Offshore Section – Off_2

The vertical current profile of Figure 2.35 shows a decrease of current intensity with the increase of depth. The vertical profile is characterized for about 70 m of water column by currents propagating towards Southwest, with maximum current speed decreasing from 0.8 m/s to 0.45 m/s. From 70 m to 100 m of W.D. the maximum current speed decreases from 0.45 to 0.35 m/s with the presence of a Northwest current. From 125 m to sea floor the Northwest current became the main flow, with speeds that increase to about 0.45 m/s at 125m of water depth and 250 m of W.D. At the sea floor the maximum current speed is about 0.2 m/s. The current rose along the vertical profile (Figure 2.36 - Figure 2.37) shows the current is mainly directed towards South until 80m of W.D, while the deep layers investigated show the trend just now described.

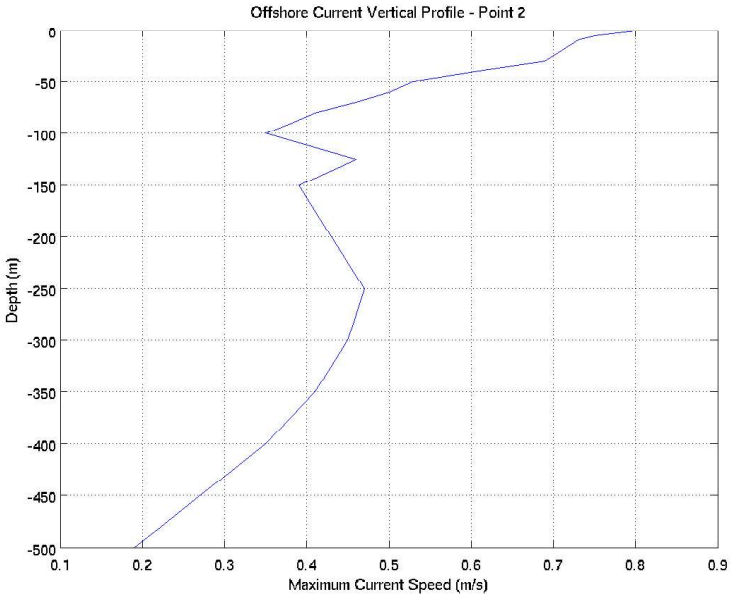

Figure 2.35: Vertical Current Profile – Offshore Section – Off_2

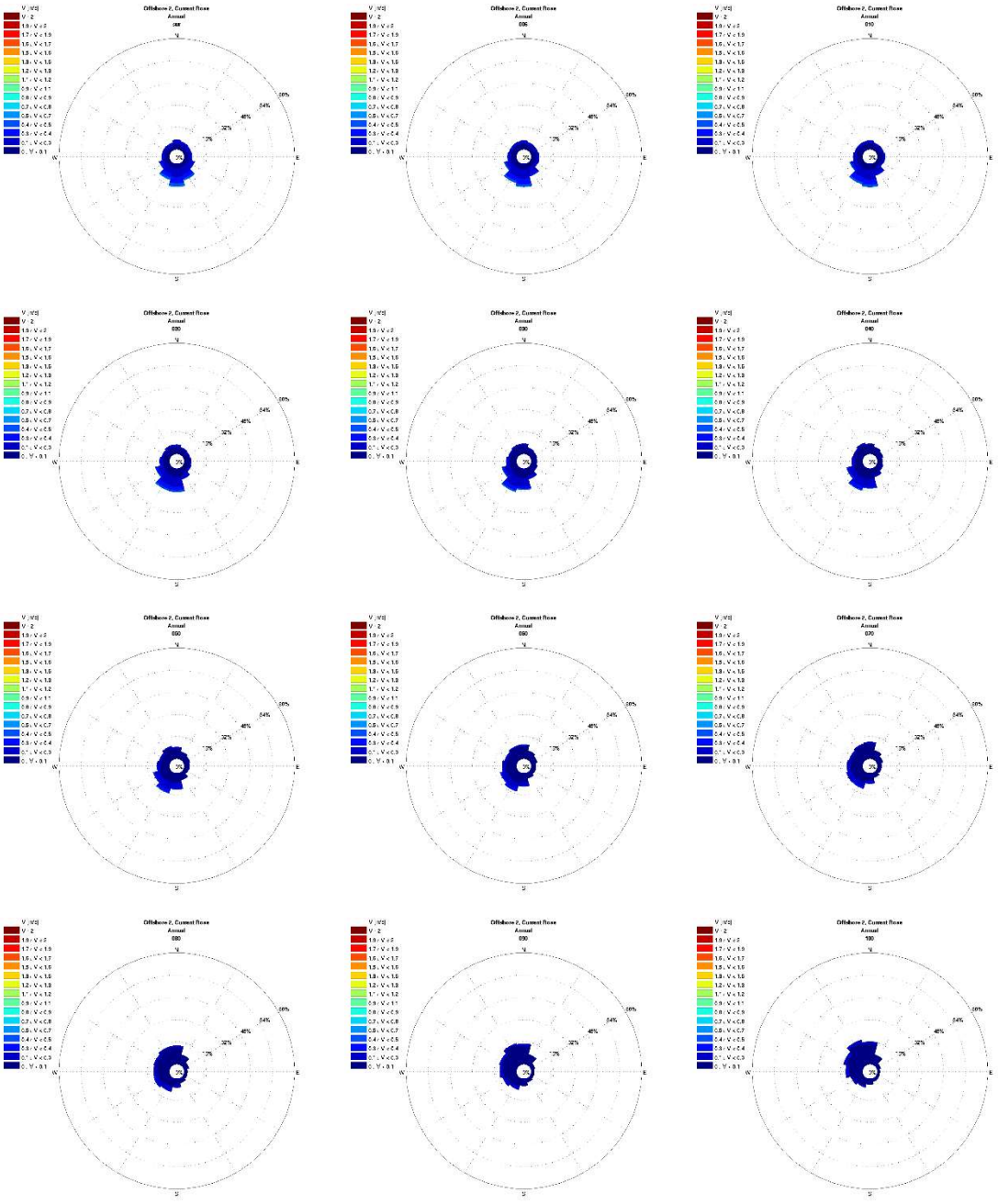

Figure 2.36: Current Rose along the Vertical Profile – Surface Layers– Offshore Section – Off2

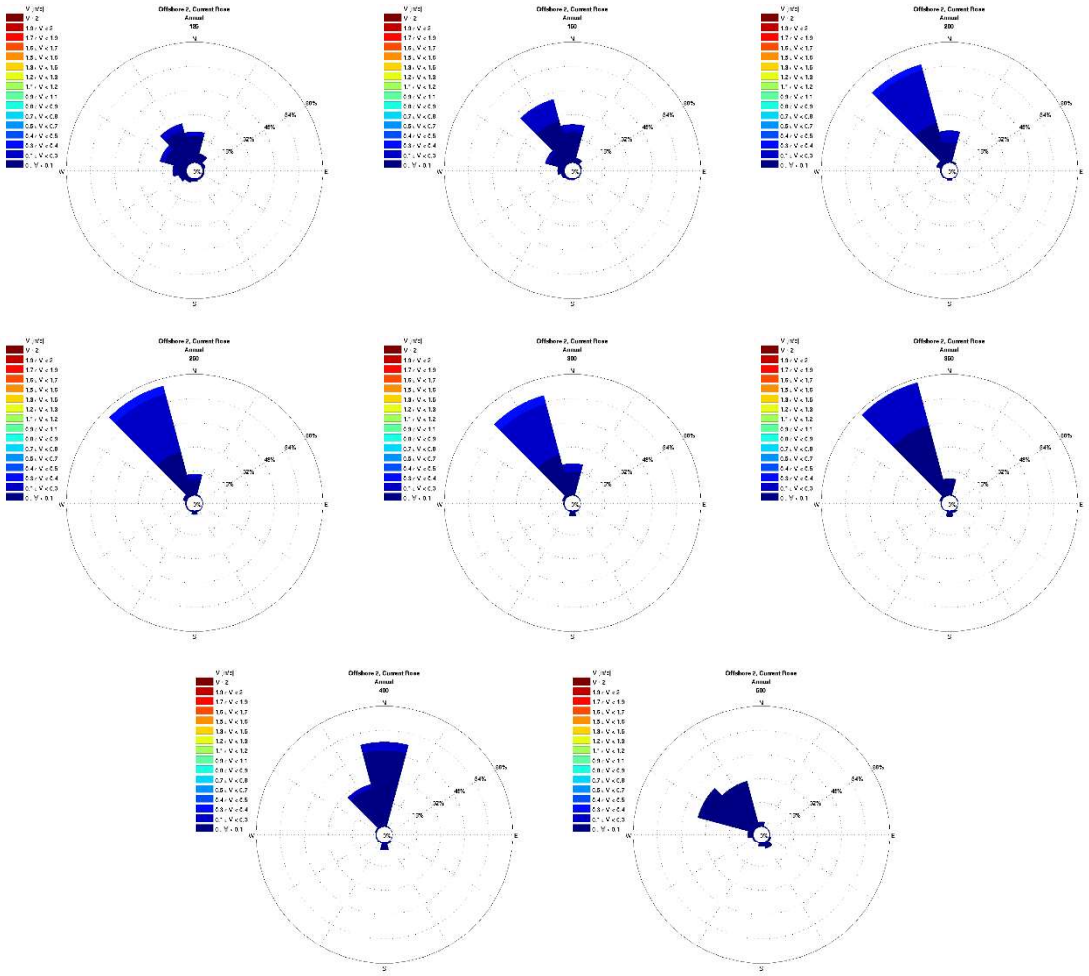

Figure 2.37: Current Rose along the Vertical Profile – Deep Layers– Offshore Section – Off2

2.2.4.2 Extreme Values

The extreme omnidirectional and directional values of surface total current, reported in Table 2., have been assessed using the Weibull distribution function (Figure 2.38) applied to the surface current regime shown in 2.2.4.1.

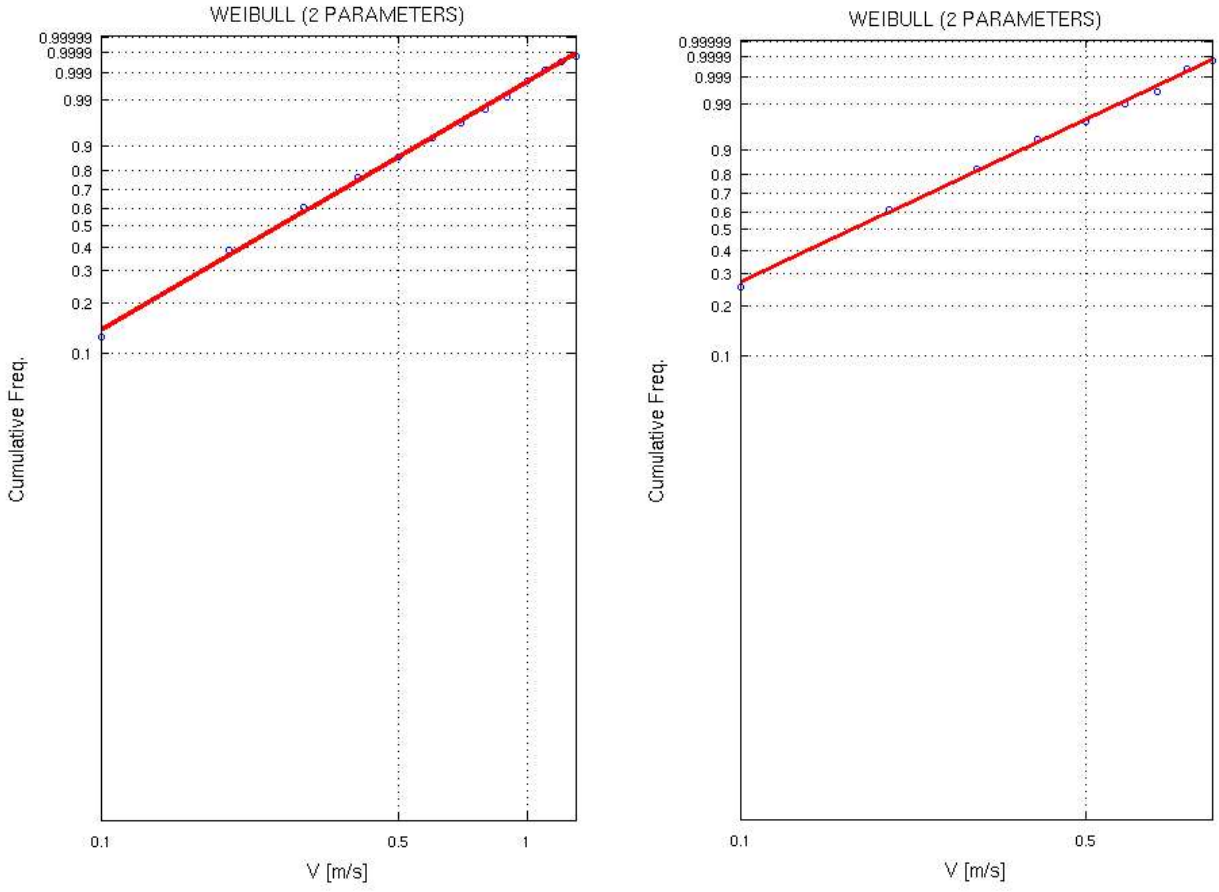

Figure 2.38: Omnidirectional Current Fitting Distribution – Offshore Section (left panel = Off_1, right panel = Off_2)

Table 2.18: Extreme Values of Surface Total Current – Offshore Section

Off1	Return Period (year)			
	1	10	50	100
Dir (°N)	V (m/s)	V (m/s)	V (m/s)	V (m/s)
OMNI	1.0	1.2	1.4	1.4
0	0.3	0.5	0.6	0.6
30	0.4	0.5	0.5	0.6
60	0.3	0.5	0.5	0.6
90	1.0	1.2	1.4	1.4
120	0.4	0.7	1.0	1.1
150	0.9	1.2	1.3	1.4
180	1.0	1.2	1.3	1.4
210	0.6	0.8	0.9	1.0
240	0.3	0.5	0.6	0.6
270	0.2	0.4	0.6	0.6
300	0.2	0.5	0.8	0.9
330	0.2	0.4	0.5	0.6

Table 2.19: Extreme Values of Surface Total Current – Offshore Section

Off2	Return Period (year)			
	1	10	50	100
Dir (°N)	V (m/s)	V (m/s)	V (m/s)	V (m/s)
OMNI	0.7	0.9	1.0	1.0
0	0.2	0.5	0.8	0.9
30	0.3	0.4	0.5	0.5
60	0.3	0.4	0.5	0.5
90	0.3	0.4	0.5	0.5
120	0.4	0.5	0.6	0.6
150	0.6	0.8	0.9	0.9
180	0.7	0.8	1.0	1.0
210	0.6	0.8	0.9	1.0
240	0.5	0.6	0.7	0.8
270	0.3	0.5	0.6	0.6
300	0.7	0.9	1.0	1.0
330	0.2	0.5	0.8	0.9

2.2.5 Physical Parameters

In this section, sea water parameters are reported as monthly vertical profile of temperature and salinity.

2.2.5.1 Temperature Profiles

The monthly average depth profile of temperature is reported in graphical form in Figure 2.39 for Point Off_1 and in Figure 2.40 for Point Off_2. From temperature profile of Point Off_1 and Off_2 it can be noted that the temperature is nearly constant along the water profile except from June to October when the summer stable thermocline forms and interests the first about 50 m of surface water column, with a maximum ΔT of about 10°C between surface and deep water.

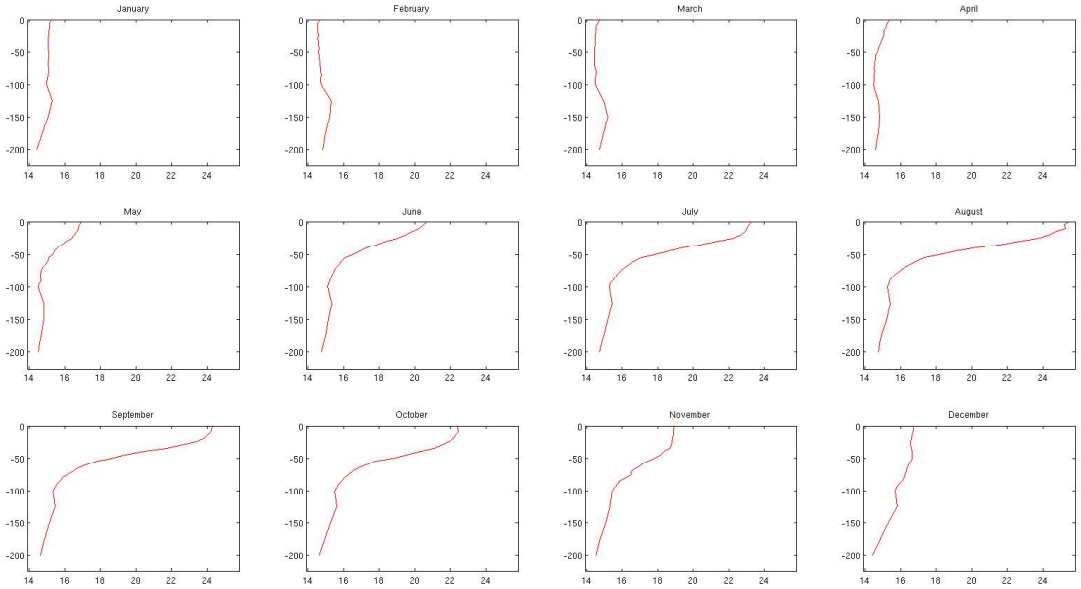

Figure 2.39: Average Monthly Water Temperature Profile – Offshore Section _ Point Off1

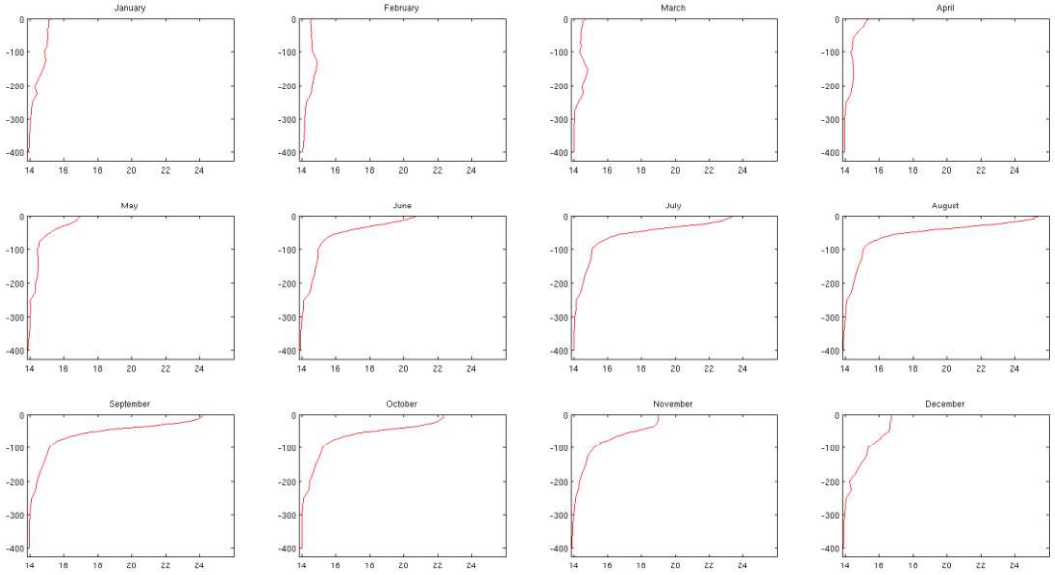

Figure 2.40: Average Monthly Water Temperature Profile – Offshore Section _ Point Off2

2.2.5.2 Salinity Profiles

The monthly average depth profile of salinity is reported in graphical form in Figure 2.41 (Off_1) and Figure 3.63 (Off_2).

From salinity profile of Point Off_1 and Off_2 it can be noted that the salinity increases with the water depth, from November to June. During Summer months due the evaporation of surface waters it can be noted the creation of relatively more saline water in the higher water profile. From Figure 2.42:(Point Off_2) it can be noted the presence of the LIW, characterized by constant water salinity from about 200 m of water depth to

the sea floor. From current profile of Figure 2.35, the NW LIW current can be recognized about from 125 m to the sea bottom. The salinity profile shows from 100 to 200 m of W.D. a sharp variation of salinity, of about 1.5 PSU, where mixing process between superficial and deep waters occurs.

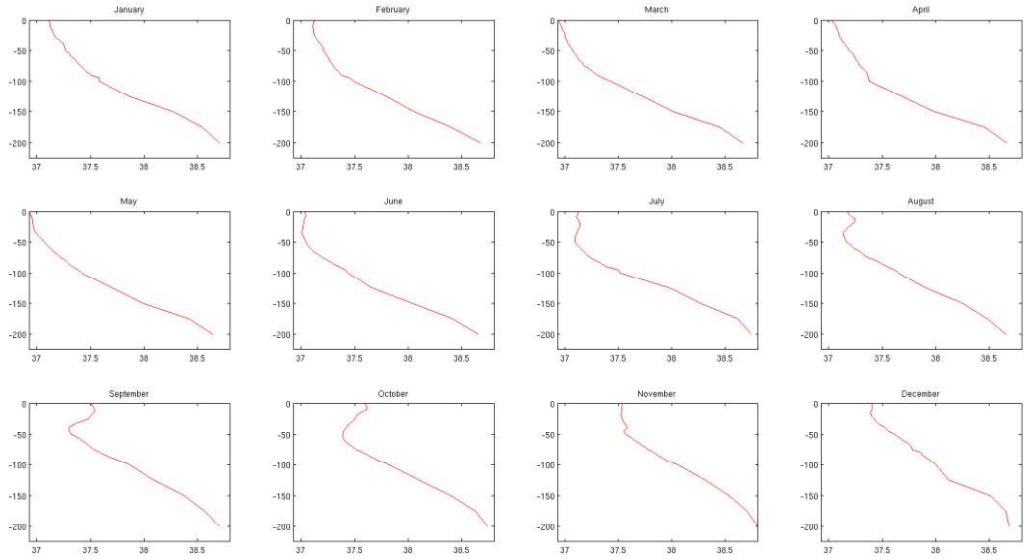

Figure 2.41: Average Monthly Water Salinity Profile – Offshore Section _ Point Off1

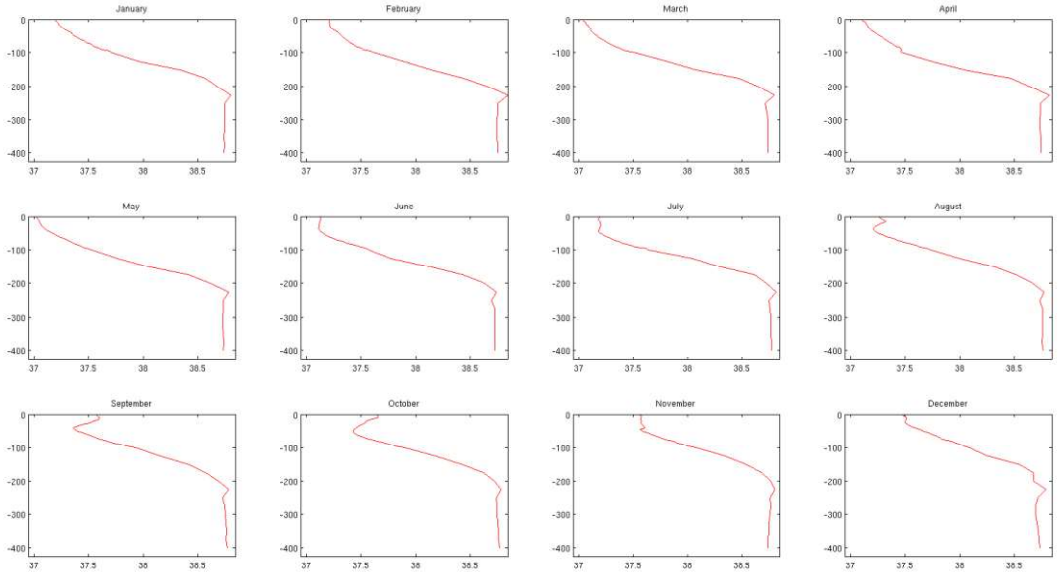

Figure 2.42: Average Monthly Water Salinity Profile – Offshore Section _ Point Off2

3. SEABED GEOLOGY AND GEOMORPHOLOGY

The content of this chapter derives from the study "RVFR18400A00012, revision 05, 29/09/2021, Marine Feasibility Studies for Tunisia-Italy Power Interconnector" by Rina-Comete.

3.1 Bathymetry

The following figure shows the bathymetrical profile along the power cable route from Italy (left side) to Tunisia (right side).
The maximum water depth is around 800 meters.

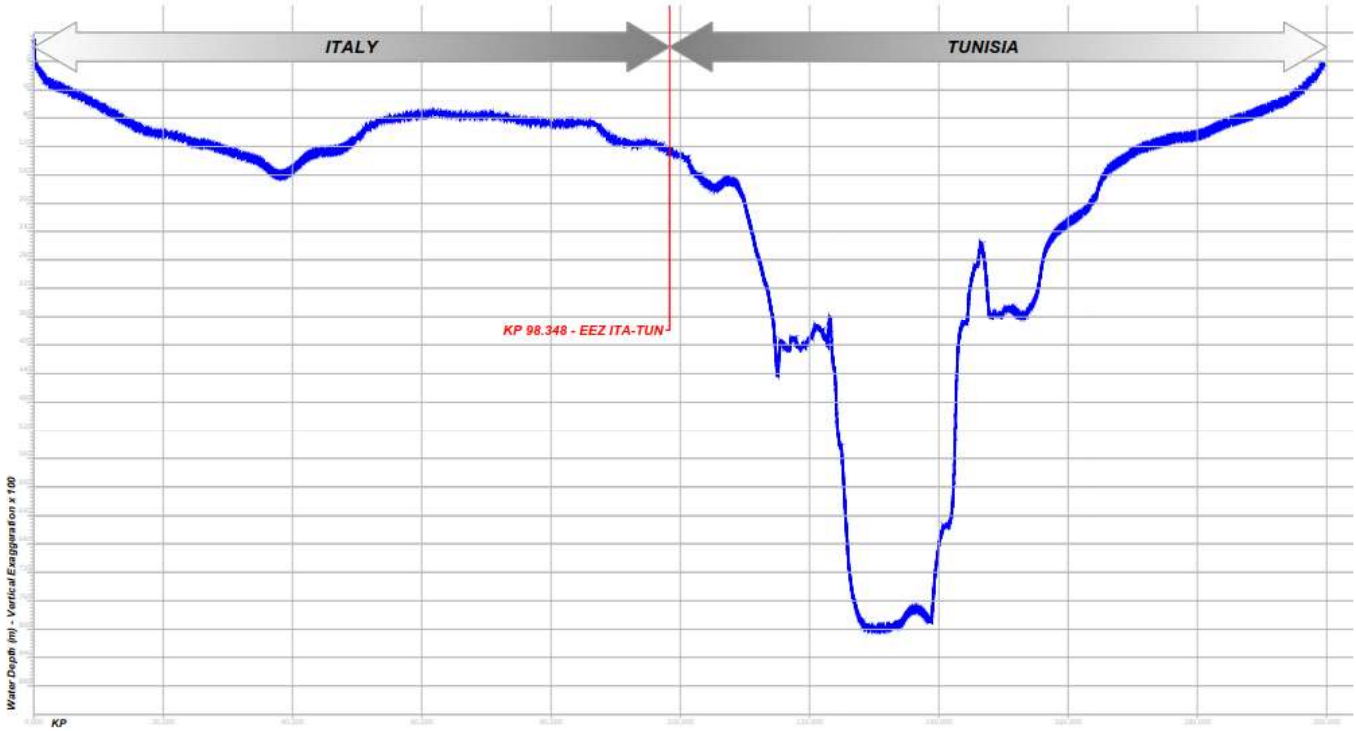

Figure 3.1: Bathymetry along the power cable route

3.2 Overview - main geological features and geohazard

The present section describes the geological features, including seabed morphology and lithology, seismic properties, volcanism, geodynamics and related geohazard.

The topics covered will be treated separately for the nearshore and for the offshore section of the cable route.

3.3 Tunisian nearshore section

3.3.1 Seabed morphology and lithology

Based on available large-scale bathymetry data the slope morphology close to the Tunisian landfall shows no particular deviation from a gently dipping gradient of less than 1°. Occasional rise can be found at depth greater than -50m WD but none that exceeds 10m in height. The homogeneous slope geometry can be described by the absence of dramatic morphological change, as well as the absence of topography in the immediate proximity of the landfall.

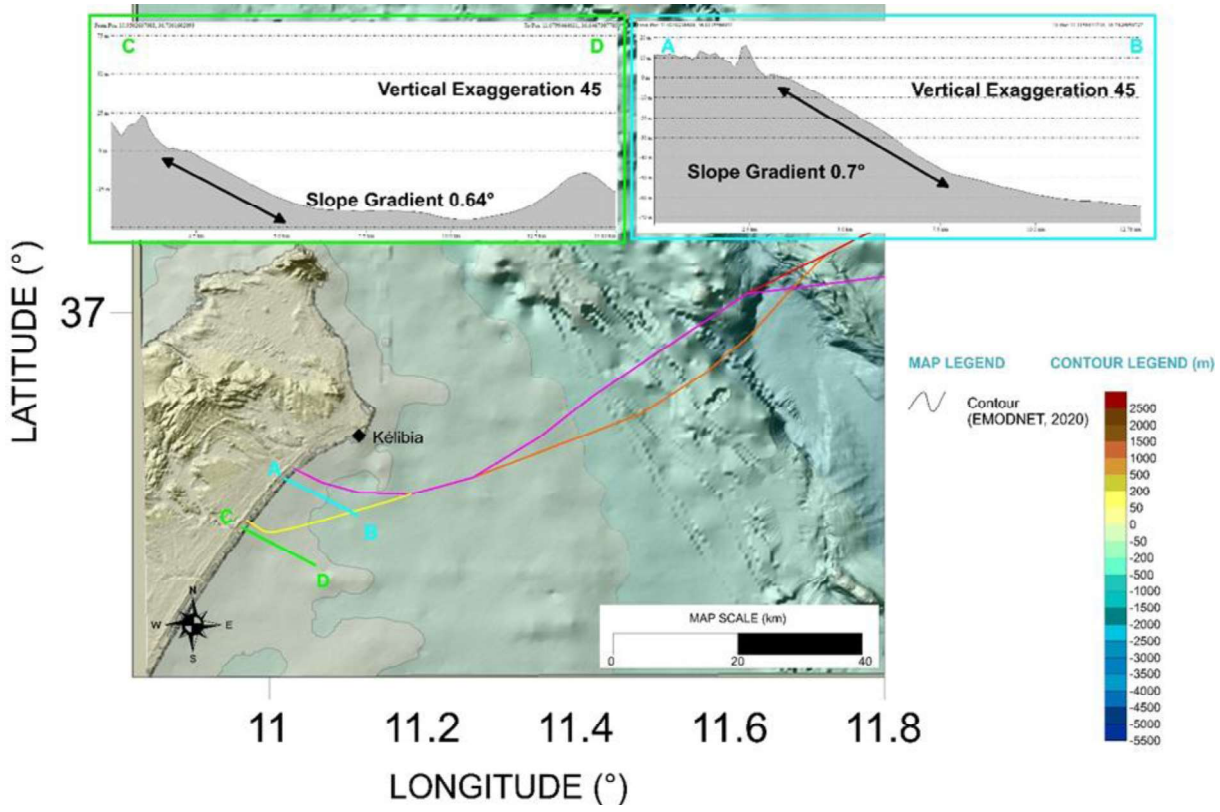

Figure 3.2: Tunisian landfall bathy-morphological setting

Water depth of about -40m is at about 5km offshore; in this section seabed gradient is of about 0.7°. From that depth downwards, the gradient further decreases, reaching -100m WD at 25km off the coastline.

3.3.2 Seismic Setting

3.3.2.1 General

The Northeastern Tunisia has been affected by moderate earthquakes throughout history, most of which occurred in the tectonically active area of Southern and Northern Atlas. Also, the Sicilian prosecution of the Maghrebides displays other faults capable of severe earthquakes that can be perceived across the Sicilian strait and in Tunisia.

3.3.2.2 Local Seismicity and Earthquake Catalogue

Figure 3.3 presents the Earthquake Catalogue from the International Seismological Centre (ISC, 2020[1]). The catalogue has been downloaded for a window of Latitude 34° to 39°N and Longitude 8° to 14°E and contains all recorded events from 1905 to June 2020 including aftershocks and foreshocks. The catalogue comprises events with magnitude larger than 3 and relies on data contributed by seismological agencies from around the world. Overall, the area of Tunisia landfall is characterized by moderate seismicity with magnitude below 4. Largest events with magnitude up to 5 are located more than 50 km apart from Tunisia landfall (Figure 3.3).

[1] http://www.isc.ac.uk/

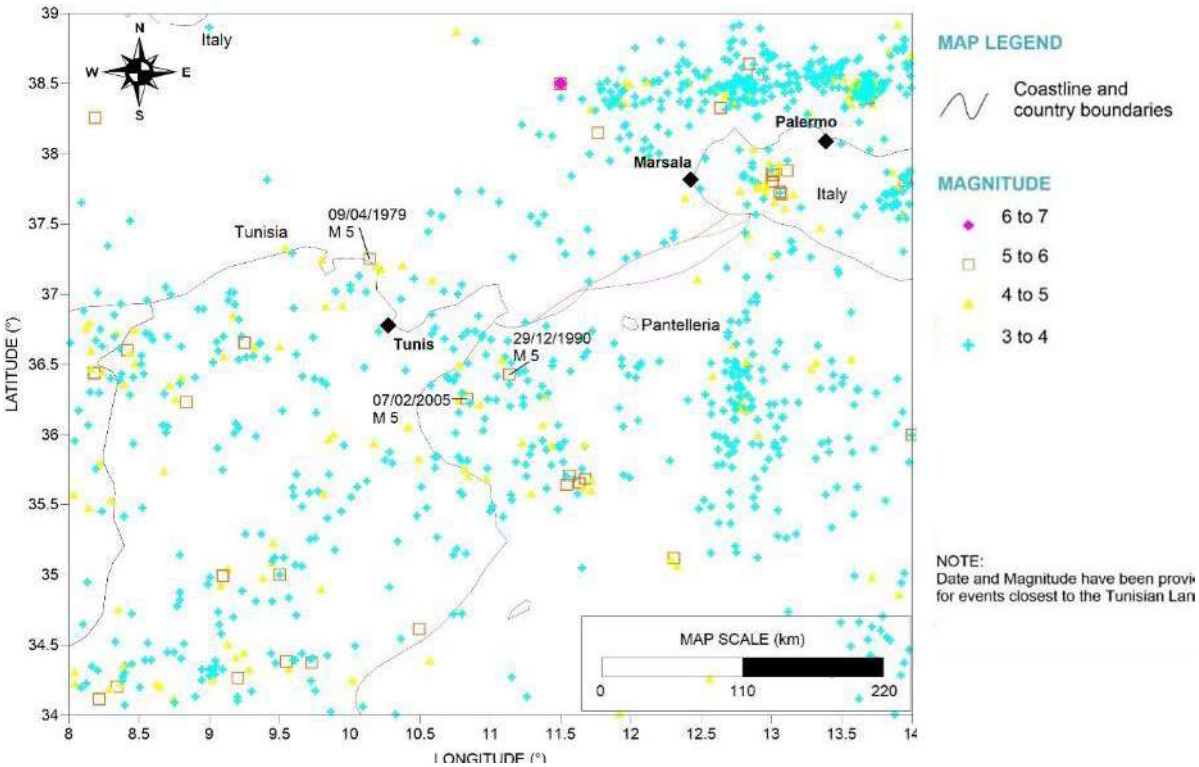

Figure 3.3: Seismicity in the Study Area (events from (ISC 2020)

3.3.2.3 Peak Ground Acceleration (PGA)

Table 3.1 lists the results obtained from several studies and codes performed in the study area aimed to give the general pictures of seismic regime in the area.

Table 3.1: PGA Value from Different Studies

Reference	Site Conditions	Return Period (yr)	PGA (g)	Description
ISO 19901-2 (ISC 2020)	Site class A/B Hard rock/rock ($V_{S,30}$>750 m/s)	1000	0.1 g	The code defines seismic design criteria for fixed offshore structures. PGA values is computed dividing the value at 5 Hz by a factor of 2.5 as per ISO standard shape spectrum.
GSHAP (Giardini et al., 2015)	Rock ($V_{S,30}$>800 m/s)	475	0.16	The GSHAP-Global Seismic Hazard Assessment Program gives worldwide coverage of PGA values for onshore locations. This source provides a good general indication of seismic hazard but can be inaccurate in areas with a complex seismotectonic regime (e.g. local faults).
3GEM (Fetheddine et al., 2012)	Rock ($V_{S,30}$ =760-800 m/s)	475	0.08-0.13	The Global Earthquake Model (GEM) Global Seismic Hazard Map (version 2018.1) depicts the geographic distribution of the PGA with a 10% probability of being exceeded in 50 years.
ESC-SESAME (International standard 2017)	Stiff Soil	475	0.08 – 0.16	The ESC-SESAME is the first unified model for PSHA for Europe and the Mediterranean (2001 and 2003). It was developed within the framework of several recent projects on global and regional seismic hazard assessment and allows for homogeneous hazard computation throughout the whole European- Mediterranean domain.

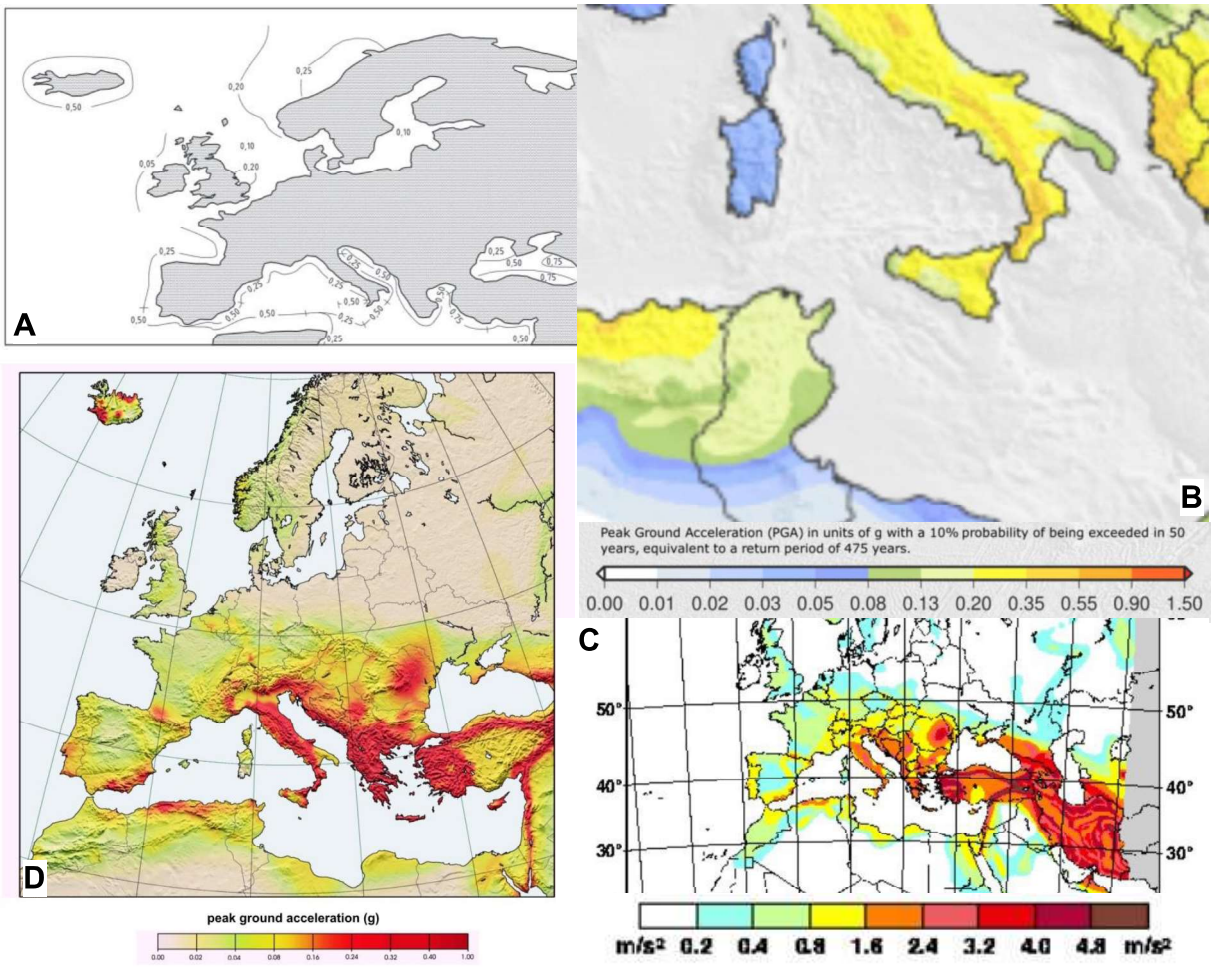

Figure 3.4: PGA Values at Tunisia landfall location; A: PGA Value 5 % damped spectral response accelerations for offshore Europe, ISO (ISC, 2020); B: PGA values according to GEM (Fetheddine et al., 2012); C: PGA values according to GSHAP (Giardini et al., 2015); D: PGA values according to SESAME (International standard 2017)

The different studies agree to a moderate value of PGA between 0.08 g and 0.16 g for 475 years return period and for rock condition at Tunisia landfall.

3.3.3 Geological Framework and regional faults

3.3.3.1 General

The study area is located on the eastern peninsula of Gulf of Tunis, north-eastern Africa, 10 km south of Kelibia city (Figure 3.5).

The area of Cap Bon and the Gulf of Tunis constitutes the extension of the Tunisian Atlas to the south and the Tell-system to the north and corresponds to a relay-zone with the Siculo-Tunisian strait and it marks the continuation of the tectonic and sedimentary structures recognized at the Cap Bon Peninsula, Tunis, Kechabta, Ghar El Melh, El Alia and Bizerte areas.

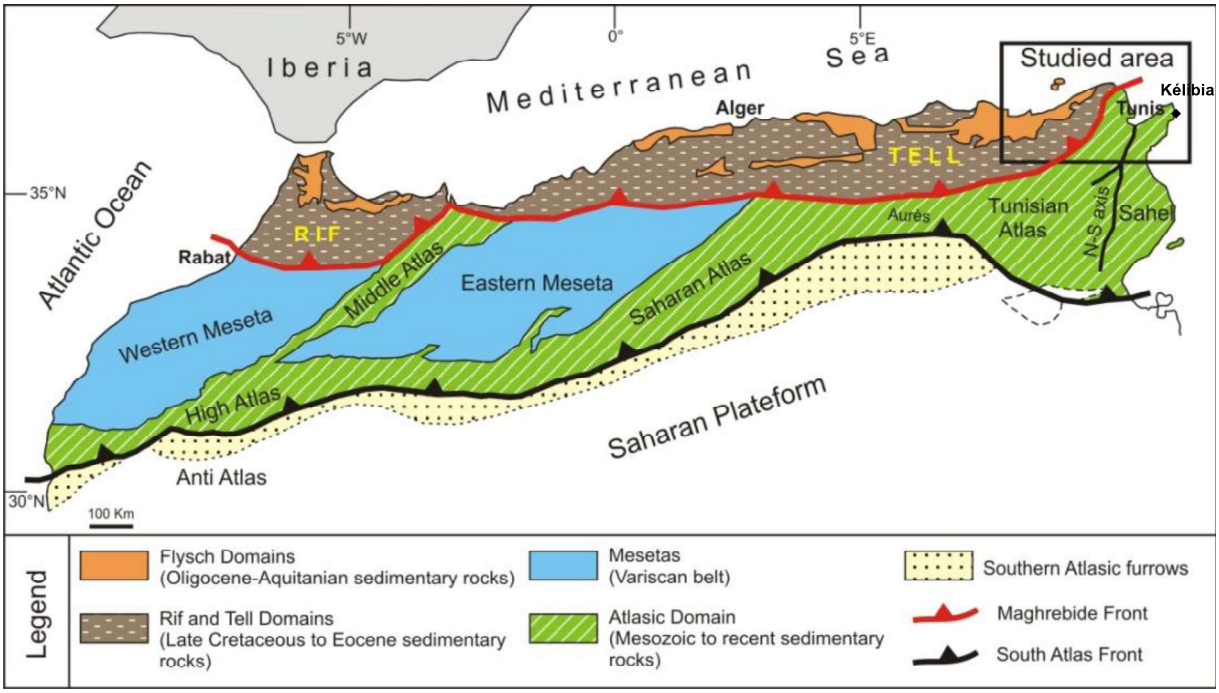

Figure 3.5: Geological sketch of the Maghreb (Ferranti et al., 2019)- RIF and TELL are geographical names of those tracts of the Atlas mountains

3.3.3.2 Geodynamic Evolution

The geodynamic evolution of the Mediterranean basins has been considered related to Africa and Europe motions and a consequence of different spreading rates along the Atlantic oceanic ridge.
Since the Late Triassic to Present, the North African domain has undergone episodes of deformation that can be correlated to plate kinematics. The Cap Bon area shows paleogeographic continuity of the known onshore sedimentary deposits and records the tectonic movements, as well as the regional sedimentary events. These tectonic and sedimentary events follow the major orogenic phases, which resulted from convergence movements between the African and Eurasiatic plates.

During the Triassic, this margin was guided by rejuvenation of the Hercynian. From the Jurassic and especially during the Early Cretaceous, an extensional event has controlled the Gulf of Tunis. Sedimentary units of deposits are marked by seismic reflections of progradational oblique configurations at the base and aggradational-retrogradational onlaps towards their tops. The N-S to NW-SE extension of the Tunisian margin caused the formation of a subsiding basin. This extensive period regionally identified through the Tunisian Atlas was accompanied by the intensive halokinetic and magmatic activities.

Since the ending of Cretaceous (Late Maastrichtian) and until the Middle-Upper Eocene, the NE-SW ancient accidents have still controlled the sedimentation in a compressional context. This compressive stress has generated the reverse movements along the NE-SW ancient lineaments that delineated deformed sub-basins with major gaps and unconformities. Tilting of the sedimentary floor long the faulted zone is marked by the avalanche breccias in Late Eocene times.

The Oligocene series are only identified near the Cap Bon peninsula, confirming the extension of the NE-SW high zone, developed during the Oligocene, in the Gulf of Tunis. This ‘‘Bald’’ zone coincides, geographically, with the domes and diapirs zones in the Tunisian Atlas (Riahi et al., 2015).

The generalized marine invasion of Middle Miocene in Mediterranean Basin is fossilized by onlapping of the Langhian limestones (Ain Grab formation). This transgression was also described in the Cap Bon peninsula and in the Gulf of Hammamet.

The NE-SW extensional processes that affected the Gulf of Tunis during the Oligocene–Early Miocene is represented by major normal faults that bordered the tilted blocks, and by transverse structures. Seismic profiles available in literature (Jimenez et al., 2001) show a complex system characterized by a clearly asymmetric structure, with a successive polarity west-dipping half-graben.

The Middle to Late Miocene is represented by thick lagunal facies deposited in isolated and sometimes deltaic basins. The lack of the Messinian deposits on the uplifted areas is due to a combination of vertical movement of border faults and a regional eustatic sea-level fall along the Mediterranean Basin.

The contemporaneous activity of normal and reverse faults with the thrust system suggests that the Siculo–Tunisian Strait may be being shaped by the occurrence of two independent tectonic processes that act simultaneously and overlap each other: the Maghrebides–Apennines accretionary prism and the Siculo–Tunisian Channel rift. In addition, progressive migration of the subduction blockage from west to east has involved a structural zone represented by the graben structures. This domain of the atlaso-pelagian trough corresponds to a thinned continental crust at the level of the Siculo-Tunisian strait and forming the Pantelleria–Linosa recent rift. Analysis of literature seismic lines shows asymmetric halfgraben structures during the Early Pliocene, indicating the extensional event. Deposits are considerably thick towards the subsiding edges and missed on the high folded structure. Extension is more pronounced with an increase in subsidence and vertical throw of major graben-bounding faults proceeding southeastward. The Upper Pliocene strata overlie the other Lower Pliocene by aggradational and retrogradational deposits, showing the NW-SE reverse displacement. Inversion of the subsidence at the Late Miocene and the end of Early Pliocene periods is probably related to rejuvenation of the NE-SW and NW-SE faults.

3.3.3.3 Structural elements

The geodynamic evolution in northern Tunisia and in the Siculo-Tunisian strait indicate the importance effect of the NE-SW, and NW-SE faults on the control of sedimentation during the Tethyan rifting and on the structuring of the central and northern Atlas domains during the Pyrenean and Alpine/Atlasic polyphasage. Extensive and compressional regime occurred through time with rejuvenation of the main systems resulting in NE-SW trending folds and NW-SE faults.

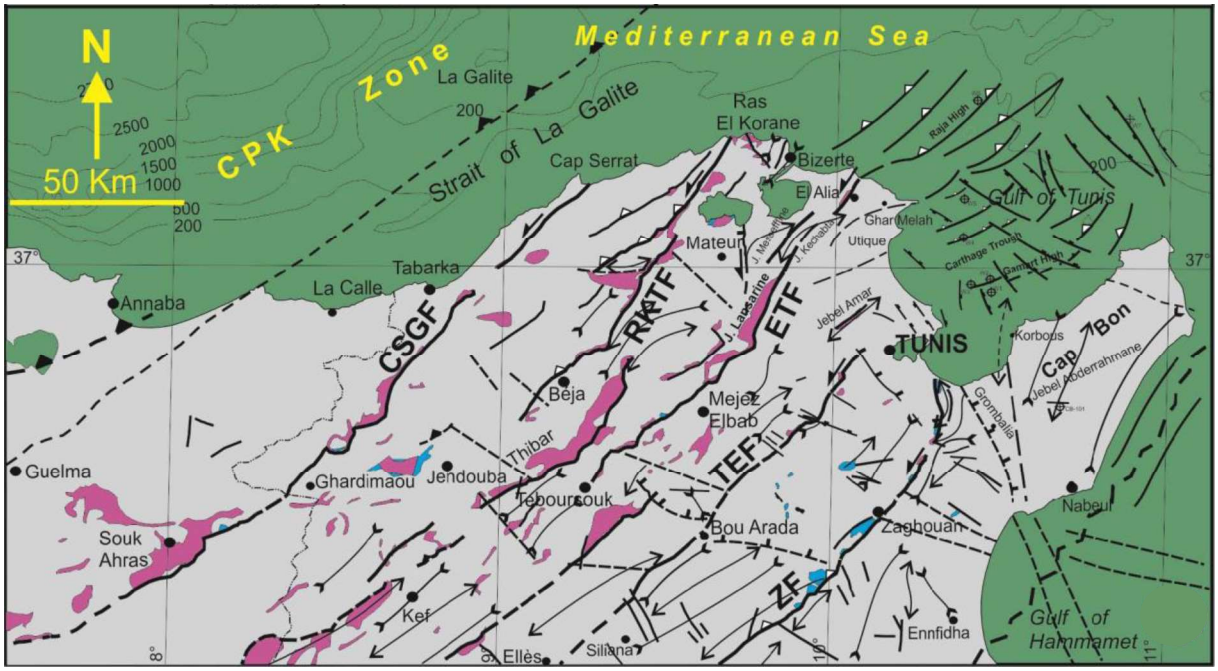

Figure 3.6: Atlasic and Alpine Domains of Tunisia and Main Structural Elements (Ferranti et al., 2019)

3.3.3.4 NE-SW Features

Northeast-southwest trending folds, generally bounded by the steep reverse faults, and associated with deep asymmetric geometries, that are organized into depressions and uplifts, characterize the area of Gulf of Tunis and Cap Born Peninsula to the north. The main element is the NE-SW El Alia-Teboursouk (ETF in Figure 3.6) system fault corridor that played an important control on the Mesozoic and Cenozoic paleogeographic evolution. Separation of the western subsiding block (Raja domain) from the other eastern block at the level of the El Alia-Teboursouk fault, suggests its major effects during the different Mesozoic and Cenozoic periods. These results let us to consider El Alia-Teboursouk system fault as a deep basement fault.

3.3.3.5 NW-SE Features

The fault pattern in the southern section of Cap Bon and of Gulf of Tunis exhibits an extensional character. Dip slip of faults trending NW–SE often display a listric geometry, and form synclines and half-grabens structures with synthetical/ antithetical tilted hanging wall blocks. The densest tectonic setting is exposed along the Gulf of Tunis belts that are marked by isolated and discontinuous ridges. The dip slip faults provide the margins of deep grabens with tilted horst blocks. Along the master faults of the grabens, the vertical offset increases, approaching the major escarpments at the border of the uplifted structures. In the offshore of the Gulf of Tunis, the movements of basement-related faults have caused halokinesis movements during the distinct phases of Jurassic extension since salt structures are always associated with faults at depth. Ascension of the Triassic salt facies continued during the Mesozoic and Cenozoic tectonic events. These diapir structures occupy the faulted/folded border of basins and participate in the structuring changes and therefore in the geodynamic evolution of the area as discussed in the previous section.

3.3.3.6 Sedimentary Distribution

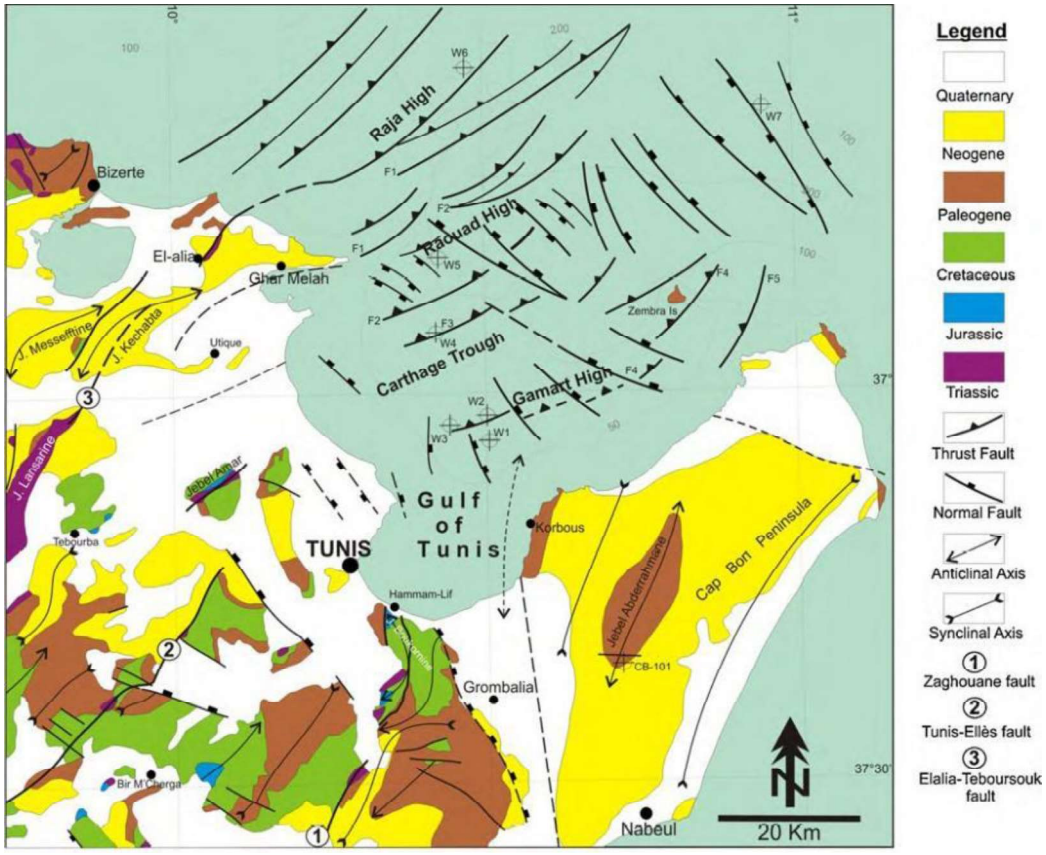

Figure 3.7: Geostructural map of NE Tunisia, from Ferranti et al., 2021.

Northeastern Tunisia displays a wide variety of geological units, Mesozoic to Cenozoic in time, deposited during various tectono-sedimentary settings from the Tethyan Rifting in the Early Mesozoic (Lower Jurassic to Early Cretaceous), Asturian and Pyrenean phases (Upper Cretaceous to Oligocene), to Atlasic phase from Miocene to actual times (Figure 3.7). Synthetic column of Geological Series of northern Tunisia is shown in Figure 3.8.

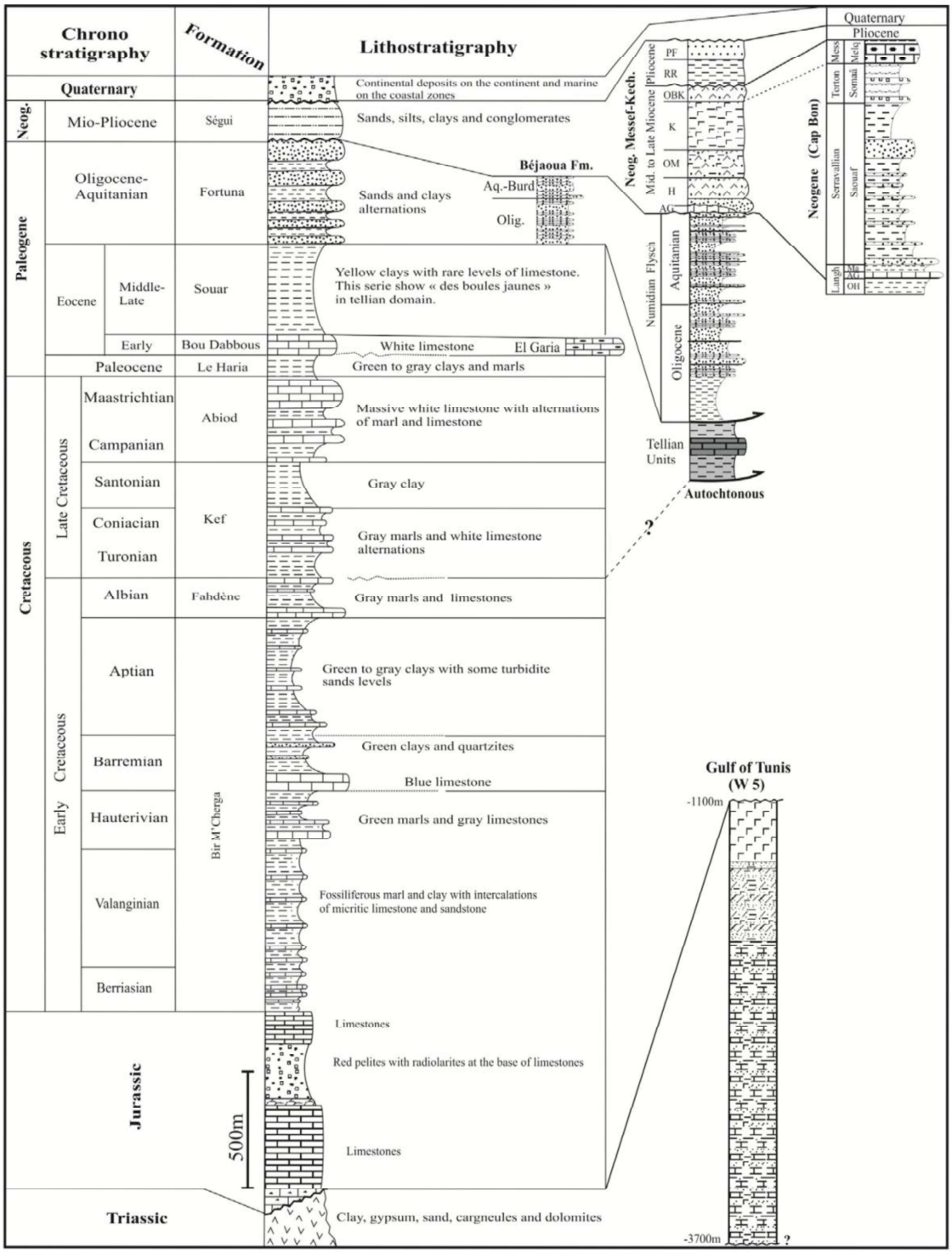

Figure 3.8: Synthetic column of Geological Series of northern Tunisia, (Ferranti et al., 2019) (AG- Ain Ghrab fm; H- Hakima fm; OM- Oued Melah fm; K- Kechabta fm; OBK- Oued Bel Khedim fm; RR- Raf-Raf fm; PF- Porto-Farina fm; OH- Oued El Hammam fm; Ma: Mahmoud fm)

A description of the main sedimentary facies, from bottom (older) to top (younger), follows.

Triassic: Triassic facies is always identified with abnormal stratigraphic position in a zone that corresponds

to the eastern extension in offshore to the domes and diapirs zones of the northern Tunisia Atlas. The facies are essentially formed by carbonates, clays, sandstones and sometimes by anhydrites.

Jurassic: The deposits remain unknown in the Gulf of Tunis because there is no well crossing these series. It largely outcrops in the Dorsale mountain range, in the northern Atlas. Jurassic sequence thickness is about 700m in the northern Tunisian trough and in the Cap Bon peninsula. The base of the Jurassic limestones and marls deposits overlays the Triassic carbonates by a downlap prograding deposits on the flanks of highs. Above, the Middle and Upper Jurassic are formed by the aggradational-retrogradational onlaps on the underlying sequence and associated with angular unconformities toward the uplifted areas.

Cretaceous: It is composed by clays, marls, limestones with some layers of sands, separated from underlying deposits by Upper Jurassic unconformity, a distinct surface characterized by a subtle toplap/onlap patterns. Interpreted seismic profiles on the slope zone in the Gulf of Tunis, show prevailing progradational oblique configurations of seismic reflectors confirming a sedimentary distribution under the effects of the master boundary faults.

Paleocene – Eocene: The sedimentary series of this epochs are formed by three different lithologic formations; at the base, the El Haria formation (Late Maastrichtian–Paleocene) is composed by marls and clays. The second Boudabous formation (Ypresian–Early Lutetian) is formed by Nummulitic limestone with some argillaceous rate. The last, on top, Souar formation (Lutetian–Priabonian) is composed essentially by clays (Ferranti et al., 2019; Khomsi et al., 2009). Thickness of these formations varies from 434m, to 307m. In the Cap Bon outcrops, the Souar formation reaches 800m of thickness.

Oligocene – Miocene: This series is represented by clay with silt and sand alternations. The upper unit of the Fortuna formation (Late Oligocene–Aquitanian) is completely missed in all the Gulf of Tunis. Towards the east, in the Cap Bon, the Fortuna formation outcrops with a thickness of 800m. Seismic sections show important hiatuses, essentially, on the top of paleohighs. These series are, overall, deposited on the Gamart Ypresian large carbonate platform (Boudabous formation), which are partially eroded. The Middle Miocene starts by the lumachellic calcareous bar of the Ain Grab formation (Langhian) and marks the beginning of the Middle Miocene transgression, identified regionally in all Tunisia. The Middle to Late Miocene series identified in the Gulf of Tunis are represented by the Saouaf (Serravallian–Tortonian–Messinian) and the Oued Bel Khedim (Messinian) formations that show a great variation of facies in the Gulf of Tunis area. These formations are composed by clays and silts and occasionally by sandy limestone at the base and by marls and salts at the top. At the top, this super-sequence is bounded by a toplap structures and is overlain by a double seismic reflector corresponding to the Upper Miocene gypsum.

Pliocene: In the Gulf of Tunis, the Pliocene deposits that make up the top-most Neogene interval are capped by the major Villafranchian unconformity. The deposits show a huge thickness represented by clays, sands, and sandstones. The horizons at the base of sequences are interpreted as representing the conformable portion of unconformities that should be developed farther up dip in the basins and on the uplifts. The deposits, which are recorded towards the faulted uplifts, are associated with Middle Pliocene unconformity. These variations are controlled by simultaneous movements of the basement caused by the transpressional strain and salt tectonics.

Quaternary and Recent Sedimentation: The area of Tunisian landfall on the eastern side of Cape Bon had been thoroughly described as mainly comprising quaternary deposits as its uppermost unit. These deposits are represented by sands with variable degree of compaction, from aeolian dune fields, to alluvium, to cemented calcareous sands. The low energy environment favors the development of sand sheets and levees around topography, as well as coastal lagoons and saltmarsh ponds. Therefore, although the main soil component remains quaternary sands, finer sediments can be locally present or interbedded in the uppermost part of the stratigraphy.

3.3.4 Submarine volcanism

For Tunisian nearshore area literature doesn't stress any volcanic structure and activity.

3.3.5 Coastal erosion

Regarding the Tunisian landfall area, the site visits outcomes underline distinct features associate with low energy, stable shoreline such as lagoons and mouth bars. This, coupled with the extremely low elevation of the entire Kélibia coast, gives the entire area a low risk to any form of slides, topping and collapsing in project area.

Figure 3.9: The long beach on the East side of Cap Bon Peninsula. Note the well-structured back beach dune.

In the following figures the geomorphological description of the coast from Kelibia to Korba. Note the continuity of the beach width and of the back beach dune presence.

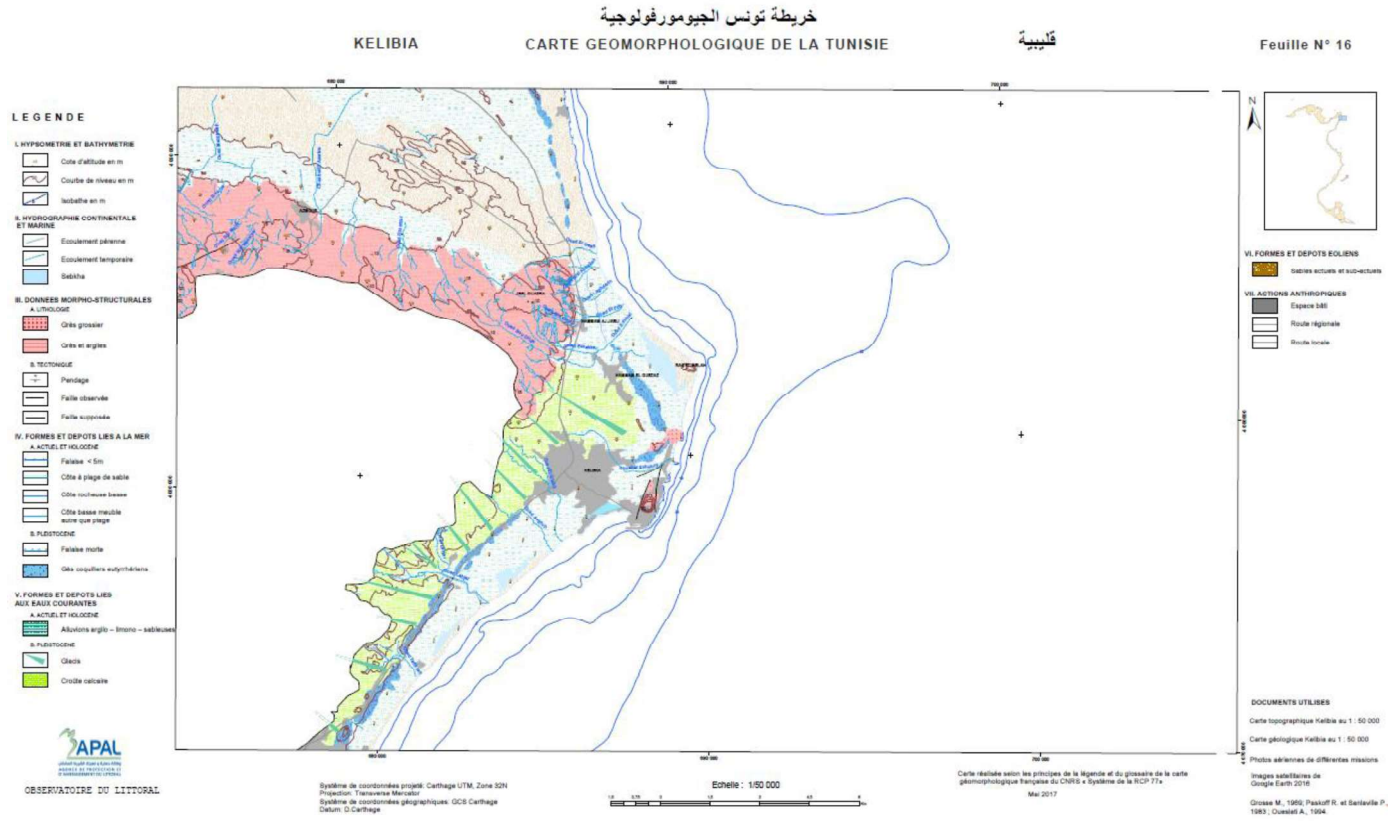

Figure 3.10: Geomorphological chart for the area of the Kelibia landfall[2]

In the figure below an extract from morpho dynamic assemblage chart[3] is shown. This is in line with APAL morpho-dynamic cartography, and also with site visit outcomes, showing that the sandy beach in the whole area is stable/very slightly regressing along the shoreline with the exception of Kelibia town southern area where erosion appear to be quite strong.

2 http://www.sigapal.tn/sigapal/images/docs/cartes/cartes_geomorph/Kelibia.pdf

3 http://www.sigapal.tn/sigapal/images/docs/CartesSyntheses/MorphodynMorcPDF/Morphodyn_assemblage_PE_Morc1b.pdf

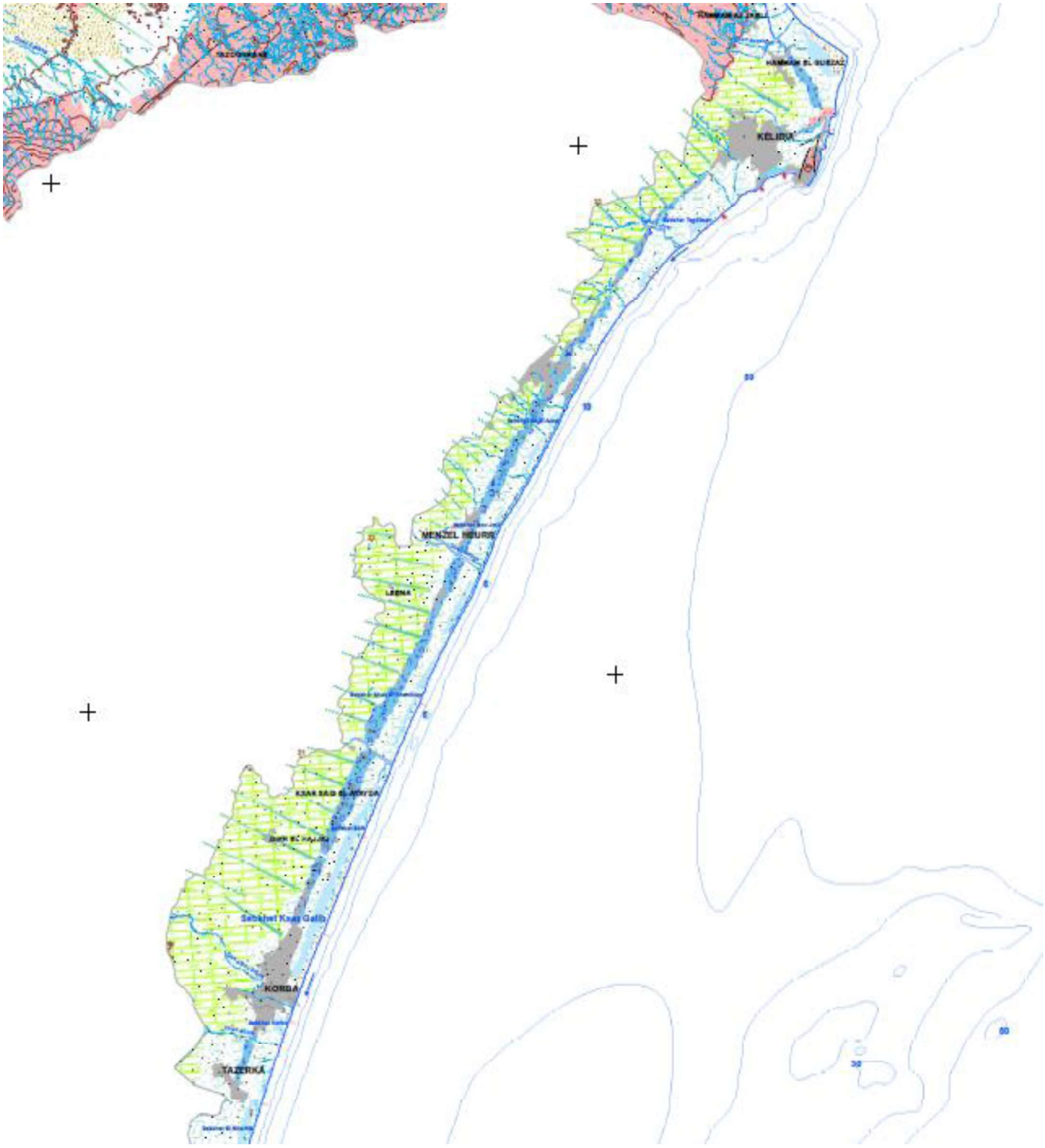

Figure 3.11: Extract of Morpho-dynamic chart of the Eastern Cap Bon Peninsula.

3.4 Offshore section

3.4.1 Overview

In this section, morpho bathymetry and general geohazard features are presented based on available large-scale bathymetry and literature review of proposed route.

The Sicily Channel is an extensional area active since the Late Miocene (i.e. the Sicily Channel Rift Zone; e.g. Reuther 1987; Corti et al. 2006). The rifting affected the pennine-Maghreb thrust belt and foreland, resulting in the formation of the Pantelleria, Malta and Linosa troughs (Colantoni 1975). Extensional processes generated normal faults, volcanic activity and major morphological structures. Volcanic activity is restricted largely to the vicinity of Pantelleria Island, Linosa Island and a series of submarine banks (e.g. Adventure Bank); for example, there are historical records of major eruptive events in 1831 (Ferdinandea Island) and 1891, 5 km northwest of Pantelleria Island (Washington 1909).

Although remaining constant, the seabed morphology along the proposed corridor from the landfalls of Marinella di Selinunte and Kélibia presents different morphological domains. After the initial gentle slope, the morphology of continental shelf maintains its almost flat gradient for more than 100km from Sicily and more than 45km from Tunisia. However, such gentle gradient becomes steeper in the Sicily Channel section of the corridor route, crossing the Channel proper, an abyssal region up to 40km wide, reaching more than 750m WD with slope gradient from 5° to 10° (Slope gradient from a large scale bathymetry dataset[4]) (Figure 3.12).

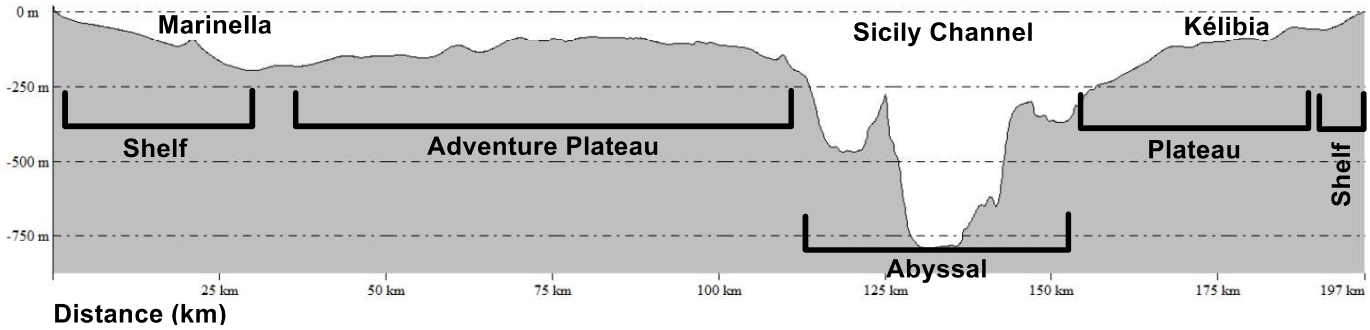

Figure 3.12: Bathymorphological sections from Sicily to Tunisia. Kartibubbo to Kélibia on top left; Marinella to Kélibia on bottom right.

Martorelli et al (2011) published a study related to presence of contourites (sedimentary deposits originated by the circulation of thermohaline oceanic currents of contour, named this way because they follow bathymetric curves) offshore of Pantelleria Island. conturites are deep sea deposits driven by deep currents. Being at the base of the continental slope, just where the current carries them, they erode on one side, forming moats, and deposit on the opposite side, forming drifts. There are also various types of drift, depending on how the current flows and how the sediment is deposited. The characteristic forms of conturites are the sediment waves, that is to say the undulations of the seabed, due both to the constant movement of conturites (and their relative current), and to the movement of the benthic organisms that continuously move the sediment. Conturites can be sandy or muddy; the former is the rarest, the latter are the most common.

[4] EMODnet Bathymetry Consortium, 2020, EMODnet Digital Bathymetry (DTM), https://portal.emodnet-bathymetry.eu/.

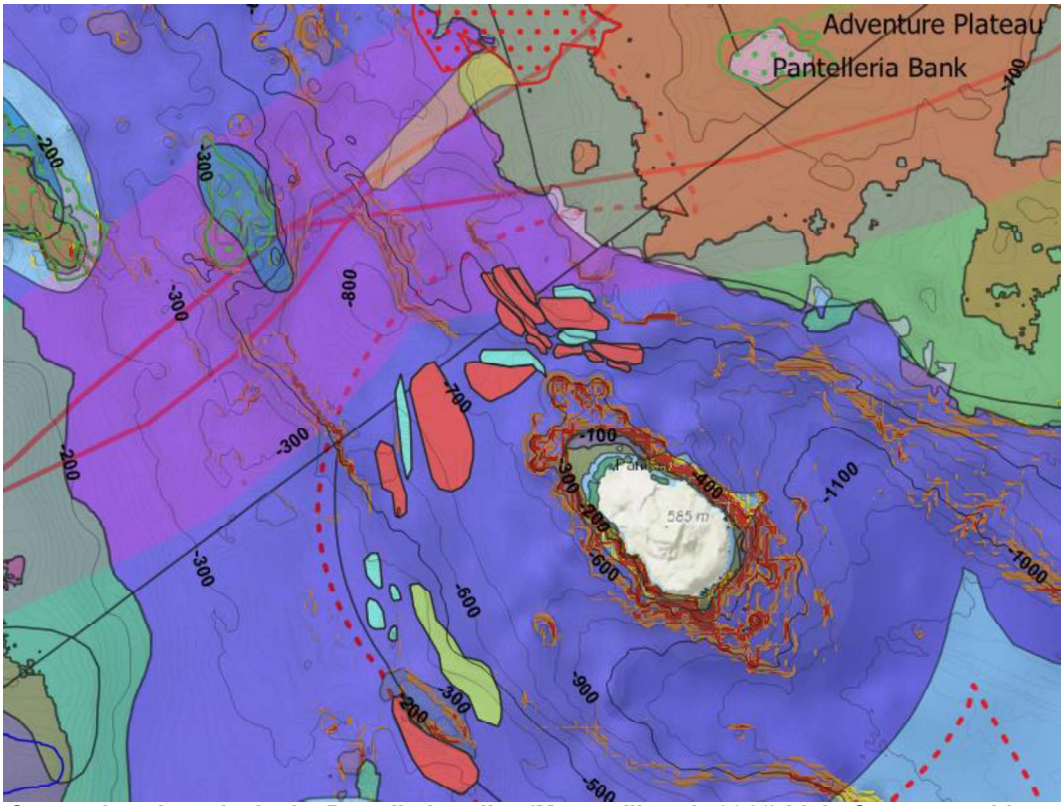

Figure 3.13: Contourites deposits in the Pantelleria valley (Martorelli et al., 2011) Light Green area: biogenic build-Up; Orange areas: Drift zones; Light Blue areas: erosion

The high slope margins of the Pantelleria valley are charachterized by both sedimentary and erosive formations, and biogenic build-ups colonized by deep-water corals (i.e. *Lophelia* and *Madrepora*). Although no live corals have yet been documented in the Pantelleria study area, the high abundance of identified biogenic buildups and their fresh morphological appearance suggest a recent origin.

The offshore route follows mostly flat sections of the seabed across Sicily Channel (i.e. Adventure Plateau); however, the channel proper section presents gradient up to 15° (based on large scale bathymetry); thus this sector can be prone to seabed instability and mass wasting processes, potentially triggered by seismic activity.

Literature review has not provided relevant information on such events or any other geohazard along the proposed corridor routes.

3.4.2 Offshore Marine Volcanism

The Sicilian Channel is a broad and shallow shelf which is geologically part of the African Plate. Its NW sector (the Adventure Plateau), where water depths rarely exceed 100 m, is punctuated by several kilometre-sized morphological highs (Figure 3.14). These elevations, formed by both sedimentary and volcanic rocks, emerged around middle Holocene time or earlier when they constituted a large archipelago. The sedimentary banks (Talbot, Ante-Talbot, Panope, Nereo and Pantelleria Vecchia), presently located at water depths 8–40 m, are composed of Miocene rocks severely deformed by a late Miocene compressional phase which produced the external sector of the Sicilian–Maghrebian thrust belt. Tortonian-aged rock samples from the Pantelleria Vecchia Bank represent patch reefs that have mostly formed on structural highs. Sedimentary analogies suggest that other sedimentary banks of the Adventure Plateau may have the same origin. Galatea, Anfitrite and Tetide represent submarine volcanic edifices emplaced on major extensional faults formed during early Pliocene – Quaternary continental rifting of the Sicilian Channel (Zvi Ben-Avram et al., 2015). The present-day morphology of the banks is the result of repeated phases of subaerial exposure and drowning, especially since the Last Glacial Maximum.

Refer to paragraph 4.2.5. for Doride Laneira and Lanassa volcanoes description.

Further, similarly to the nearshore area, in not possible to exclude presence of mud volcanoes in the offshore area, recently found and described in southern Sicily channel along faults adjacent to the Scicli fracture zone (Holland et al., 2003; Zeppilli et al., 2011).

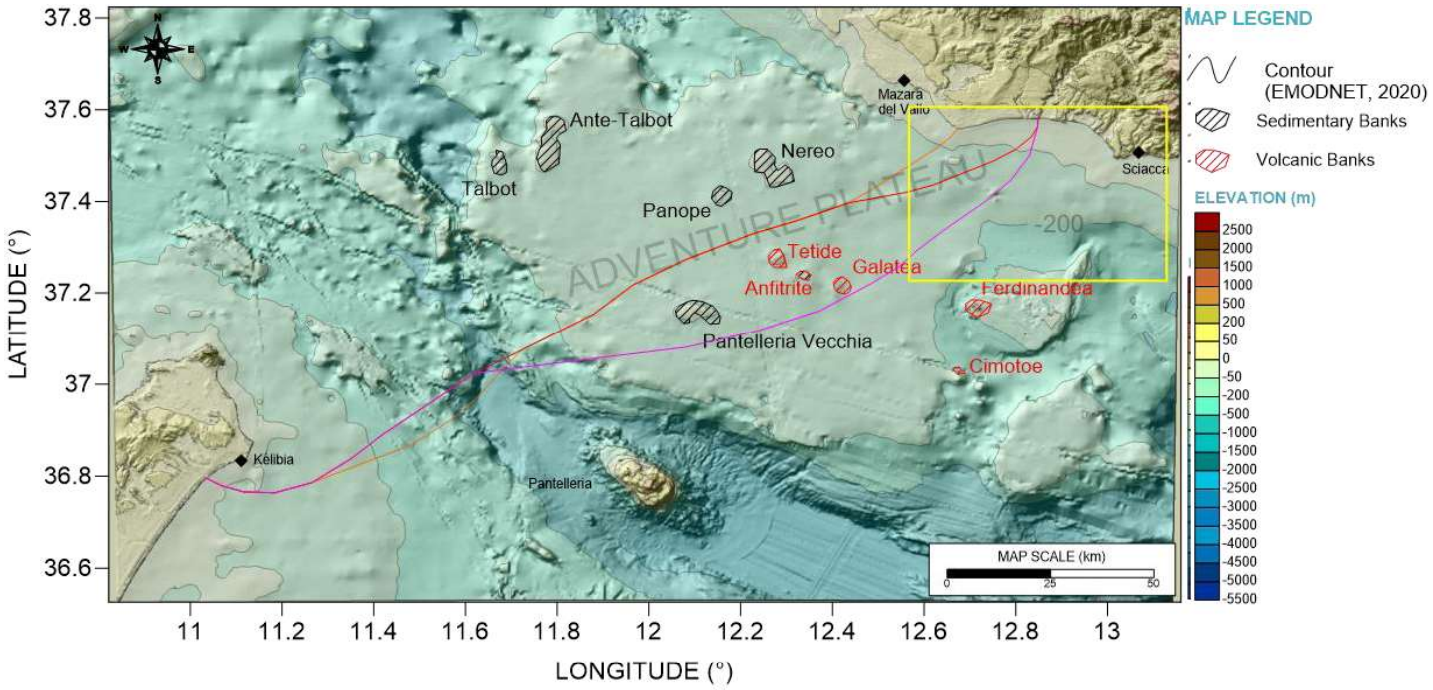

Figure 3.14: Offshore Banks of Adventure Plateau; rectangular area is described.

3.4.3 Geohazard overview

Based on available data and literature review, a large scale preliminary geohazard identification is summarized in the following table:

Table 3.2: Preliminary Geohazard Summary

Geohazard	Description	Landfall ITA	Shelf ITA	Channel	Shelf TUN	Landfall TUN
Earthquakes	The area is characterized by moderate to high seismicity. PGA values increasing towards Sicily. Offshore section's PGA need to be evaluated with dedicated study.	PGA 0.15 to 0.35 g (475 yr return period)	PGA 0.15 to 0.35 g (475 yr return period)	Unknown (PGA value decreasing from Sicily to Tunisia)	PGA 0.08 to 0.16 g (475 yr return period)	PGA 0.08 to 0.16 g (475 yr return period)
Faults	Fault system reported throughout the Sicily Channel.	Capo Granitola and Sciacca Fault Systems	Capo Granitola and Sciacca Fault Systems	Pantelleria Graben (activity unknow)	No active regional faults	No active regional faults

Geohazard	Description	Landfall ITA	Shelf ITA	Channel	Shelf TUN	Landfall TUN
Volcanoes	Volcanism limited to Adventure Plateau.	None	Closest volcanoes to corridor route are: Shallow water - Climene, Doride, Actea. Offshore - Tetide, Anfitrite, Galatea, (Activity unknown)	None	None	None
Mud Volcanoes	Possible presence close to faults and volcanoes	none	Possible	Possible	Unlikely	None
Pockmarks due to gas release	Possible presence close to faults and volcanoes	none	Possible	Possible	Unlikely	None
Landslides and MTD	Mass wasting processes limited to Channel sector	Unlikely	Unlikely	Possible (to be verified with geophysical survey)	Unlikely	Unlikely
Hydrodynamic effects (i.e. sand waves)	Bottom currents capable of mobilize sediment, especially in shallow waters. Deepwater bottom currents cannot be ruled out at this stage.	Unlikely	Possible	Highly Possible	Possible	Unlikely
Rock outcrops	Landfall areas show sandy deposits but rocky outcrops cannot be ruled out. Rock outcrop – sub crop can be present in the Channel.	Possible	Possible	Possible	Unlikely	Unlikely
Liquefaction	Sandy sediments are reported especially at landfalls and shelves.	Possible	Possible	Unlikely	Possible	Possible
Presence of gas (i.e. mounds, pockmarks, etc.)	Presence of gas-related features closely related to data resolution, thus is not possible to evaluate at this stage. No major such features are reported in literature.	Unknown	Unknown	Unknown	Unknown	Unknown
Tsunamis	Possible record along Sicily coast. Tsunami are GH just for landfall facilities.	Possible	None	None	None	Possible

3.5 Bibliography

Basili R., Valensise G., Vannoli P., Burrato P., Fracassi U., Mariano S., Tiberti M.M., Boschi E. (2008). The database of individual seismogenic Sources (DISS), version 3: summarizing 20 years of research on Italy's earthquake geology. Tectonophysics 453, 1-4;pp 20-43.

Bousquet, J.C. and G. Lanzafame (1986). Déformations com-pressives quaternaires au bord sud de l'Etna, C. R. Acad.Sc. Paris, 303, 235-240.

Colantoni P (1975) Note di geologia marina sul Canale di Sicilia. Giorn Geol 40(1):181–207.

Corti G, Cuffaro M, Doglioni C, Innocenti F, Manetti P (2006) Coexisting geodynamic processes in the Sicily Channel. In: Dilek Y, Pavlides S (eds) Postcollisional tectonics and magmatism in the Mediterranean region and Asia. Geol Soc Am Spec Publ 409:83–96.

Ferranti, L., F. Pepe, G. Barreca, M. Meccariello, C. Monaco, 2019, "Multi-temporal Tectonic Evolution of Capo Granitola and Sciacca Foreland Transcurrent Faults (Sicily Channel)", Tectonophysics, Vol.765, pp. 187-204.

Fetheddine, M., Z. Taher, M. Ben Chelbi, M. Bédir and F. Zargouni, 2012, "Role of the NE-SW Hercynian Master Fault Systems and Associated Lineaments on the Structuring and Evolution of the Mesozoic and Cenozoic Basins of the Alpine Margin, Northern Tunisia", Tectonics – Recent Advances, InTech, Chapter 6.

Giardini, D., J. Woessner, D. Laurentiu et al., 2015, "The 2013 European Seismic Hazard Model: key components and results", Bull. Earthquake Eng 13, 3553–3596.

Holland W.C., Etiope G., Milkov A., Michelozzi E., (2003). Mud volcanoes discovered offshore Sicily. Marine Geology, 199 (1-2): 1-6.

Jiménez, M. J., D. Giardini, G. Grünthal and the SESAME Working Group, 2001, "Unified Seismic Hazard Modeling throughout the Mediterranean Region", Bollettino di Geofisica Teorica ed Applicata, Vol. 42, pp. 3-18.

Khomsi, S. et al., 2009, "New insights on the structural style of the subsurface of the Tell units in north-western Tunisia issued from seismic imaging: Geodynamic implications", C. R. Geoscience, Vol. 341, pp. 347–356.

Lavecchia G., Ferrarini F., de Nardis R., Visini F., Barbano M.S. (2007)., Active thrusting as a possible seismogenic source in Sicily (southern Italy): Some insights from integrated structural-kinematic and seismological data. Tectonophysics 445,3-4;pp 145-167.

Lodolo E, Renzulli A, Cerrano C, Calcinai B, Civile D, Quarta G and Calcagnile L (2021) Unraveling Past Submarine Eruptions by Dating Lapilli Tuff-Encrusting Coralligenous (Actea Volcano, NW Sicilian Channel). Front. Earth Sci. 9:664591.

Martorelli E., Petroni G., Latino Chiocci F., and the Pantelleria sciantific Party (2011). Contourites offshore Pantelleria Island (Sicily Channel. Mediterranean sea): depositional erosional and biogenic elements.
Reuther CD (1987) Extensional tectonics within the central Mediterranean segment of the Afro-European zone of onvergence. Mem Soc Geol Ital 38:69–80.

Riahi, S. et al., 2015, "Age, Internal Stratigraphic Architecture and Structural Style of the Oligocene–Miocene Numidian Formation of Northern Tunisia", Annales Societatis Geologorum Poloniae, Vol. 85, pp. 345–370.

Stucchi M., C. Meletti, V. Montaldo, A. Akinci, E. Faccioli, P. Gasperini, L. Malagnini, G. Valensise, 2004, “Pericolosità sismica di riferimento per il territorio nazionale MPS04 Data set”, Istituto Nazionale di Geofisica e Vulcanologia (INGV).

Vattano, M., C. Di Maggio, G. Madonia, V. Agnesi, S. Monteleone, 2017, “Geomorphological Evolution of Western Sicily, Italy”, Geologia Carpathica, Vol. 68, 1, pp. 80 – 93.

Washington HS (1909) The submarine eruption of 1831 and 1891 near Pantelleria. Am J Sci 27:131–150.
Zecchin M., E. Lodolo, D. Civile, L. Zampa e F. Accaino, 2019, “A series of volcanic edifices discovered a few kilometers off the coast of SW Sicily”, Marine Geology, Vol.416, pp. 105999.

Zeppilli D., Mea M., Corinaldesi C., Davovaro R., (2011) Mud volcanoes in the mediterranean Sea are hot spots of meiobenthic species. Progress in Oceanography

4. UNDERWATER NOISE

4.1 Ambient noise

4.1.1 Overview

In the marine environment a background noise is produced by natural processes due to physical (e.g. surface waves, wind, volcanism, earthquakes) or biological causes (e.g. bioacoustics signals produced by marine species). Namely:

- Wind: wind noise could reach 85 - 95 dB @1 μPa2/Hz, with spectra main energy concentration at low frequencies;
- Rain: rain can cause short periods of high underwater noise levels with flat spectra that can reach up to 80 dB @1 μPa2/Hz.

Other relevant noise sources at sea are human activities, for example (Simmonds et al., 2004):

- marine traffic: the main sources of noise are engines and thrusters. Usually marine vessels emission spectra show a prevalence of low frequencies (less than 1kHz);
- energy – related activities: main concern is raised about seismic surveys, which usually generate high levels due to massive and repeated use of air guns in a relatively restricted area for a long period. Other very loud activities are linked with the construction of offshore windfarms (pile diving). Least concern raises the oil & gas exploration and production activity itself, which usually shows relatively low sound levels;
- military and research activities: these activities are considered to be particularly harmful due to the usage of sonars and air guns on wide areas. These types of sources, as mentioned above, are usually both particularly loud and differ from each other mainly for the frequency range (high for sonars and low for air guns).

Marine traffic is at present the main anthropogenic source, especially at low frequencies (< 300 Hz). According to some studies carried out in North -Eastern Pacific deep waters, background noise at low frequencies has risen in the last 40 years at the rate of +3dB each 10 years, mainly because of commercial shipping (Andrew et al., 2002; McDonald et al., 2006). In the northern hemisphere, where numerous marine mammals' species are known to live, the effects of interaction between the intense marine traffic and some animals' abilities has been recorded. The main cause of this interaction is the bioacoustics signals masking effect (Figure 4.1).

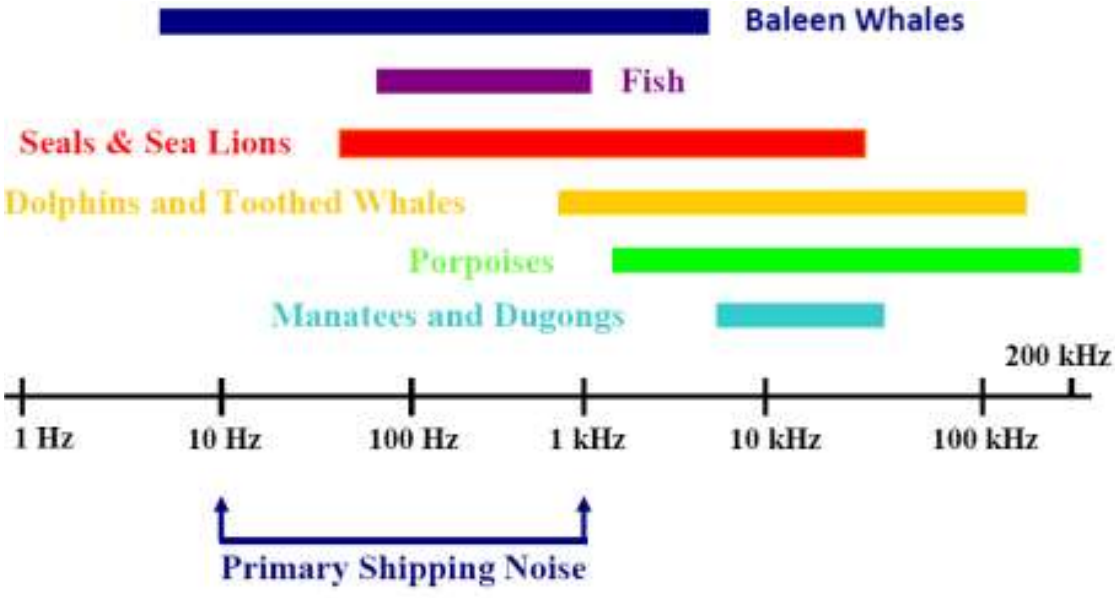

Figure 4.1: Comparison between bioacoustics sounds frequencies and shipping noise frequencies (Southall, 2005)

The marine traffic plays a main role in the rise of background noise levels in the oceans and it will be of increasing concern in the future, as forecasts show an increase trend for shipping at global scale even though at European level the Plan for the so–called Motorways of the Sea is setting policy to implement a more sustainable commercial shipping.
Shipping noise is mainly composed by low frequencies (<100 Hz). It is mainly generated by:

- cavitation;
- vibration of mechanic elements and structures;
- displacement of water masses due to the ship movement.

The most likely sources of ambient noise across the study area have been identified in:

- Local shipping;
- Distant shipping;
- Industrial noise;
- Seismic surveys;
- Offshore oil and gas facilities.

4.1.2 Main anthropogenic noise sources in the project area

The area of interest comprises deep, offshore waters in which the dominant noise source will be distant shipping in the absence of wind and precipitation (travelling vessels are sources of low-frequency acoustic waves which propagate efficiently through the water mass and thus affect underwater noise levels at large distances from the major shipping lanes) and shallow coastal areas, where a multitude of potential anthropogenic sources contribute to the ambient noise. It should also be noted that a seasonal variability is expected, due to variations in noise contributions through the year and seasonal differences in acoustic propagation loss.
As per a national analysis of the uses of the Italian maritime areas, the south-western coast of Italy is heavily interested by commercial routes on the axis Bosforus/Suez-Gibraltar (mainly container ships and oil tankers) and fishery activities, both in the proximities of the coast (with the Mazara del Vallo harbor, one of the main centers for fishery and fish commercial distribution, along with the harbor of Porto Palo) and at open water, where the fishery area GSA16 lays.
The contribution of service routes from/to Sicily and the islands in the Strait (Pantelleria, the Pelagie islands and Malta) is also relevant. These routes, moreover, intensify in the summer, when the area welcomes significant touristic flows, due to a variety of points of interest (e.g. beaches, cultural and naturalistic sites). During summer, the number of pleasure boats also increases, due to the tourism industry.
The coastal areas host a multitude of harbors, with different dimensions and main vocations, but all of them are mainly multipurpose.

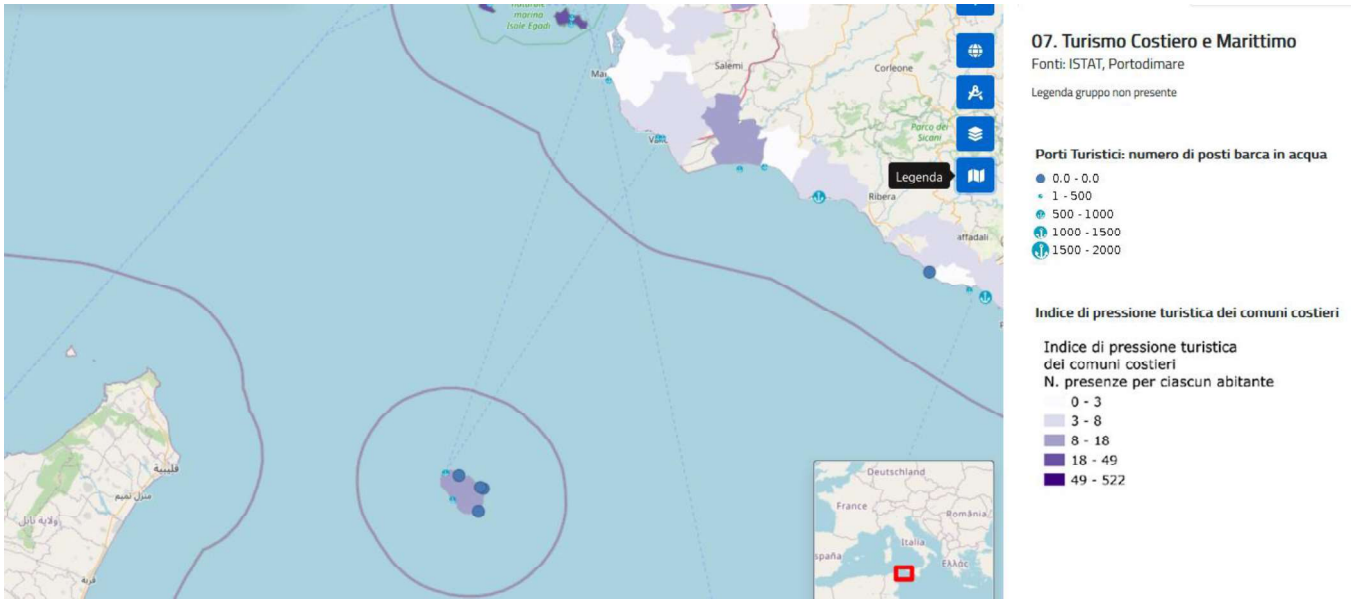

Figure 4.2: Main touristic ports and touristic density index in South Sicily coastal regions (Portale del Mare, November 2022)

Different types of ships could affect the marine ambient noise to a different extent on the basis of tonnage and cruise speed. It is also to be noted that different types of boats could also be linked to different sound spectral distribution. In the following images some characteristic noise spectra are represented.

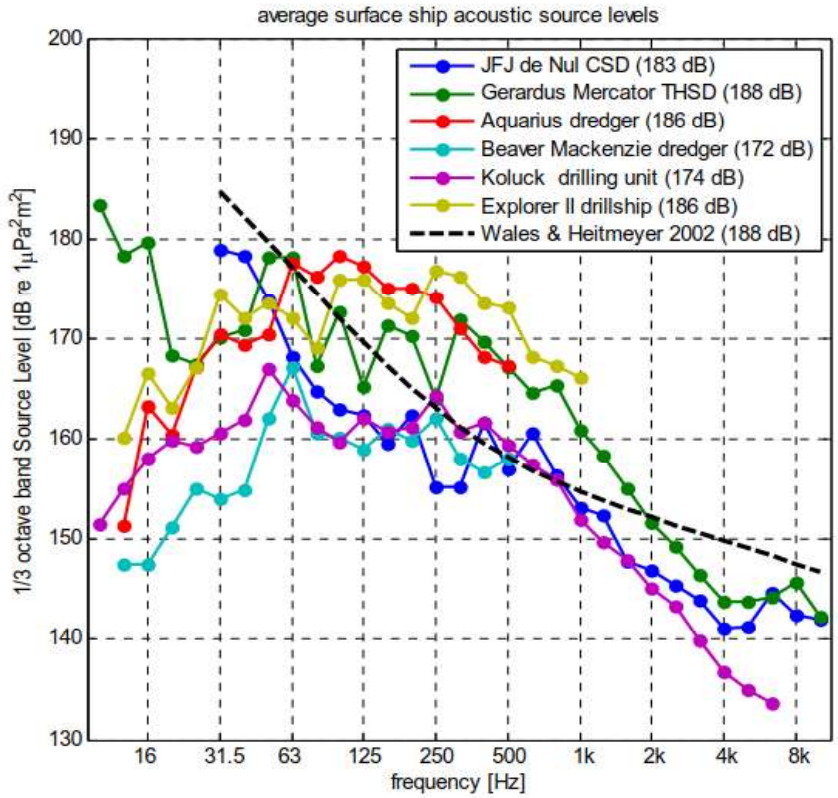

Figure 4.6. 1/3-octave band source level spectra of underwater noise for marine dredging and offshore drilling, compared with the average source level of transiting merchant ships (Wales & Heitmeyer, 2002). The data for the *JFJ de Nul* Cutter Suction Dredger and the *Gerardus Mercator* Trailing Suction Hopper Dredger are taken from the Sakhalin data and the other spectra from Richardson *et al.* (1995). The levels between brackets in the legend give the broadband integrated source level in dB re 1 μPa^2m^2.

Figure 4.3: Sound spectra for various types of ship (Ainslie 2009)

In the image below, the density of routes per square km per month is reported.

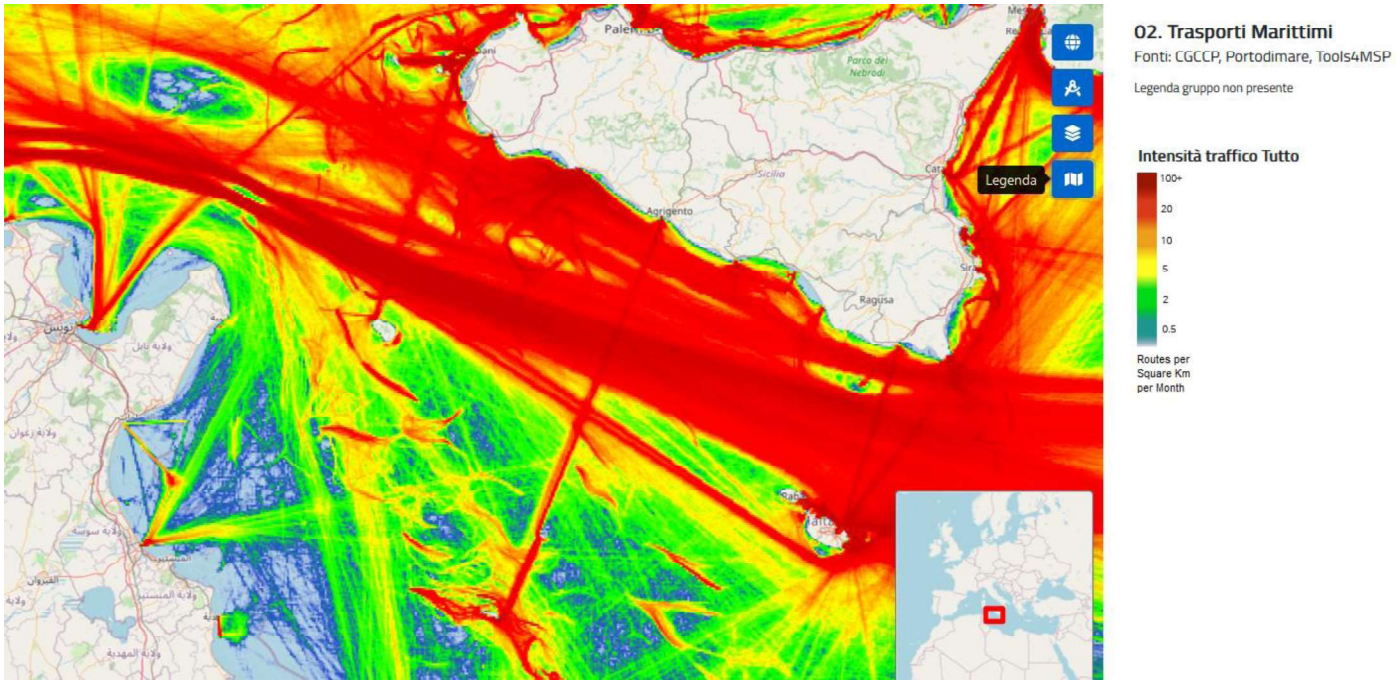

Figure 4.4: Marine Traffic distribution in the Sicily strait (Central Mediterranean Sea) (Portale del Mare, November 2022)

In the Sicily strait there are also hydrocarbon production and exploration activities: the areas that are open to new exploration instances are represented hereafter and include also the project area.

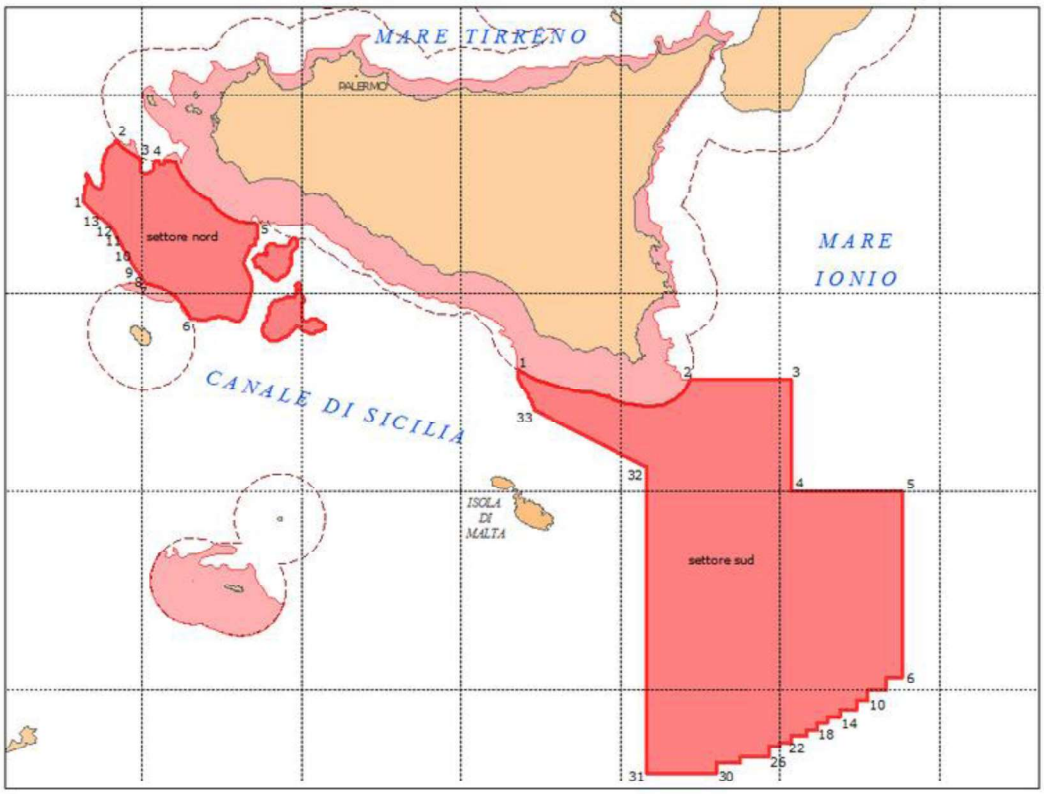

Figure 4.5: Available areas for new exploration instances in Southern Sicily (C zone) – (UNIMIG, October 2022)

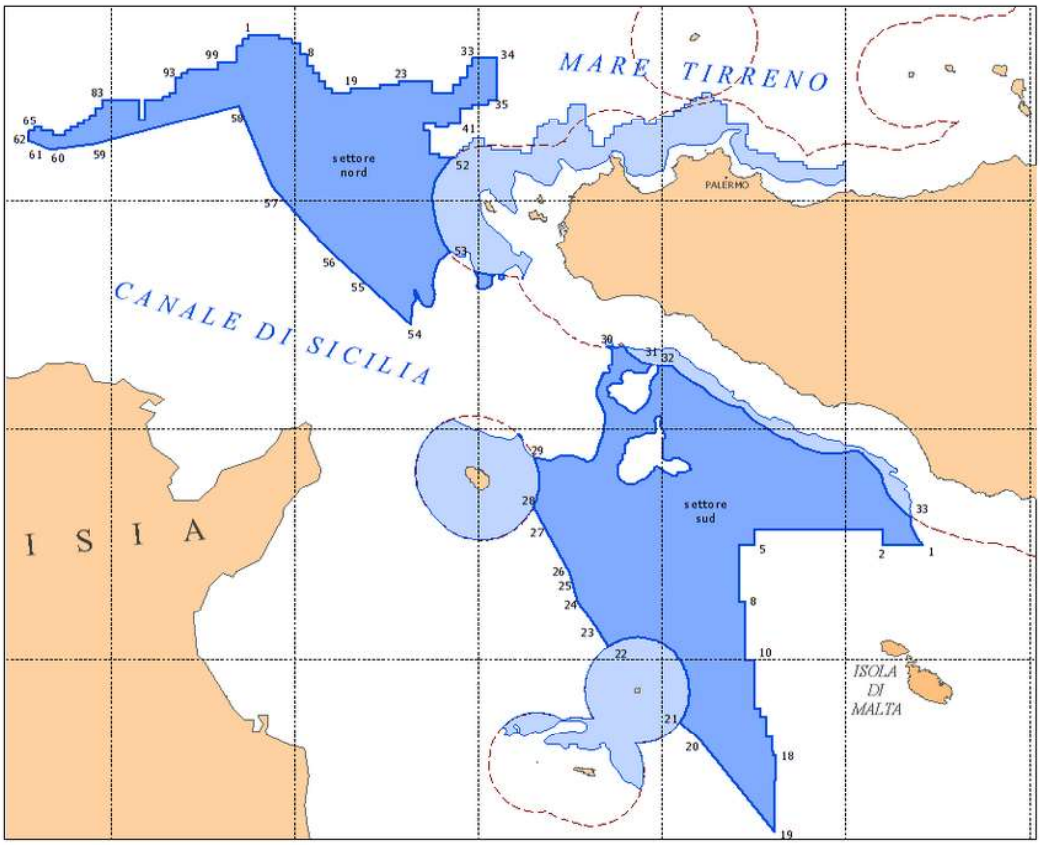

Figure 4.6: Available areas for new exploration instances in Southern Sicily (G zone) – (UNIMIG, October 2022)

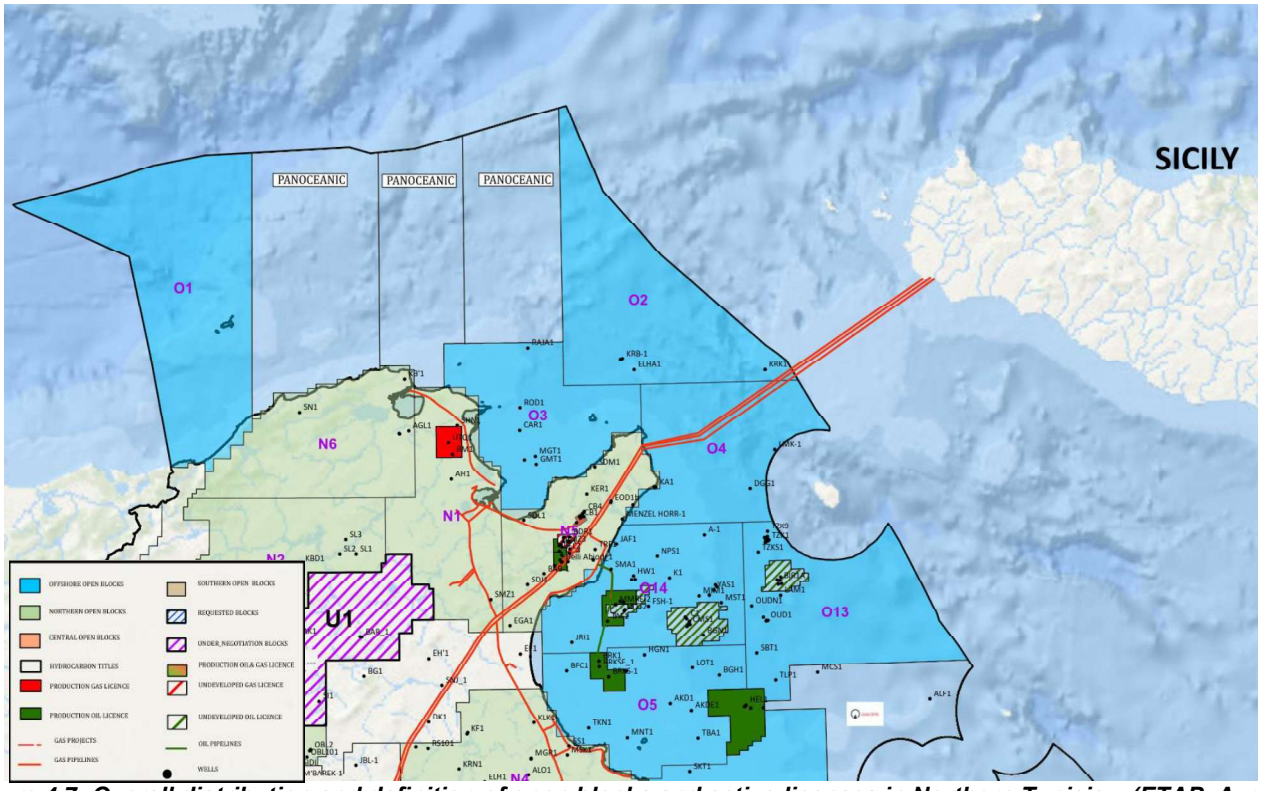

Figure 4.7: Overall distribution and definition of open blocks and active licenses in Northern Tunisia – (ETAP, August 2022)

The exploration and production areas already active are mainly distributed in the Gela Gulf in Italy and in the Hammamet Gulf in Tunisia. These activities could affect the ambient noise of the whole area, even if in the far field.

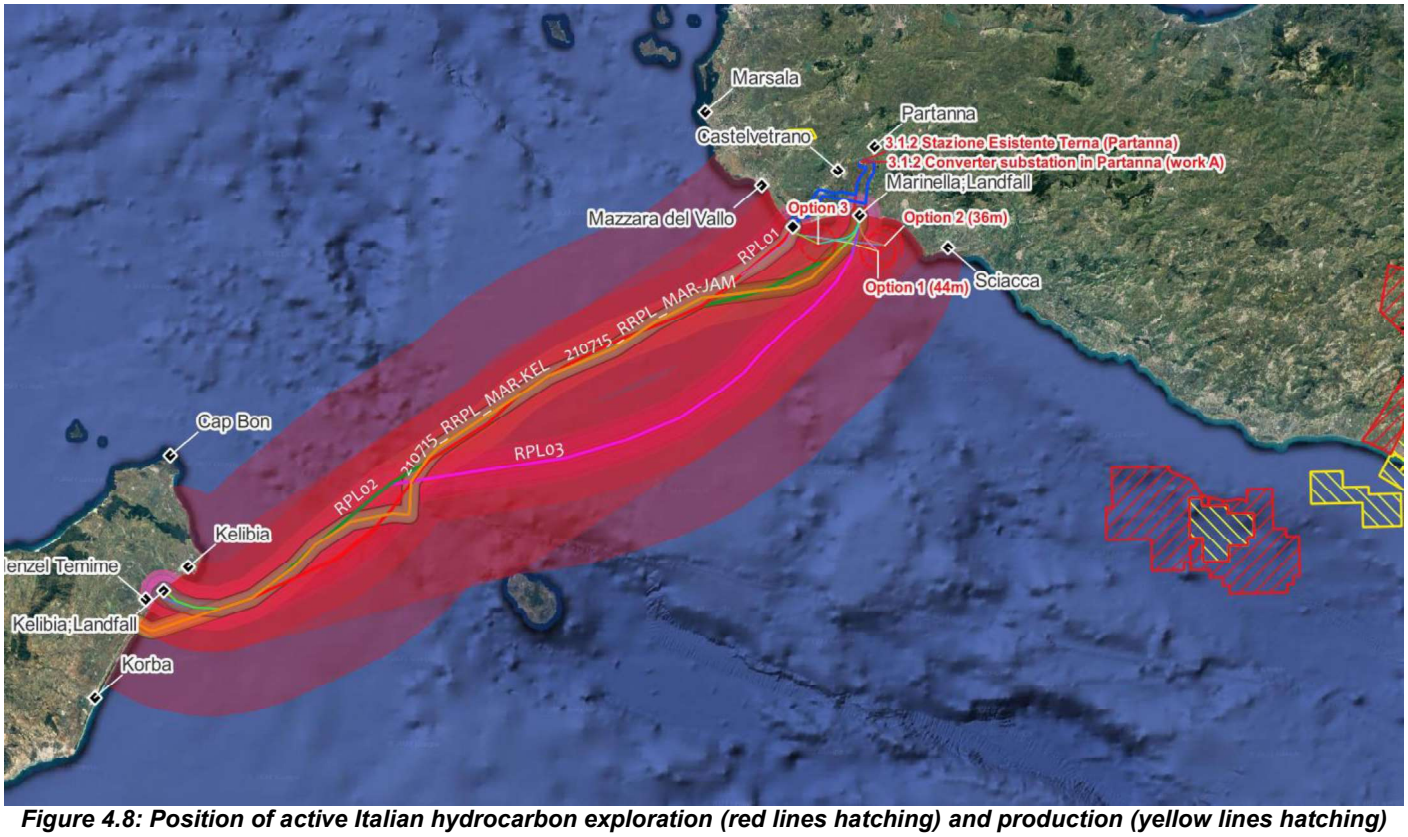

Figure 4.8: Position of active Italian hydrocarbon exploration (red lines hatching) and production (yellow lines hatching) areas in the Sicily strait (UNIMIG)

The area is also interested by seismic surveys aimed at both exploration and research. This kind of activities are of main concern for the status of ambient noise and for the impact potentially induced on fauna.
In 2018, a monitoring of the ambient noise in Italian seas has been performed in order to assess the initial status of the marine environment as a baseline for the definition of MSFD Descriptor 11 thresholds.
In the Descriptor 11 Paper Report (EEA, 2018) the following map is reported: unfortunately, color scale or recorded data analysis are not reported.

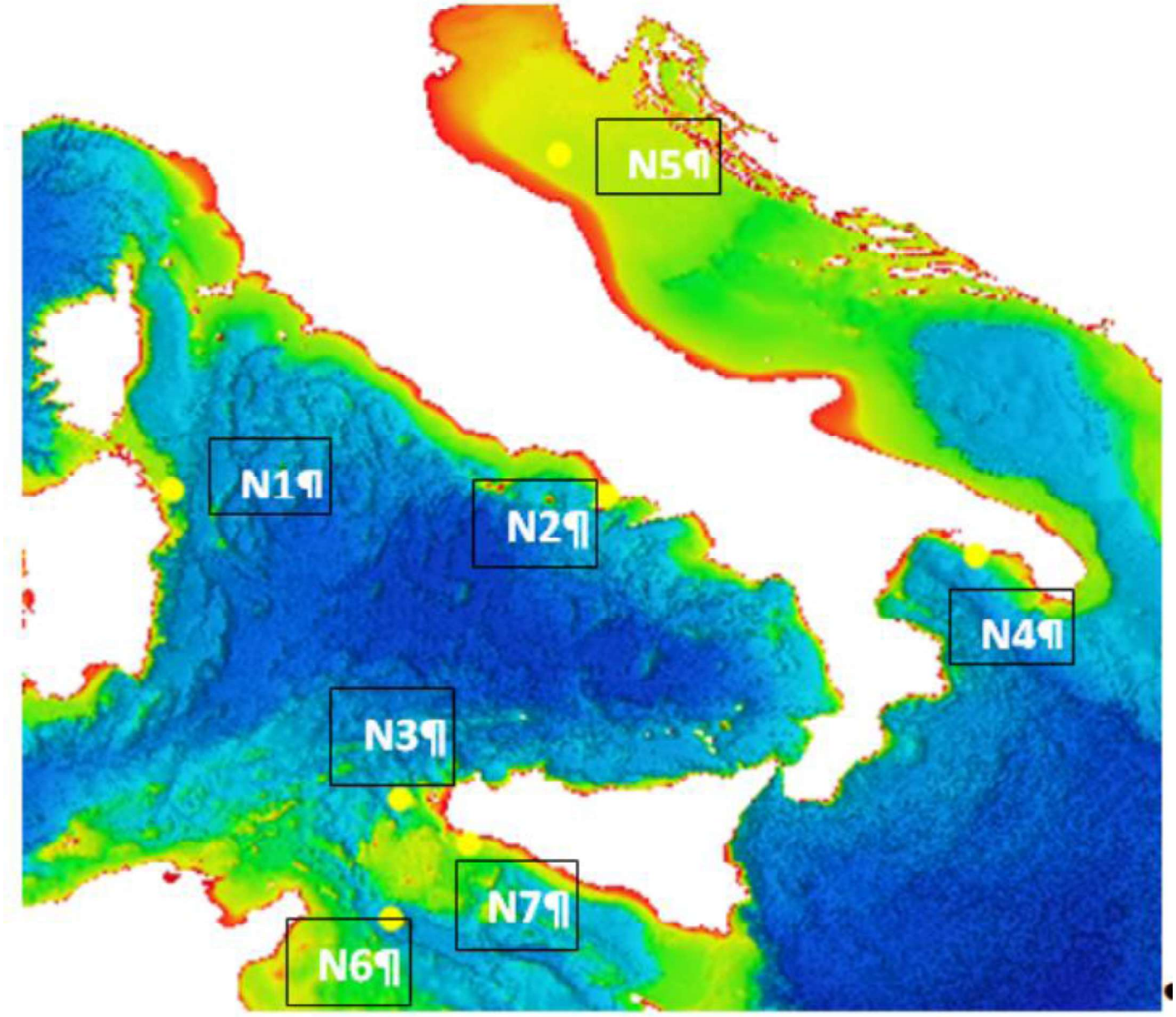

Figure 4.9: Map of the monitored ambient noise in the Mediterranean (EEA 2018)

What could be seen is that in the Sicily strait the monitored ambient noise results to be higher than in other Mediterranean regions also far from shore.

4.2 Receptors

4.2.1 Main marine fauna of the Sicily strait

With regards to sensitive receptors, it is to be noted that the area is considered to be of high interest as a fish nursery. As identified in the IBAT report, moreover, a variety of species could be found in the area.
The main targets of noise are mammals and sea turtles due to the sensitivity of their auditory systems, developed in order to use bioacoustics signals to communicate, mate and feed.
The marine mammal and turtle species which have been detected in the Mediterranean subregion according to IBAT are listed in the following table along with their UINC red list classification:

Genus	Binomial	Common name	Category (UINC)	Population trend	Assessment date
Balaenoptera	*Balaenoptera physalus*	Fin Whale	EN	Decreasing	12/01/2021
Physeter	*Physeter macrocephalus*	Sperm Whale	EN	Decreasing	16/11/2020
Grampus	*Grampus griseus*	Rissos Dolphin	EN	Decreasing	24/11/2020
Delphinus	*Delphinus delphis*	Common Dolphin	EN	Decreasing	15/11/2020
Globicephala	*Globicephala melas*	Long-finned Pilot Whale	EN	Decreasing	29/03/2021
Ziphius	*Ziphius cavirostris*	Cuviers Beaked Whale	VU	Decreasing	27/01/2018
Chelonia	*Chelonia mydas*	Green Turtle	EN	Decreasing	30/04/2004
Caretta	*Caretta caretta*	Loggerhead Turtle	VU	Decreasing	23/08/2015
Dermochelys	*Dermochelys coriacea*	Leatherback	VU	Decreasing	21/06/2013

Along with mammals and sea turtles, a variety of sharks and fishes, also endangered, have been detected in the area.

4.2.2 Noise sensitivity

The marine mammals species above listed, for what concerns noise sensitivity, belong to different auditory groups, defined on the base of NOAA's Technical Guidance for Assessing the Effect of Anthropogenic Sound on Marine Mammal Hearing (2018), namely:

- Low frequency: fin whales;
- Mid-frequency: dolphins, sperm whales, Risso's dolphins, pilot whales, beaked whales.

The "Technical Guidance for Assessing the Effects of Anthropogenic Sound on Marine Mammal Hearing" (Version 2.0, 2018) is a guideline developed by the U.S. National Marine Fisheries Service. This Guideline provides updated thresholds for onset of temporary (TTS) and permanent thresholds shifts (PTS) for impulsive and non – impulsive sound sources on different kinds of marine mammals. The guideline divides marine mammals in groups on the basis of their auditory range and defines, for each auditory group, weighting functions to be applied to sound sources in order to assess perceived levels for each group.
In the following table the auditory groups are defined, while in the following image weighting functions are shown.

Hearing Group	Species (not exhaustive List)	Generalized Hearing Range
Low – frequency (LF) cetaceans	Baleen whales	7 Hz to 35 kHz
Mid – frequency (MF) cetaceans	dolphins, toothed whales, beaked whales, bottlenose whales	150 Hz to 160 kHz
High – frequency (HF) cetaceans	true porpoises, river dolphins	275 Hz to 160 kHz

Phocid pinnipeds (PW)	true seals	50 Hz to 86 kHz
Otariid pinnipeds (OW)	sea lions, fur seals	60 Hz to 39 kHz
Sirenians (SI)	manatee	6 kH to 20 kHz

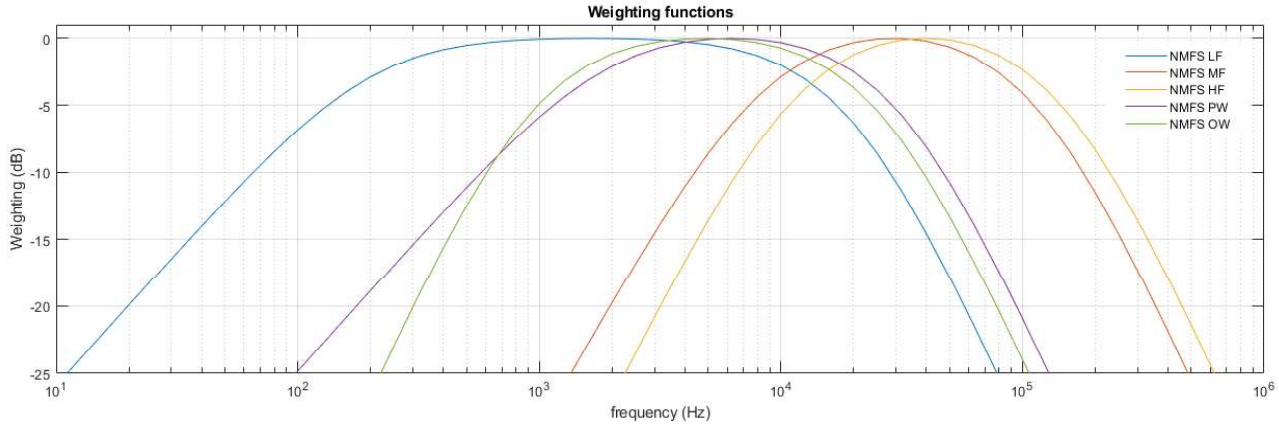

Figure 4.10: NOAA NMFS weighting functions for cetaceans' auditory groups

These weighting functions have to be applied in order to assess the overall effect of a sound source through a lasting period of time using the "equal energy approach" (exposures with equal SEL result in equal effects, regardless of the duration or duty cycle of the sound, NOAA 2018). NMFS recommends an accumulation period of 24h. For impulsive sources, then, peak thresholds (non – weighted) are set.
Behavioral thresholds are also provided from NMFS ("Level B" criterion) still not updated and distinctively defined for all auditory groups, which sets "behavioral disruption" thresholds for impulsive and non – impulsive sound sources.
This lack of up-to-date thresholds for behavioral effects depends on the fact that behavior in animals depends on a huge number of factors, so that the response to a stimulus can vary not only between species but also within the same species depending on factors such as sex, age, size and motivation (feeding, mating, etc.). Moreover, no reliable data can be derived from the observation of captive animals in order to forecast wild animals' behavioral response to stimuli as a huge difference in general behavior has been noted.

4.3 Good Environmental Status criteria and baseline

Italy has a national application of the Marine Strategy Framework Directive (2008/56/CE) in the D.Lgs. 190/2010. The Commission Decision (2010/477/EU) on criteria and methodological standards on good environmental status of marine waters defines two criteria and two indicators for underwater noise as follows (European Commission, 2012):

- 11.1. Distribution in time and place of loud, low and mid frequency impulsive sounds: Proportion of days and their distribution within a calendar year over areas of a determined surface, as well as their spatial distribution, in which anthropogenic sound sources exceed levels that are likely to entail significant impact on marine animals measured as Sound Exposure Level (in dB re 1µPa2.s) or as peak sound pressure level (in dB re 1µPa peak) at one meter, measured over the frequency band 10 Hz to 10 kHz
- 11.2. Continuous low frequency sound: Trends in the ambient noise level within the 1/3 octave bands 63 and 125 Hz (center frequency) (re 1µPa RMS; average noise level in these octave bands over a year) measured by observation stations and/or with the use of models if appropriate.

The national legislation identifies the areas on which to determine the parameters (Marine Reporting Units - MRU) with the three main Mediterranean sub-seas Adriatic, Ionian & Central Mediterranean and West Mediterranean. Although the MRUs have been set, no information is available on the current status of the two sub-descriptors, neither a registry of the known sources in the MRUs is available.

For what concerns Tunisia, even though it is not part to European Union, it is involved in the IMAP-MPA project, which overall objective is to contribute towards the achievement of the Good Environmental Status (GES) in the Mediterranean Sea and Coast through the consolidation of the Ecosystem Approach (EcAp)

process for MPAs management and sustainable development. As The IMAP-MPA project builds on the results and achievements of the EcAp-Med II project "Mediterranean Implementation of the Ecosystem Approach, in coherence with the European Union Marine Strategy Framework Directive" the MSFD criteria and GES definitions used in the European context could be considered as applicable also to Tunisia.

4.4 References

ACCOBAMS, 2017. ACCOBAMS-MOP6/2016/Res.6.17 Anthropogenic Noise.

ACCOBAMS, 2015. ACCOBAMS-MOP5/2013/Res.5.15 Addressing The Impact Of Anthropogenic Noise.

ACCOBAMS, 2013. ACCOBAMS-MOP5/2013/Doc.24 Methodological Guide: “Guidance On Underwater Noise Mitigation Measures.”

ACCOBAMS, 2010. ACCOBAMS-MOP4/2010/Res.4.17 Guidelines To Address The Impact Of Anthropogenic Noise On Cetaceans In The Accobams Area.

ACCOBAMS, 2007. ACCOBAMS-MOP3/2007/Res.3.10 Guidelines To Address The Impact Of Anthropogenic Noise On Marine Mammalsin The Accobams Area.

ACCOBAMS, 2004. ACCOBAMS-MOP2/2004/Res.2.16 Assessment And Impact Assessment Of Man-Made Noise.

Ainslie, M.A., de Jong, C.A.F., Dol, H.S., Blacquière, G., Marasini, C., 2009. Assessment of natural and anthropogenic sound sources and acoustic propagation in the North Sea. TNO-DV 2009 C085.

Andrew, R.K., Howe, B.M., Mercer, J.A., Dzieciuch, M.A., 2002. Ocean ambient sound: Comparing the 1960s with the 1990s for a receiver off the California coast.

Casale, P., Margaritoulis, D., 2010. Sea turtles in the Mediterranean: distribution, threats and conservation priorities.

Coll, M, Santojanni, A, Palomera, I, Arneti, E, 2010 Ecosystem assessment of the North-Central Adriatic Sea: towards a multivariate reference famewok. Marine Ecology Progress Series, 417, 193-201. doi: 10.3354/meps08800

Erbe, C., Reichmuth, C., Cunningham, K., Lucke, K., Dooling, R., 2016, Communications masking in marine mammals: a review and research srategy. Marine Pollution Bulletin 103, 15-38.

Gilbert, K.E., White, M.J., 1989. Application of the parabolic equation to sound propagation in a refracting atmosphere. The Journal of the Acoustical Society of America 2, 630–637. https://doi.org/DOI: 10.1121/1.397587

IUCN, 2012. Marine Mammals and Sea Turtles of the Mediterranean and Black Seas.

IUCN-MMPATF, 2017 Northen Adriatic IMMA Factsheet. IUCN joint SSC/WCPA Marine Mammal Protected Areas Task Force

Mazor, T., Beger, M., Mcgowan, J., Possingham, H.P., Kark, S., 2016. The value of migration information for conservation prioritization of sea turtles in the Mediterranean. Global Ecology and Biogeography 25, 540–552.

McDonald, M.A., Hildebrand, J.A., Wiggins, S.M., 2006. Increases in deep ocean ambient noise in the Northeast Pacific west of San Nicolas Island, California. Journal of the Acoustical Society of America 2, 711–718. https://doi.org/10.1121/1.2216565

McPherson, C., Li, Z., Quijano, J., 2019. Underwater sound propagation modelling to illustrate potential noise exposure to Maui dolphins from seismic surveys and vessel traffic on West Coast North Island, New Zeland. New Zeland aquatic Environment and Biodiversity Report No. 217

Ministero delle Infrastrutture e della Mobilità Sostenibili - SID il Portale del Mare (https://www.sid.mit.gov.it/mappa)

Rako, N, Fortuna, C.M., Holcer, D, Mackelwoth, P, Nimak-Wood, M, Pleslic, G, Sebastianutto, L, Vilibic, I, Wiemann, A, Picciulin, M, 2013 Leisure boating as a trigger for the displacement of the bottlenose dophins of the Cres-Losinj archipelago (northen Adriatic Sea, Croatia). Marine Pollutant Bulletin

Science Communication Unit, University of the West England, 2013. Science for Environment Policy Future Brief: Underwater Noise. Report produced for the European Commission DG Environment.

Simmonds, M., Dolman, S., Weilgart, L., 2004. Oceans of Noise. WDCS Science Report.

Southall, B.L., 2005. Shipping Noise and Marine Mammals: A forum for Science, Management and Technology, in: National Oceanic and Atmospheric Administration (NOAA) International Symposium. NOAA, Arlington, Virginia, USA, p. 40.

Southall, B.L., Bowles, A.E., Ellison, W.T., Finneran, J.J., Finneran, R.L., C.R. Greene Jr., D. Kastak, D.R. Ketten, J.H. Miller, P.E. Nachtigall, W.J.Richardson, J.A. Thomas, Tyack, p. l., 2007. Marine Mammal Noise Exposure Criteria: Initial Scientific Recommendations. Aquatic Mammals 33.

Stokes, K.L., Broderick, A.C., Canbolat, A.F., Candan, O., Fuller, W.J., Glen, F., Levy, Y., Rees, A.F., Rilov, G., Snape, R.T., Stott, I., Tchernov, D., Godley, B.J., 2015. Migratory corridors and foraging hotspots: critical habitats identified for Mediterranean green turtles. Diversity and Distributions 21, 665–674. https://doi.org/10.1111/ddi.12317

UN Environment CMS, 2017. UNEP/CMS/Resolution 12.14 ADVERSE IMPACTS OF ANTHROPOGENIC NOISE ON CETACEANSAND OTHER MIGRATORY SPECIES.

UNEP, 2012. Initial integrated assessment of the Mediterranean Sea: fulfilling step 3 of the ecosystem approach process.

UNEP CMS, 2017a. UNEP/CMS/COP12/Doc.24.2.2. CMS Guidelines on Environmental Impact Assessments for Marine Noise-generating Activities.

UNEP CMS, 2017b. UNEP/CMS/COP12/Inf.11/Rev.1, 2017 Technical Support Information to the CMS Family Guidelines on Environmental Impact Assessment for Marine Noise-Generating Activities.

UNEP-MAP-RAC/SPA, 2015a Adriatic Sea: Important areas of conservation of cetaceans, sea turtles and giant devil rays.

UNEP-MAP-RAC/SPA 2015b Adriatic Sea: Description of the ecology and identification of the areas that may deserve to be protected.

Urick, R.J., 1984. Ambient Noise in the Sea.

U.S. Dept. of Commer., NOAA, 2018. 2018 Revision to: Technical Guidance for Assessing the Effects of Anthropogenic Sound on Marine Mammals Hearing (Version 2.0). Underwater Thresholds for Onset of Permanent and Temporary Threshold Shifts.

Van der Graaf, A., Ainslie, M.A., André, M., Brensing, K., Dalen, J., Dekeling, R.P.A., Robinson, S., Tasker, M.L., Thomsen, F., Werner, S., 2012. European Marine Strategy Framework Directive - Good Environmental Status (MSFD GES): Report of the Technical Subgroup on Underwater Noise and other forms of energy. Final Report.

5. BIODIVERSITY

5.1 Introduction

The Strait of Sicily divides the Mediterranean Sea into two main basins: the western Mediterranean Basin with more Atlantic influence and the eastern Mediterranean Basin. The two basins remain to some extent disconnected (Cartes et al. 2004).

The topography of the Strait of Sicily consists of shallow banks along the Sicilian and Tunisian coasts where the water depth ranges from 50 to 200 m.

The Strait of Sicily separates the island of Sicily from the coasts of Tunisia. It has a minimum width of about 150 km (between Cape Bon and Mazara del Vallo), a length of about 600 km, and a mean sill of about 400 m depth. It is characterized in the southwest by the wide Tunisian continental shelf and in the northeast by the Sicilian shelf.

The bank on the Tunisian side covers a substantial part of the surface area in the strait. Deeper channels with depths to around 1,000 m exist between the shallow banks. Proceeding southeast from Sicily the depth ranges from 50m to around 600m in the shelf break region (UNEP, 2015).

These two banks are separated by deep water areas from which arises the volcanic island of Pantelleria. Morphologically, the Strait of Sicily exposes irregular bottoms, canyons, seamounts and banks. Maximum depths are reached in three different basins: Pantelleria basin (1,317 m), Malta basin (1,721 m) and Linosa basin (1,529 m) where sediments tend to pile up. It communicates with the western and eastern basins by a narrow sill, NW of Pantelleria Island (400–500 m deep), and a wider channel, SE of Malta (500–600 m deep), respectively. The complex topography of the Strait influences water circulation characterized by filaments, meanders and eddies. These lead to the production of upwelling along shelf edges locally increasing biological productivity. Moreover, its banks have been reported to accommodate important nursery and spawning areas for many fishery resources further exposing the important and sensitive nature of this area.

The Strait is characterized by several oceanographic phenomena. This ecotonal nature is best demonstrated by the co-occurrence of two species of one of the largest Mediterranean gastropods of the genus Charonia, C. lampas lampas found in the western basin and C. tritonis variegata in the eastern basin. The two sub-regions are further divided into four main sub-basins (western Mediterranean, Adriatic Sea, Ionian Sea and Aegean-Levantine Sea) characterized by distinctive hydrodynamics and water circulation patterns.

The Contracting Parties of the Convention on Biological Diversity recognized the Strait of Sicily as an “Ecologically or Biologically Significant Area” (EBSA) in 2014 (Figure 5.1)[5].

In addition, the Regional Activity Centre for Specially Protected Areas (RAC/SPA) started to assess in 2015 the possibility of creating one or more Specifically Protected Areas of Mediterranean Importance (SPAMIs) in the Strait. Moreover, the General Fisheries Commission for the Mediterranean Sea adopted during its 40th meeting (30 May 2016–03 June 2016), a multiannual management plan for the fisheries exploiting the European hake and the deep-water rose shrimp in the Strait of Sicily. The majority of information about its fish diversity though comes from traditional trawl surveys with most of it remaining unknown. The highest species richness in the Strait was recorded at depth of 0–50 m and significantly decreased to remain almost constant in deeper layers.

[5] EBSAs are special areas in the ocean that serve important purposes, in one way or another, to support the healthy functioning of oceans and the many services that it provides. They are not legally binding and are mostly used by countries to support marine spatial planning in national waters and to inform international negotiations on managing areas beyond national jurisdiction.

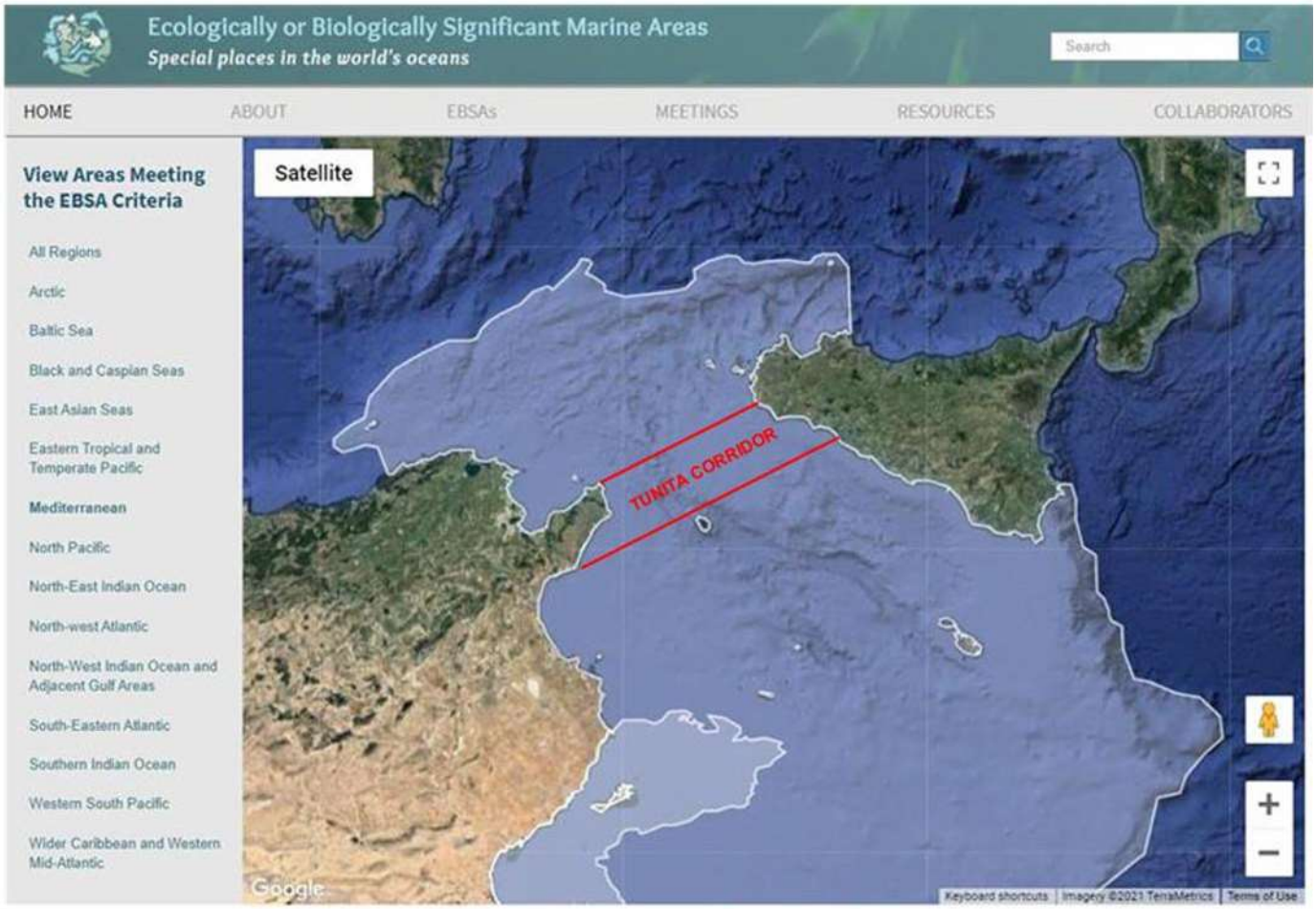

Figure 5.1: Sicilian Channel EBSA

Marine biodiversity is not uniform along this channel and is affected by its complex topography and the hydrodynamic forces in the area. The sections below present the main marine biodiversity components of the Strait of Sicily.

5.1.1 Kelibia Important Marine Mammal Area (K-IMMA)

The cable route crosses the Kelibia Important Marine Mammal Area (K-IMMA).
The perimeter of the IMMA is shown in the following figure.
The trigger species for declaring the K-IMMA was the Mediterranean subpopulation of the Common bottlenose dolphin - *Tursiops truncatus* that was previously classified as Vulnerable.
Nevertheless, the IUCN Red List of Threatened Species re-assessed this subpopulation in 2021 and listed it as Least Concern (https://www.iucnredlist.org/species/16369383/215248781). Accordingly, the conservation status of this species in the area of works is not of main concern.
Nevertheless, applying the precautionary principle for the conservation of species of main concern, vessels are to be equipped with Marine Mammal Observers (MMO) during cable laying operations to spot and identify species like cetaceans and marine turtles amongst others and to monitor on-board adherence to related environmental guidelines. In case of close encounters, the MMO may request halting works until the danger subsides.

Figure 5.2: Location of K-IMMA (source: https://www.marinemammalhabitat.org/imma-eatlas)

Figure 5.3: Cable route (in red) across Kelibia IMMA (perimeter in yellow)

5.2 Flora

In the Strait of Sicily, three main marine seagrasses are present: *Cymodocea nodosa*, *Posidonia oceanica* and *Zostera noltii* (less common).
The overall description of the nearshore area is based on data published on EMODNED portal (EUNIS/full-detail classification map), on ARPA Sicily monitoring reports, scientific literature and interpretation of seabed morphology. The identified seabed habitats are:

- *Posidonia oceanica* beds (A5.535 EUNIS classification- Habitat 1120* "Habitat Directive") - source: EMODNET; ARPA monitoring reports;
- Infralittoral fine sand (A5.23 EUNIS classification) – source: EMODNET;
- Facies of dead "mattes" of *Posidonia oceanica* (A5.5353 EUNIS classification) - source: EMODNET; ARPA monitoring reports;
- Infralittoral rock and other hard substrata (A3 EUNIS classification- habitat 1170 "Habitat Directive") – source: EMODNET;
- Mediterranean biocenosis of coastal detritic bottoms (A5.46 EUNIS classification) – source: EMODNET;
- Mediterranean coralligenous communities moderately exposed to hydrodynamic action or Mediterranean
- coralligenous communities sheltered from hydrodynamic action (A4.26 or A4.32 EUNIS classification) – source: EMODNET; scientific publication; interpretation of seabed morphology;
- Mediterranean communities of shelf-edge detritic bottoms (A5.47 EUNIS classification) – EMODNET.

Nearshore surveys identified three main flora species, *Posidonia oceanica*, *Cymodocea nodosa*, and *Caulerpa sp*. on the cable route.
The project will apply the HDD (Horizontal Directional Drilling) technique that involves drilling from land towards the sea therefore avoiding any negative impacts on sea grass habitats.

5.2.1 Posidonia oceanica

Posidonia oceanica is endemic to the Mediterranean Sea and forms extensive underwater meadows from the surface to over 40m depth with a temperature range between 10 and 30°C. The species propagates mainly via vegetative reproduction through rhizome elongation and cuttings with the fruit requiring 6 – 9 months to ripen. They usually drop off between May and July and float for a while before settling.
Currently, *P. oceanica* is listed as "Least Concern" by the IUCN Red List.
Posidonia oceanica life cycle:

- Summer: During these warm water temperatures, Posidonia leaves are covered by a large number of epiphytic organisms that seek substrate, protection and food from the plant. This leads the plant to develop a brownish shade, causing difficulties in photosynthesis and breathing. During these months, its growth in height is minimal.
- Autumn: Posidonia sheds off its dry leaves and associated epiphytes. At this time, new deep green leaves begin to sprout and flowering begins. The leaf growth continues until the beginning of spring.
- Winter: During winter, falling temperatures slow down the growth of the leaves that started in autumn. The flowering process though continues and the meadows turn into deep green forests.
- Spring: The water temperature increases therefore the growth of the leaves accelerates. The first fruits emerge, the seeds germinate.

Based on the above, and regarding works that disturb *Posidonia*, two windows represent themselves that allow reducing impacts to the minimum by order of priority:
1) Summer season from beginning August until the end of September; and
2) the Winter season between the beginning of December and the end of February.
Visual inspection that the plants have shed all their fruits if works are to be conducted in the summer should determine the beginning of works while visual inspection about the stage of the developing fruits and length of the leaves is also important for winter works (leaves are usually still sprouting and if fruits started to develop, they are not too ripe).

5.2.2 Cymodocea nodosa

Cymodocea nodosa is a key seagrass species in the Mediterranean Sea, forming extensive and patchy meadows in shallow coastal and transitional ecosystems. It is found between the surface and 50 m depth and is recorded to also grow in sheltered environments in two distinct belts, one shallower and the other deeper than *P. oceanica* meadows. It is considered a pioneering species and thought to be more tolerant to environmental fluctuations than *P. oceanica*. A succession of *C. nodosa* communities has been shown to often precede P. oceanica colonization of habitats. It is a perennial species that spreads horizontally and can lose its leaves in winter. This pioneering characteristic makes the species very tolerant to disturbance and exhibits high recovery rates and therefore is not heavily impacted by project works.
Currently, *Cymodocea nodosa* is listed as “Least Concern” by the IUCN Red List.

5.2.3 Caulerpa sp.

Caulerpa sp. is a green marine macro-algae native to tropical waters of the Indian, Pacific and Atlantic oceans. In the 1980s, a specifically bred cold-resistant clone of *C. taxifolia* spread by accident in different parts of the Mediterranean Sea from a public aquarium in Monaco. Known as the ‘aquarium strain’, it grows rapidly between the months of July and November, is known to smother seagrasses and are extremely difficult to eradicate. In the Mediterranean, it reproduces by vegetative dispersion with the probability of reestablishment of fragments (composed of stolon, blade and rhizoid) being greater in summer at shallow depths than in the other seasons or in deep waters.
In order to mitigate the spread of this species, works are best carried-out in the winter season when sea water temperatures are at their lowest.

5.3 Fauna

5.3.1 Cetacean Fauna

The strait of Sicily hosts various cetaceans species associated with deep waters; Vella and Vella (2012) suggested that the strait of Sicily hosts various cetaceans species associated with deep waters and to prey on species found in deep waters.
Mainly the striped dolphin (*Stenella coeruleoalba*), the common dolphin (*Delphinus delphis*) and the bottlenose dolphin (*Tursiops truncatus*) represent the “Toothed Whales” in the strait of Sicily (Aissi, Mehdi & Vella, Adriana. 2015).
Literature and ferries observation identify also other whale and dolphin subpopulations as listed in Table 5.1.

Table 5.1: Main cetacean subpopulations in the Strait of Sicily

Cetacean Subpopulation	Description
Stenella Coeruleoalba (Striped Dolphin)	Striped dolphin in the Mediterranean is currently proposed to be listed on the IUCN Red List as Vulnerable. The Mediterranean population of striped dolphin is particularly exposed to high levels of chemicals and heavy metals, which have severe effects on their reproduction and immune system. It qualifies for listing as Vulnerable based on criterion A4 (UNEP, 2015). The Striped Dolphin subpopulation is distributed close to submarine slopes and escarpments of the strait of Sicily according to regular monitoring sightings using ferries sightings financed by ACCOBAMS (Agreement on the Conservation of Cetaneans of the Black Sea, Mediterranean Sea and Contiguous Atlantic Sea). This study pointed out a similar habitat use (preference to open waters) as major Mediterranean areas where striped dolphins were spread over neritic and pelagic environments. Although overall the striped Dolphin is the most abundant cetacean in the Mediterranean, both in the eastern and the western basins, this ichtyo-teutophageous (fish and squid eater) species is considered covering major of pelagic waters in this area. (UNEP, 2015). Moreover during the 2013 survey by the Italian CNR (National Centre for Research) 3 groups of Stenella Coeruleoalba were found.
Delphenus Delphis	The Delphenus Delphis (short-beaked common dolphin) is a small cetacean species with a wide distribution. In 2003 the Mediterranean common dolphin 'subpopulation' was listed as endangered in the IUCN Red List of Threatened Animals, based on criterion A2, which refers to a 50% decline in abundance over the last three generations, the causes of which 'may not have ceased or may not be understood or may not be reversible' (Bearzi et al., 2003). The species is present in the Sicily Channel (Cavalloni, 1988; Arcangeli et al., 1997) with larger groups being observed around Malta (Vella, 1998, 1999) and the Cap Bon area (Northern Tunisia) (Benmessaoud et al., 2012). In these two areas, the common dolphins reportedly associate with bluefin tuna Thunnus thynnus. Both shallow and deeper water habitats are utilized where it may be observed also in association with bottlenose dolphins or striped dolphins (Benmessaoud, pers. com). Indeed, the species is today relatively abundant in the Sicily channel around Malta and in the Cap Bon North-Eastern Tunisia (Figure 16). Although common dolphins were considered relatively abundant in much of the Mediterranean until a few decades ago, large-scale population decline has occurred, and today they survive only in small portions of their former Mediterranean range. Indeed, these dolphins have become rare or are completely absent in some Mediterranean ex-suitable habitat. Standing data of this species in the strait of Sicily is rather inexistent, however rare stranding events were recorded along the Tunisian (Karaa, 2009) and Maltese coastline (Vella, 2005). The 2013 survey by the Italian CNR (National Centre for Research) identified 4 groups of Delphenus Delphis.
Tursipos Truncatus (Bottlenose Dolphin)	The bottlenose dolphin is one of the most frequently observed cetaceans in the Mediterranean (e.g. Gnone et al., 2011). They occur in most coastal waters of the basin and have been reliably reported in the waters of Tunisia, Sicily, Pantelleria, Malta and Lampedusa. They have been studied only in relatively small portions of the basin, and wide areas remain largely unexplored (Bearzi et al., 2008).

Cetacean Subpopulation	Description
	The species was classified as Vulnerable and is also listed in the Annex II of the Habitats Directive(Council Directive 92/43/EEC), as a Species of Community Interest. (Reeves et al., 2006). This species are widely distributed throughout the Mediterranean and occur in most coastal waters. They occur regularly around many of the region's offshore islands and archipelagos (Bearzi et al. 2008). Stranding events of this species is very common in the strait of Sicily. Indeed, bottlenose dolphin is the most regularly identified species stranded along the Tunisian coasts. Though the bottlenose dolphin is one of the cetacean species mostly adapted to, and associated with shallow waters, its offshore relatives can spend most of their time in deeper waters and dive to over 400 m for their prey. During the 2013 survey by the Italian CNR 59 groups of T.Truncatus were detected.
Fin Whale (Balaenopetra Physalus)	The fin whale is the largest free-ranging predator found in the Mediterranean. Mediterranean fin whales are currently defined as a distinct subpopulation from those in the North Atlantic, perhaps extending out to southern Portugal (IWC 2009). Analysis of the bottom topography of the strait of Sicily points out the existence of attractive top predators features, considered a likely suitable features to the Mediterranean fin whale sub-population during winter. Fin whale presence in this area has been supported also by the stranding data accessible from the ''Mediterranean Database of Cetacean Strandings'' (MEDACES) and the Tunisian stranding network. Due to the endangered status of the fin whale world around, and not especially in the Mediterranean basin, this specie has been protected under both the Endangered Species Act (ESA) (as endangered) and the Marine Mammal Protection Act (MMPA). Although, it is listed as "endangered" by the IUCNand is listed in Appendix I of the Convention on International Trade in Endangered Species of Wild Fauna and Flora (known as CITES). Thus, fin whale distribution in the Sicily Channel may underline the importance of these areas as having a special importance for life history of this specie. In 2013 the Italian CNR (National Centre for Research) published a study regarding the Bottlenose dolphin presence in the coastal area from Capo San Marco and Capo Feto (Boldricchi et al. 2013); one group of Balaenoptera physalus was found.
Sperm whale (Physeter macrocephalus)	Sperm whale observation in the strait of Sicily is restricted to few occasions during the monitoring of this area throw ferries.The relatively common occurrence of sperm whale mortality events along the Tunisian coastline is quiet constant year round with highest relative frequencies during spring and summer. These events were mainly taking place in the western Mediterranean part exclusively for single individuals. No mass stranding were reported in this area and body lengths varied from 6 to 14 m. Although there are historical accounts of large groups of sperm whale in the strait of Sicily, recent visual and towed hydrophone surveys indicate rather low densities (Lewis et al., 2007). However, monitoring at the NEMO-ONDE neutrino detection array sited 20km off the east coast of Sicily had provided detections of sperm whales year round with a peak in April and October. Acoustic length measurement indicates that animals with a range of body lengths are present but none exceeded 15m, indicating an absence of the oldest male sperm whales.

5.3.2 Caretta Caretta

Caretta Caretta is a charismatic species, protected by international conventions (e.g., Bern Convention, Annex II; Washington Convention—CITES, Annex II) and by European national and regional laws (e.g., Habitat Directive 92/43, Appendices II and IV). IUCN Assessment: "Vulnerable" (Vecchioni et al., 2022).
It has been subject to several investigations lately especially with regards to its nesting areas and the negative effects of marine pollution of this endangered species.

5.3.3 Fisheries

Significant ecological and biological components coexist spatially in a relatively limited area considered as a biodiversity hotspot within the Mediterranean (Tunisia, Malta, Libya, Italy, and Egypt). Seamounts and deep-sea corals are found close to Sicily including mounds of white corals, which are vulnerable species and provide valuable habitat for a number of other species.
The complex oceanographic conditions in this area lead to high productivity and result in good conditions for fish spawning, and therefore the relationships between environmental variables and distribution and abundance of living resources need further elucidation. For example, environmental parameters such as salinity and temperature may act as barriers and lead to differences in fish assemblages. Furthermore, environmental enrichment processes, as those occurring along the southern Sicilian coasts or along the southern Tunisian coasts affect food resources concentration and strongly influence the density of some species, therefore determining their availability to fisheries.
The Sicilian Channel is an important spawning ground for a number of commercially important fish species, including bluefin tuna, swordfish and anchovy, as well as a number of demersal fish species. An important nursery area for the endangered white shark. The Sicilian Channel is thought to be the last important habitat for the critically endangered Maltese skate.
To go deeper, analysis of environmental factors in summer periods found that most of the variability in small pelagic fish assemblages was due to the habitat differences between the northern Strait of Sicily and southern Tunisian waters. The anchovy Engraulis encrasicolus and the sardine Sardina pilchardus are the two main small pelagic supporting local fisheries. On a yearly basis, the MEDIAS program estimates their biomass and distribution through acoustic surveys.
Even though bluefin tuna spawns in several Mediterranean regions, the eastern coast of Sicily seems to concentrates large number of eggs and larvae. Traditional fishing activities ("tonnare") in this region as in other regions around the world have switched to purse seine and longlines. As for the swordfish (Xiphias gladius), it is the second most important large pelagic species in the Mediterranean Sea. The International Commission for the Conservation of Atlantic Tunas (ICCAT) recognizes a single Mediterranean stock of X. gladius with the Strait of Sicily being the most important spawning ground for the species. Furthermore, the Strait is a biodiversity hot spot for a great number of shark species, some of which have become rare or are no longer present in other regions of the Mediterranean. In this context, the Strait was identified as one of the most important spawning areas of the resident and genetically distinct white shark (Carcharodon carcharias).
The Strait of Sicily is also one of the areas with the greatest richness of demersal species in the Mediterranean basin that are greatly affected by fishing activities. Many fishes of commercial interest occupy the meso-littoral layer such as red mullets (e.g. Mullus surmuletus; Mullus barbatus) and the pandora bream (Pagellus erythrinus). Common other demersal species such as the Sea robins Lepidotrigla cavillone, the flatfishes Solea kleini and the scorpion fish Scorpaena scrofa can also be found. Studies carried out in Maltese waters identified significant differences in species diversity and abundance between protected and unprotected areas further documenting the impacts of fishing on marine ecosystems. More specifically, the area is particularly known or its rich community of elasmobranchs and accommodates the largest number of species in the north Mediterranean Sea. The greatest diversity though was reported from the offshore bank on the western part of the south Sicilian shelf. Fish diversity consistently increased with habitat complexity and was distinguished by the presence of uncommon and poorly known species and by the aggregation of vulnerable elasmobranchs such as Myliobatis aquila. Furthermore, the continental slope of the Adventure Bank at depth of more than 200 m is dominated by soft-bottom communities including species of tropical or subtropical origin (e.g., the giant red shrimp Aristaeomorpha foliacea; the deep-water rose shrimp Parapenaeus longirostris). Several studies have also found that the outer edges of the Adventure and Malta banks play essential recruitment roles of important commercial species such as the hake Merluccius merluccius and the deep-water rose shrimp P. longirostris.

Along the coast of the Middle East and North Africa until the Strait of Sicily, some NIS have recently become commercially valuable and have entered local fisheries. Such species are expected to increase across the whole basin due to the doubling of the Suez Channel in 2015. Even though the Strait of Sicily acted as a biogeographic barrier to a sudden expansion of NIS in the western Mediterranean, this role has been modified as response to rising temperatures due to climate change.
Furthermore, deep-sea coral assemblages (habitats for fish and invertebrate communities) act as marine biodiversity hotspots and are indicators of the vulnerability of marine ecosystems. In the Mediterranean Sea, deep-sea coral habitats are associated with commercially important crustaceans. Since they are highly vulnerable to human impacts such as fishing due to their life history traits, their abundance has dramatically declined due to the effects of trawling.
The waters south of Sicily [Geographical Sub Area (GSA) 16, according to the FAO General Fishery Commission for the Mediterranean (GFCM)], corresponding to the northernmost sector of the Strait of Sicily, are among the most productive areas for demersal fisheries in the Mediterranean (Milisenda et al., 2017; Di Lorenzo et al., 2018; Falsone et al., 2020). The landings of the following seven species accounted for approximately 8% of the total Mediterranean landings for cephalopods (FAO Fisheries and aquaculture software, 2021): horned octopus Eledone cirrhosa (Lamarck, 1798), Musky octopus Eledone moschata (Lamarck, 1798), broadtail shortfin squid Illex coindettii (Verany, 1839), European squid Loligo vulgaris (Lamarck, 1798), common octopus, Octopus vulgaris (Cuvier, 1797), common cuttlefish Sepia officinalis (Linnaeus, 1758), and lesser flying squid Todaropsis eblanae (Ball, 1841).

5.3.4 Phytoplankton and Zooplankton Communities

Few studies have addressed the environmental factors affecting phytoplankton and zooplankton communities in the Central Mediterranean. Specifically, more advanced models are required to clearly describe the processes driving energy exchange from primary producers up to top consumers.
Some studies though reported that Chlorophyll in the Strait of Sicily ranged between 14 and 60 mg m−2 in the 0–100 m depth stratum. Primary productivity was higher in the western sector of the area (Adventure bank) with values up to 524.61 mg m−2 day between 0 and 20 m depth compared to the minimum value of 218 mg m−2 day in the south-eastern sector. Oceanographic surveys carried out in the Eastern Mediterranean in the 90's showed an increased abundance of meso-zooplankton in the Strait with the recorded mean value almost one order of magnitude greater than in other areas. In June 1999, zooplanktonic biomass values displayed clear spatial patterns with high density values in the western region corresponding to upwelling areas. In addition, zooplanktonic biomass recorded higher values in neritic waters than in pelagic and coastal waters.

5.3.5 The benthos

Information on the benthic communities of the Strait is limited due to the few and scattered studies in time and space. It also seems that knowledge is mostly lacking on the main benthic communities on the offshore banks.

Current knowledge shows that benthic communities in the Strait of Sicily are mostly dominated by rheophilic species with an Atlantic affinity. Hard substrates of infralittoral bottoms are dominated by the sea-grass meadows of Posidonia oceanica while deeper bottoms of the circalittoral are colonized by populations of large brown algae such as Cystoseira, Sargassum, and Laminaria as well as an array of other species.

In the Strait of Sicily, the circalittoral are often sandy with grains ranging from coarse to very fine with abundant larger detritus of organic origin such as shell fragments and calcareous plants. These sedimentary bottoms are swept by unidirectional and oscillating currents and host populations of calcareous red algae (Maerl beds), sponges (e.g. Crambe crambe), cnidaria (e.g. Eunicella cavolini, Astroides calycularis), polychaetes (e.g. Serpula vermicularis), brachiopods (e.g. Argyrotheca cuneata), bryozoa, crustaceans (e.g. Lissa chiragra), echinoderms (e.g. Ophidiaster ophidianus), bivalves (e.g. Manupectenpes felis, Lima vulgaris) and sea squirts (Rhodosomacallense). The observed sea urchin Cidaris cidaris are considered as outsiders coming from the bathyal zone. Soft seaweeds are also abundant. At low depth, the green seaweed Cladophora fracta is predominant, elsewhere other algae are common (e.g. Dictyota dichotoma, Laminaria rodriguezii). L. rodriguezii beds are of particular concern since they serve as nursery grounds for the catsharks Scyliorhinus canicula and S. stellaris. In addition, the Strait of Sicily presents some species of sub-tropical origins such as

the Portuguese sole Synaptura lusitanica and the corb Umbrina ronchus, Cynoponticus ferox, Facciolella oxyrhyncha, and Epigonus constanciae amongst many others.

The hard bottoms of the deeper bathyal layer are distinguished by huge 'buildings' produced by madrepores (e.g. Madrepora oculata, Lophelia prolifera), generally forming scattered clumps of 'white coral assemblages' locally known as 'cannelleri'. These formations make such grounds dangerous for trawl fishing and other activities on the sea floor. At higher depths, a less hard white coral, Dendrophyllia cornigera, also presents obstacles for activities taking place at the sea floor. In these areas, the most typical biological indicator species is the rare Sea pen Funiculina quadrangularis since its occurrence is closely related to the abundance of food supply. The brachiopod Terebratula vitrea dominates in a few zones, but is always associated with F. quadrangolaris as is the pink shrimp Parapenaeus longirostris. The Norway lobster, Nephrops norvegicus has also been recorded. As for cartilaginous fishes, they are well and constantly represented by dogfishes (e.g. Etmopterus spinax, Scyliorhinus canicula) and skates (e.g. Raja oxyrinchus, R. miraletus).

It is worthy to note that a geo-biological exploration of rocky bottoms located between 350 and ca. 800 m depth identified several sites with diverse deep-water scleratinian corals community as well as large colonies of antipatharians and gorgonians. At depths ranging between 90 and 800 m, numerous deep coral species have been identified such as Corallium rubrum, Dendrophyllia cornigera, Desmophyllum cristagalli, the white corals Lophelia pertusa and Madrepora oculata in addition to the black coral Leiopathes glaberrima. Furthermore, an extended coral forest constituted almost exclusively of L. glaberrima was discovered between 250 and 400 m offshore the south coast of Malta. In addition, large clusters of the giant barnacle Pachylasma giganteum, one of the few living populations recorded in the Mediterranean were also reported in the area.

5.4 Marine survey

Marine survey's route and organization is described in paragraph 1.2.
The results in terms of habitats identified along the route are illustrated hereafter for the two alternative landfalls of Kelibia and Menzel Horr and for the offshore route.

5.4.1 Nearshore survey

5.4.1.1 Kelibia

5.4.1.1.1 Power cable

Kelibia working area is largely influenced by Posidonia oceanica. Starting from the coast, Posidonia extends from 3.0m of water depth (WD) at KP 199.570 to its lower limit at 29.0m WD at KP 197.405 on the route.
Posidonia meadow spreads all across the survey corridor. The Figure 5.4. shown the Posidonia visual inspection Lower limit, highlighted in green, and the locations of the ROV images. Posidonia is observed growing over matte (Figure 5.4, photo 1 and 4), matte and probably calcareous algae (photo 2) or sand (photo 3).

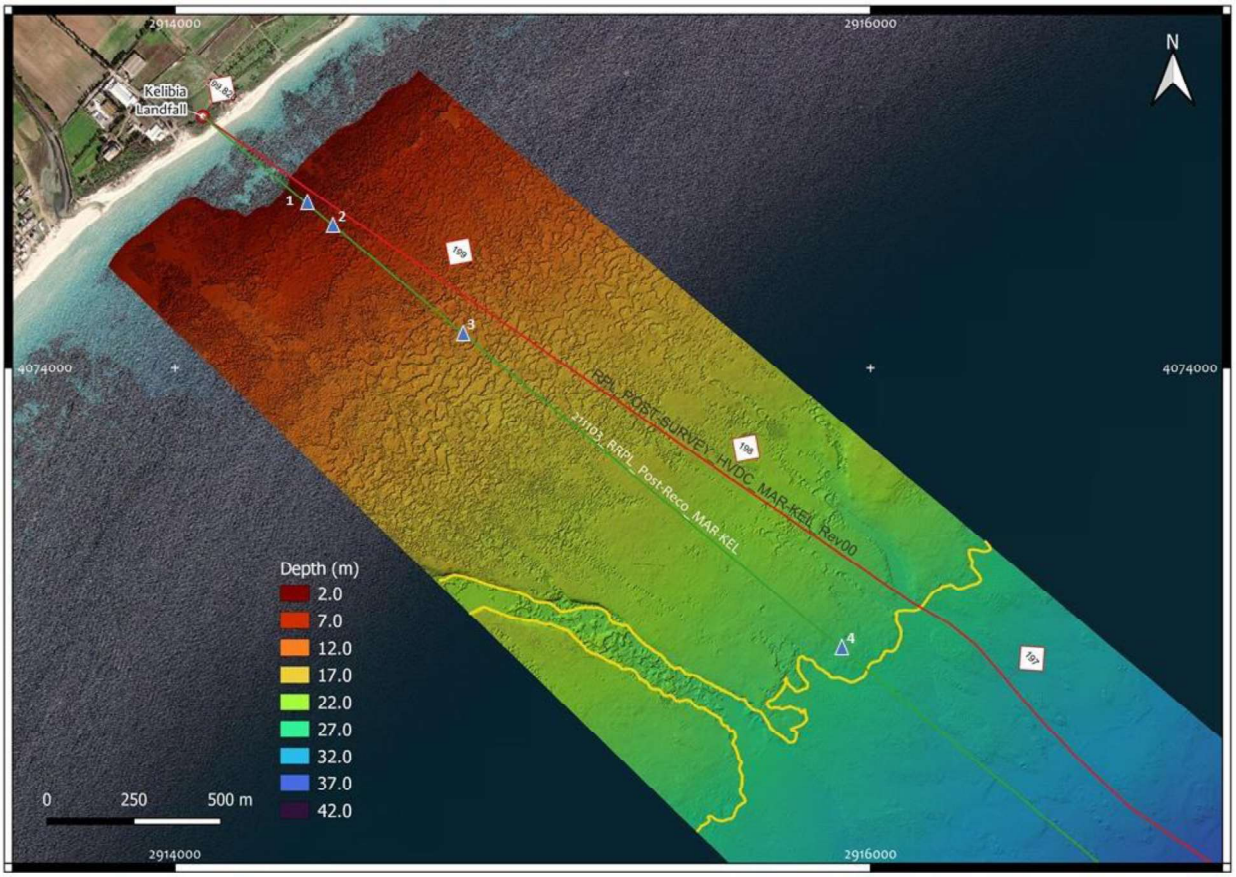

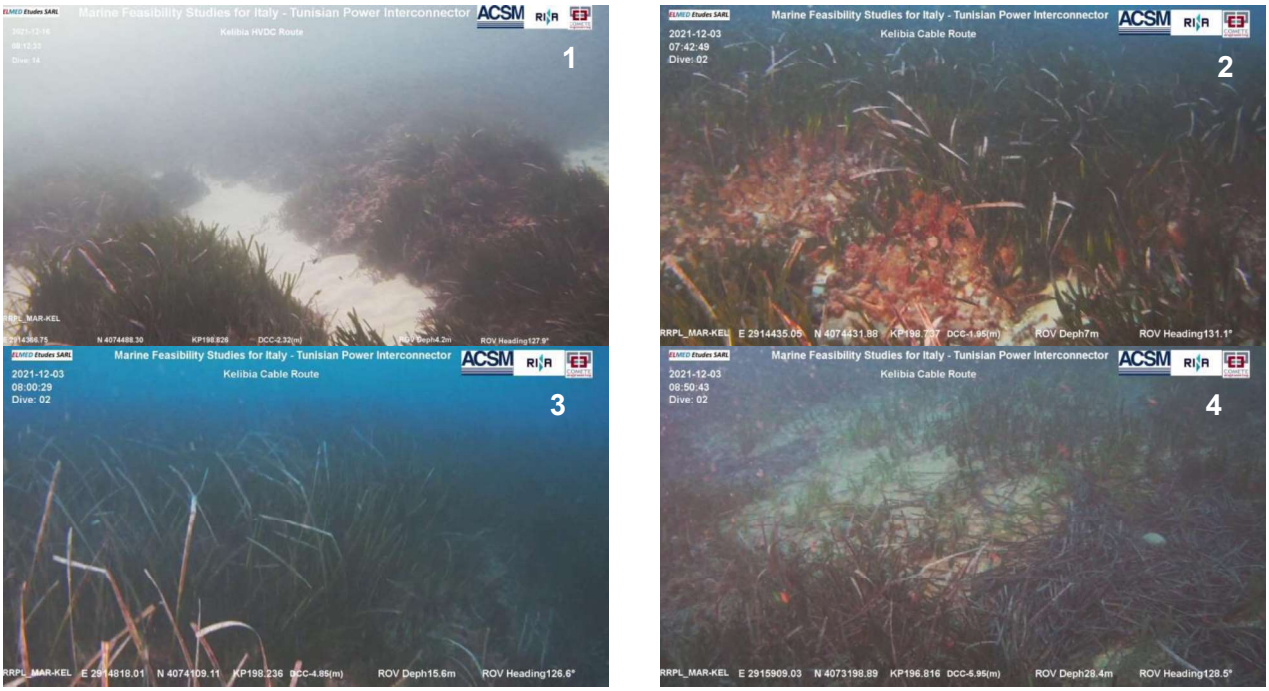

Figure 5.4: Posidonia distribution along the route

Biogenic concretions were detected from the start of the Nearshore survey area at KP 195.887 up to the limit of the Posidonia meadow at KP 197.320. The nature of these “rock” patches seems to be biogenic from the ROV Visual Inspection images, showing local presence of pre-coralligenous (in the photic area) and

coralligenous (in the aphotic area) substrates. (Figure 5.5). Coralligenous substrates result from the growth of red calcareous encrusting algae (mainly *Lithophyllum spp*.) and represent a key habitat of the Mediterranean continental shelf because of their structural and functional importance, as well as for their high aesthetic value (Chimenti et al., 2017). Due to the fact that coralligenous habitat may host a high variety of species (i.e. sponges, gorgonians, crustaceans, mollusks Ruitton et al.) they are often included in IUCN red lists and considered a sensitive habitat by European Habitat directive 92/43/CE Annex I (habitat code:1170, reef) and in the EU Marine Strategy Framework Directive 2008/56/EC, (MSFD). In Figure 5.5 some gorgonians are shown growing on sandy seabed, indicating the presence of a hard substrates covered by sandy sediments.

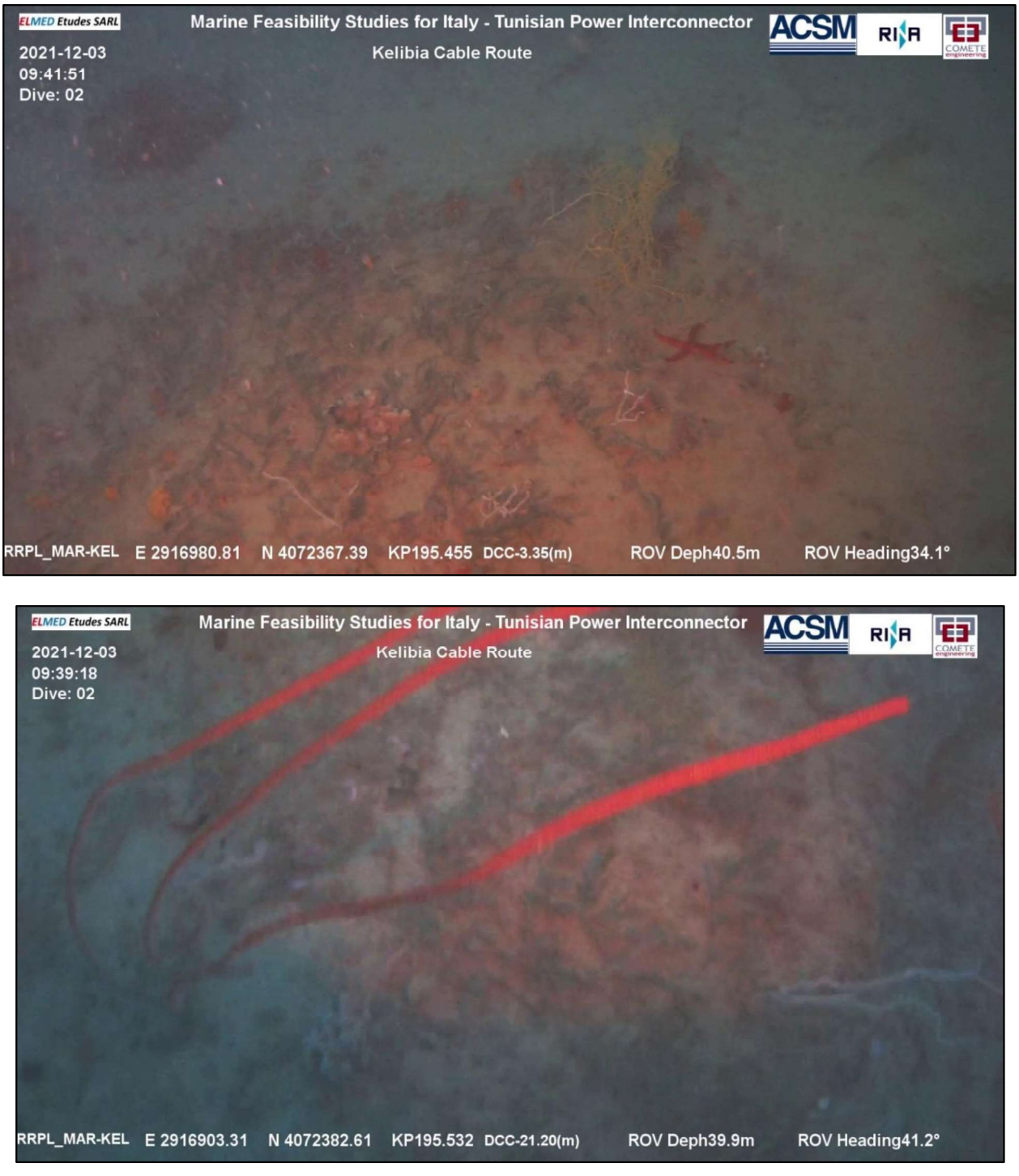

Figure 5.5: Biogenic concretion examples within Kelibia survey area

The biogenic concretions indicate locally hard seabed patches between large extensions of fine to coarse sand possibly covered by *Caulerpa sp (*probably *taxifolia)* assemblages (Figure 5.6). Please note how a confident *Caulerpa* species determination will be only possible through future samplings and analysis (Figure 5.6).

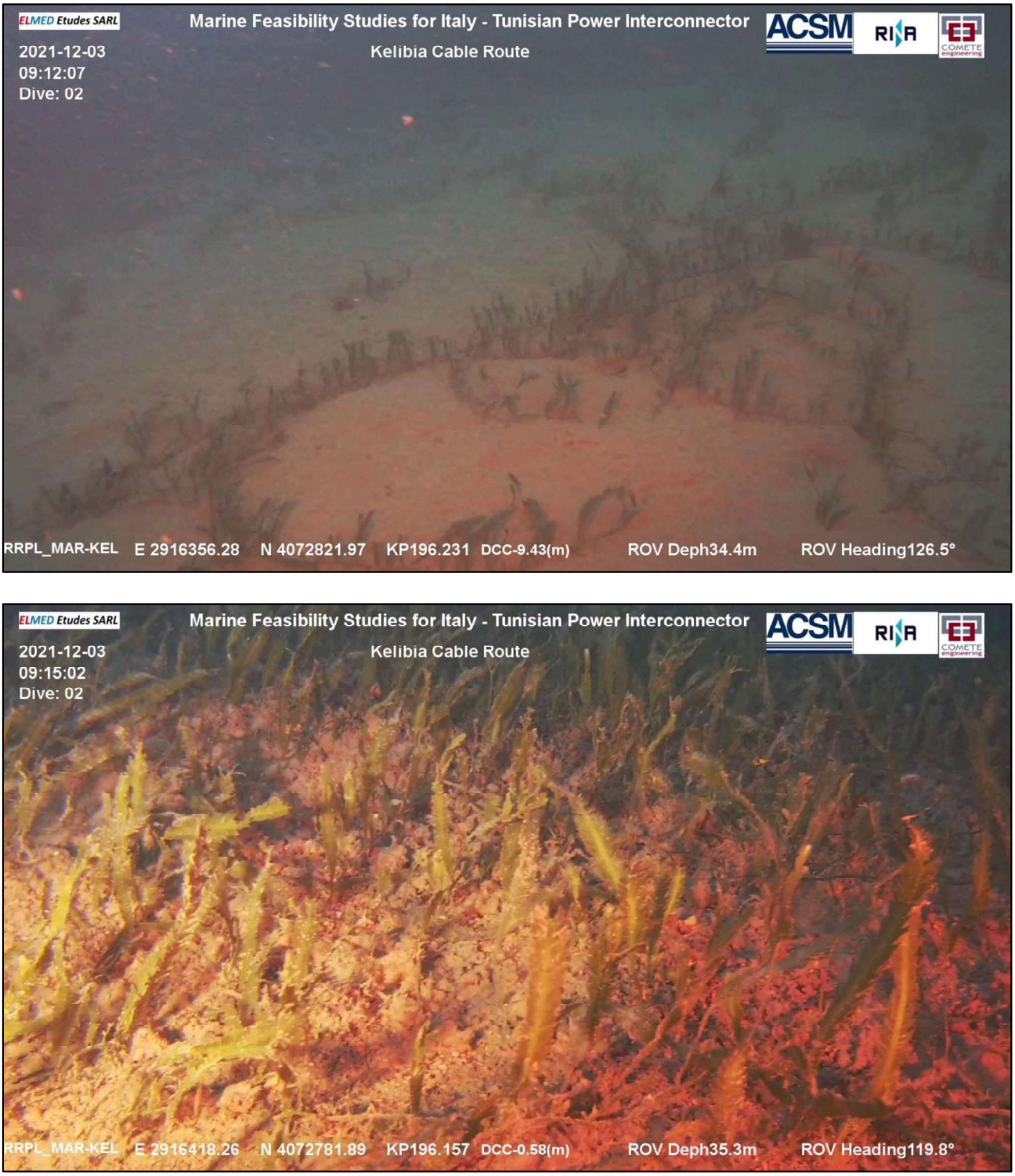

Figure 5.6: Sandy seabed with possible *Caulerpa sp* examples within the Kelibia survey area

The large number of scars found within the Kelibia area indicates an intense fishing and anchoring activity (Figure 5.7). It is to be highlighted that this part of the Tunisian coast is often used by all sort

of vessels as a shelter area in case of rough weather conditions in the Sicily Channel thus new anchor scars may be found at any time.

No other anthropic activities evidence have been detected.

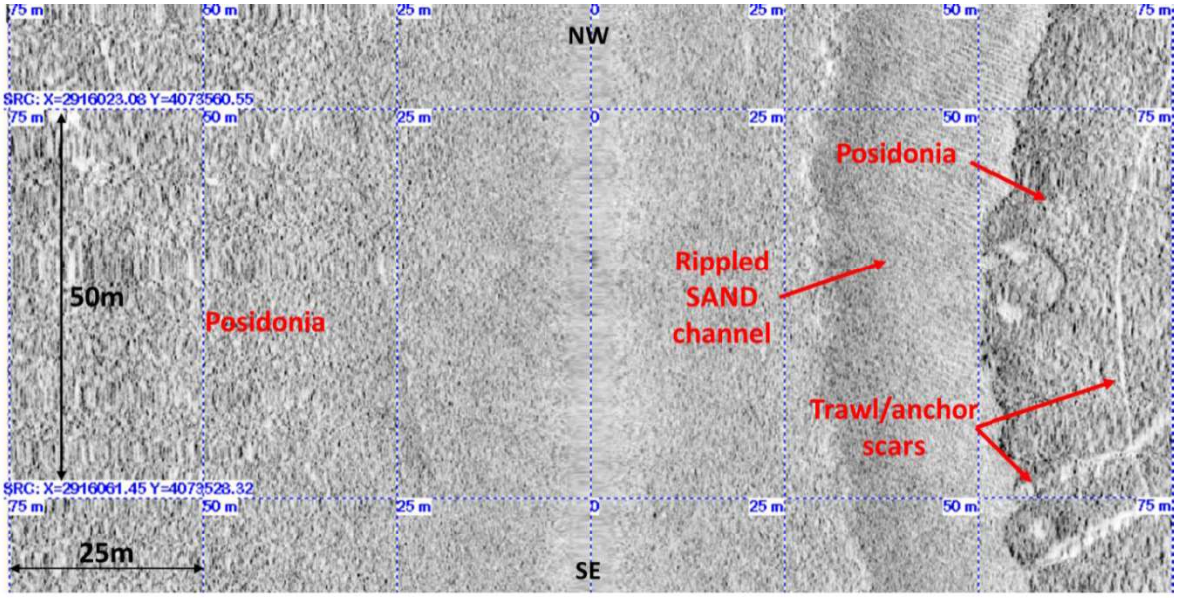

Figure 5.7: Example of scars within Kelibia survey area

5.4.1.1.2 Electrode cable

Kelibia MVDC working area is largely influenced by Posidonia oceanica. Starting from the coast, Posidonia extends from 2.6m WD at KP 0.320 to its lower limit at 29.1m WD at KP 2.382 on the route.

Posidonia meadow spreads all across the survey corridor, growing over matte and probably calcareous algae (Figure 5.8-photo 1), sand (-photo 2 and 3) and matte (-photo 4). In Figure 5.8. the Posidonia visual inspection Lower limit is highlighted in yellow and the image locations of the ROV VI pictures are shown.

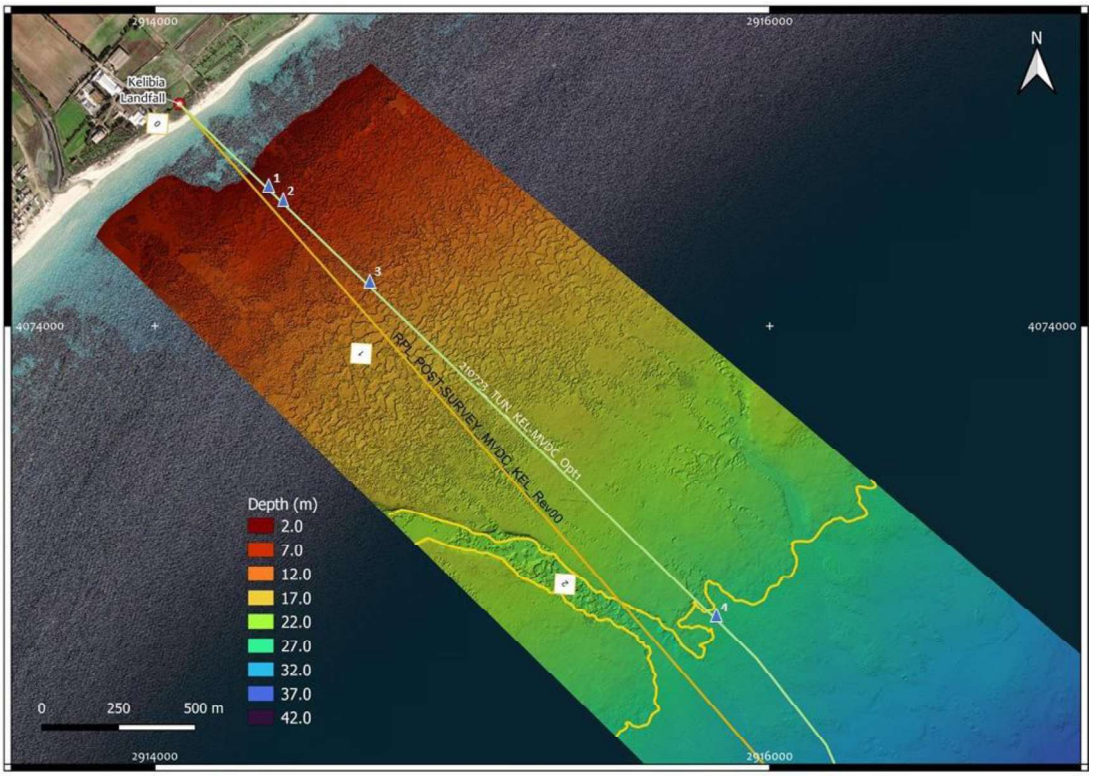

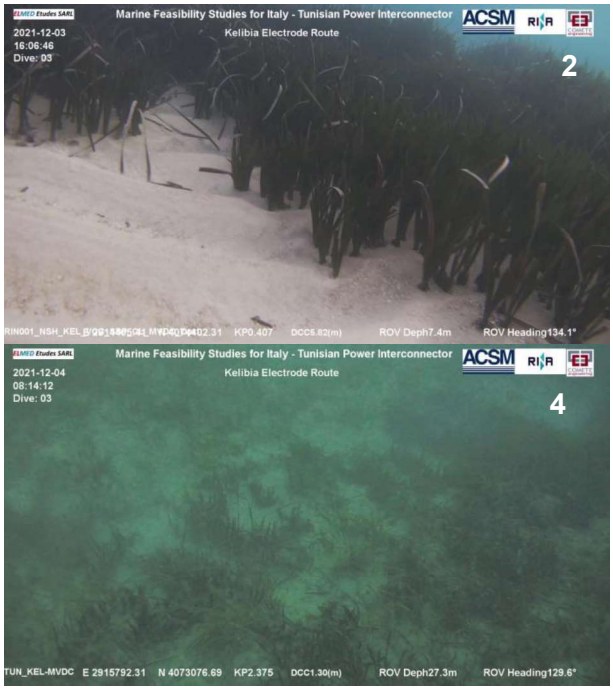

Figure 5.8: Posidonia distribution along the route

Biogenic concretions were detected from the end of the Posidonia meadow at KP 2.453 up to the end of the route at KP 8.772. As in Kelibia HVDC survey area, the nature of these “rock” patches seems to be biogenic from the ROV Visual Inspection images, showing local growth of pre-coralligenous assemblages in Figure 5.9 some gorgonians are shown growing on sandy seabed, indicating presence of hard substrates covered by fine sediments within large extension of fine to coarse sand seabed.

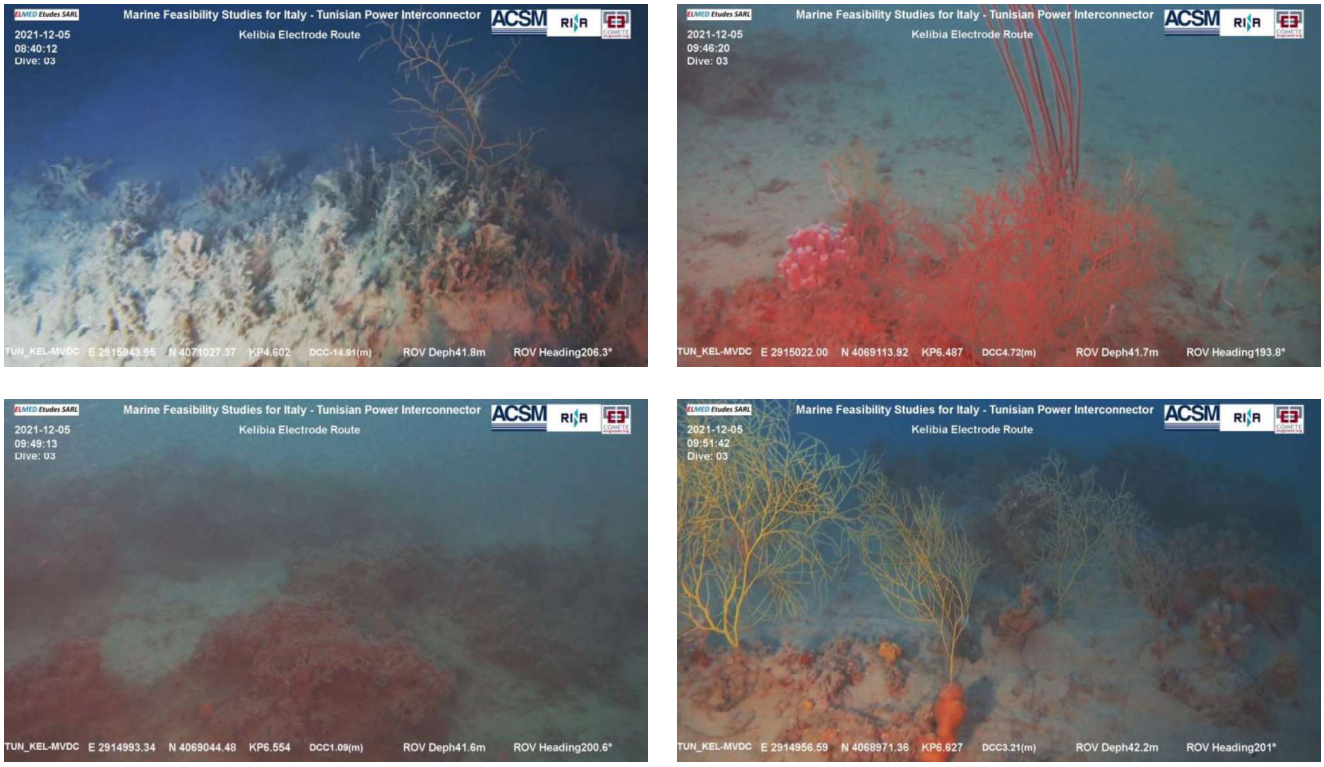

Figure 5.9: Biogenic concretion examples within the Kelibia MVDC survey area

In additions, sandy areas are seen covered with *Caulerpa* sp. *(*probably *taxifolia)* assemblages. *Caulerpa* specie determination will be possible only through samplings and analysis (Figure 5.10).

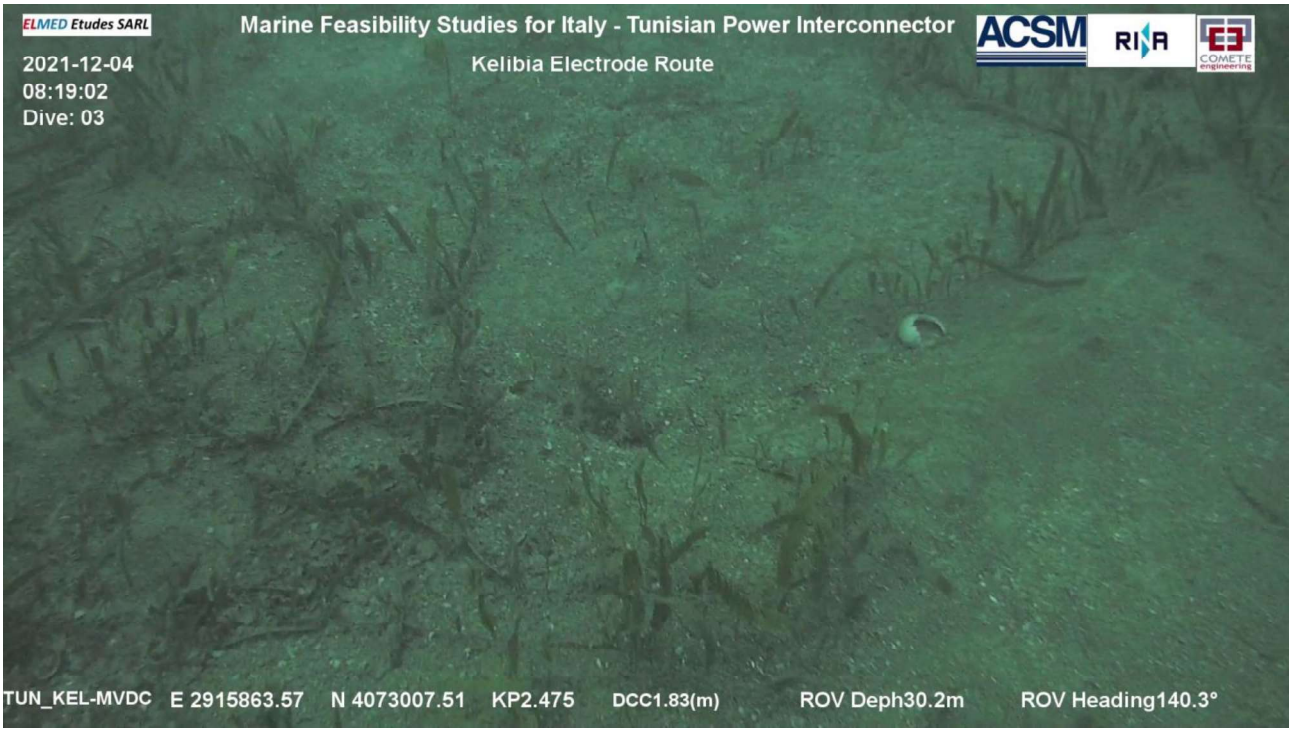

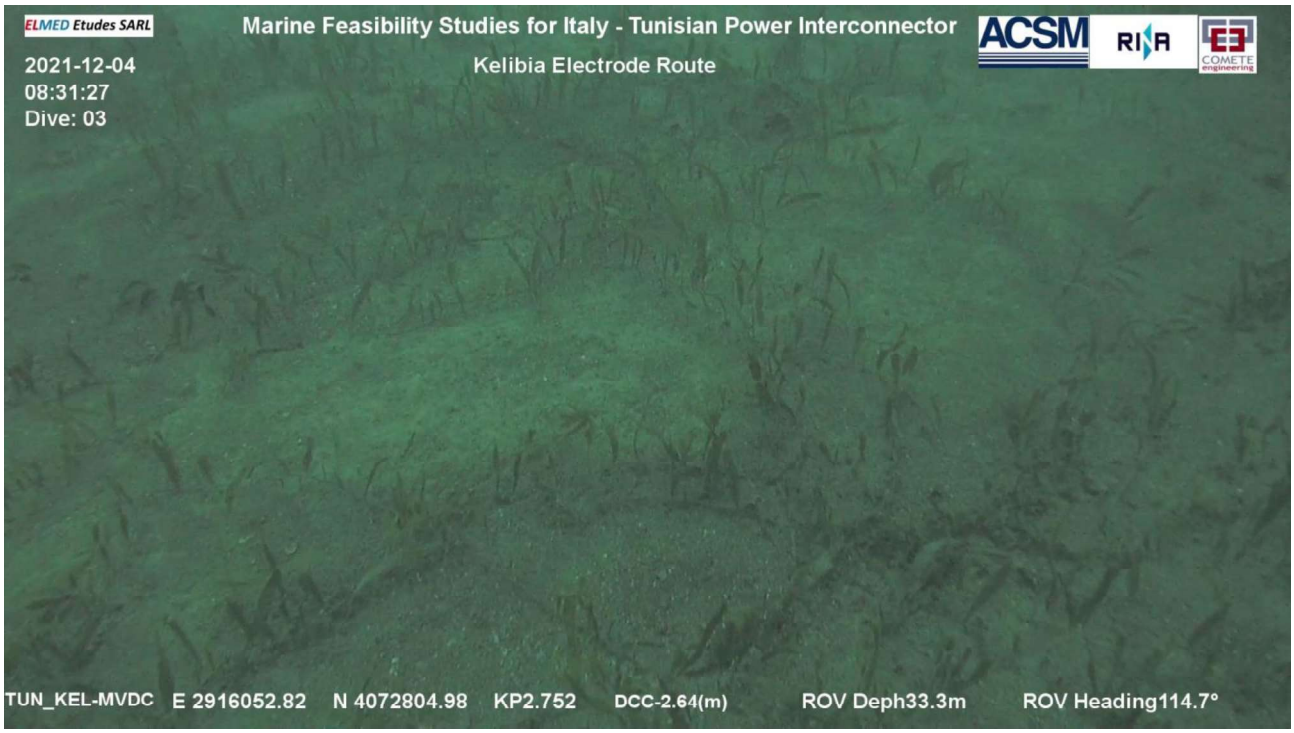

Figure 5.10: Sandy seabed with *Caulerpa sp* examples within the Kelibia MVDC survey area

The large number of scars found within the Kelibia-Option1 MVDC area indicates an intense fishing and anchoring activity (Figure 5.11). It is to be highlighted that this part of the Tunisian coast is often used by all sort of vessels as a shelter area in case of rough weather conditions in the Sicily Channel thus new anchor scars may be found at any time.

No other anthropic activities evidence have been detected.

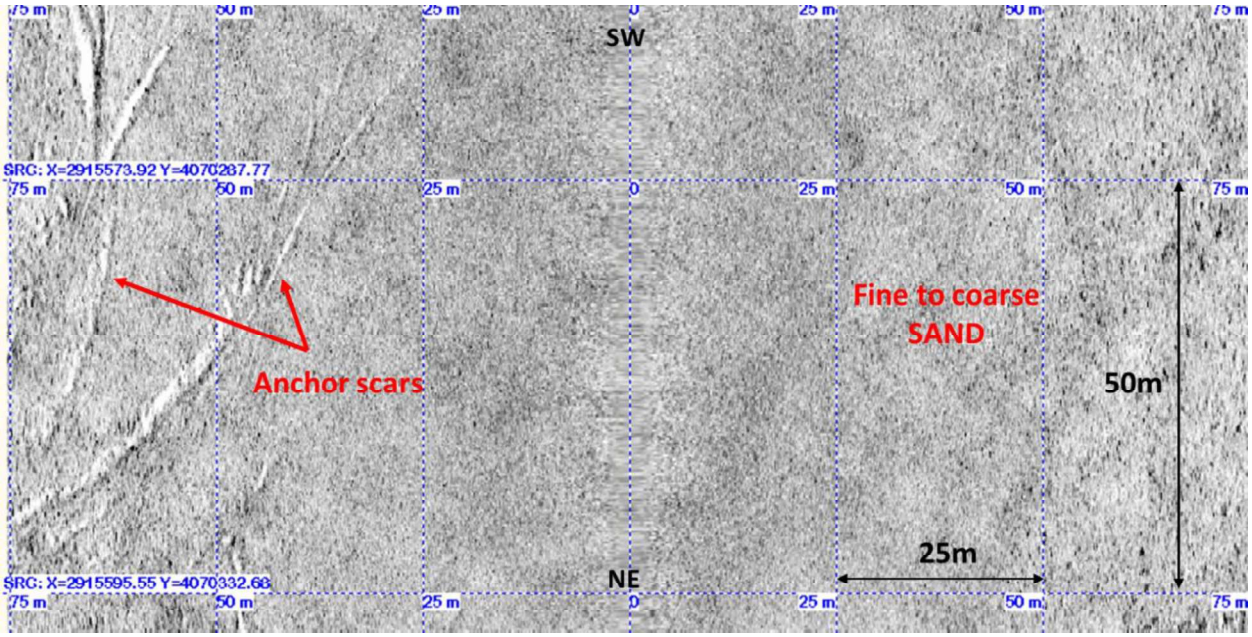

Figure 5.11: Example of anchor scars within Kelibia-Opt1 MVDC survey area (KP 5.704)

5.4.1.2 Menzel Horr

5.4.1.2.1 Power cable

Menzel Horr working area is influenced by Posidonia oceanica on its nearshore area. Starting from the coast, Posidonia extends from 6.3m of water depth (WD) at KP 205.209 to its lower limit at 23.0m WD at KP 203.141 on the route.

Posidonia meadow spreads along the Eastern part of the survey corridor. In this area, most of the Posidonia meadow is replaced by *Caulerpa sp*, the ROV Visual Inspection findings consist in almost dead *matte* and Posidonia leaves (Figure 5.12).

A small patch of Posidonia is present on the western part at about 100m of the route. Between this small patch and the main meadow, there is a narrow area 150m wide free of Posidonia and covered with fine to coarse loose sediment (SAND).

The limits of the Posidonia meadow are highlighted in yellow in Figure 5.12 and Figure 5.13, together with images collected during the ROV visual inspection.

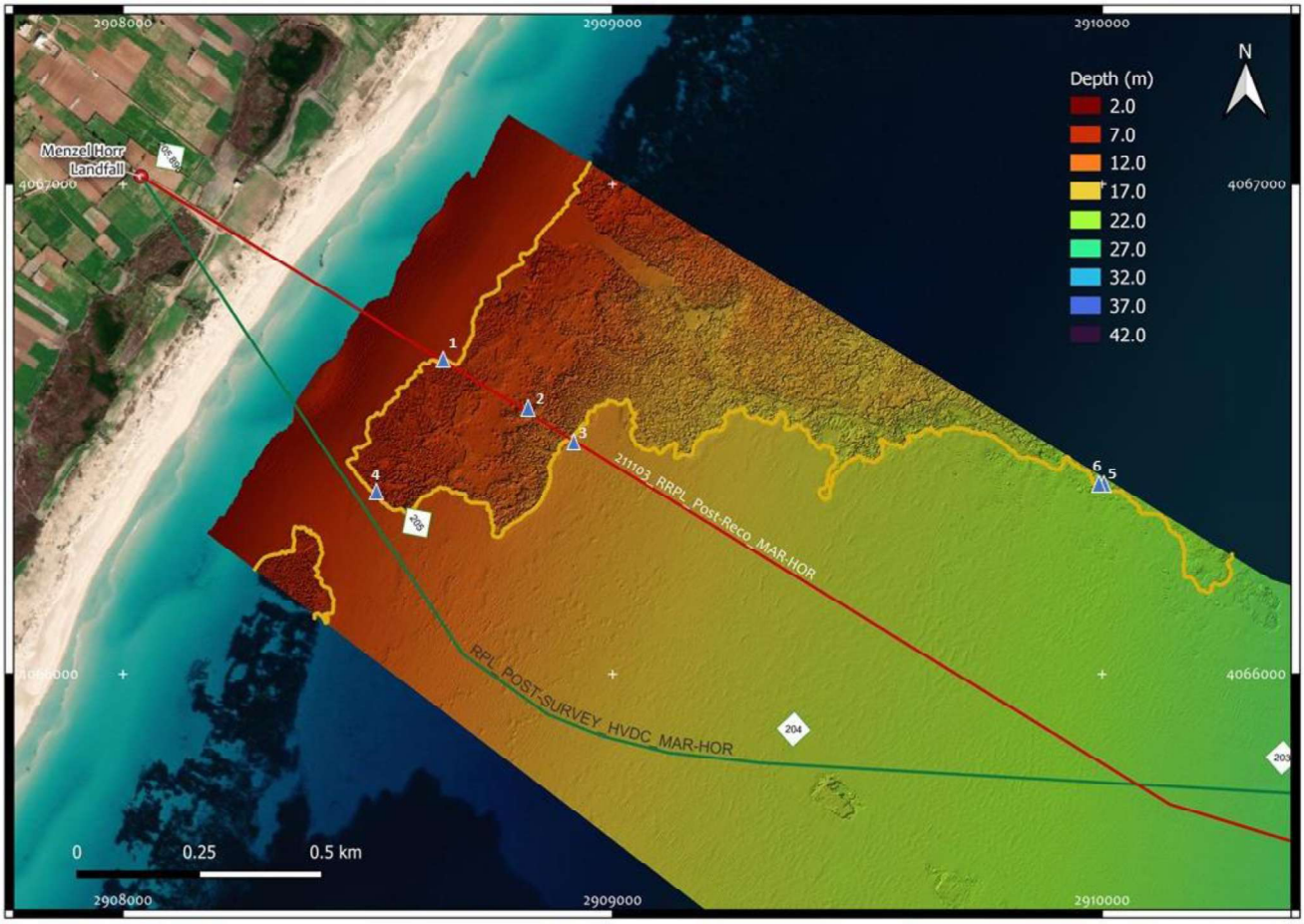

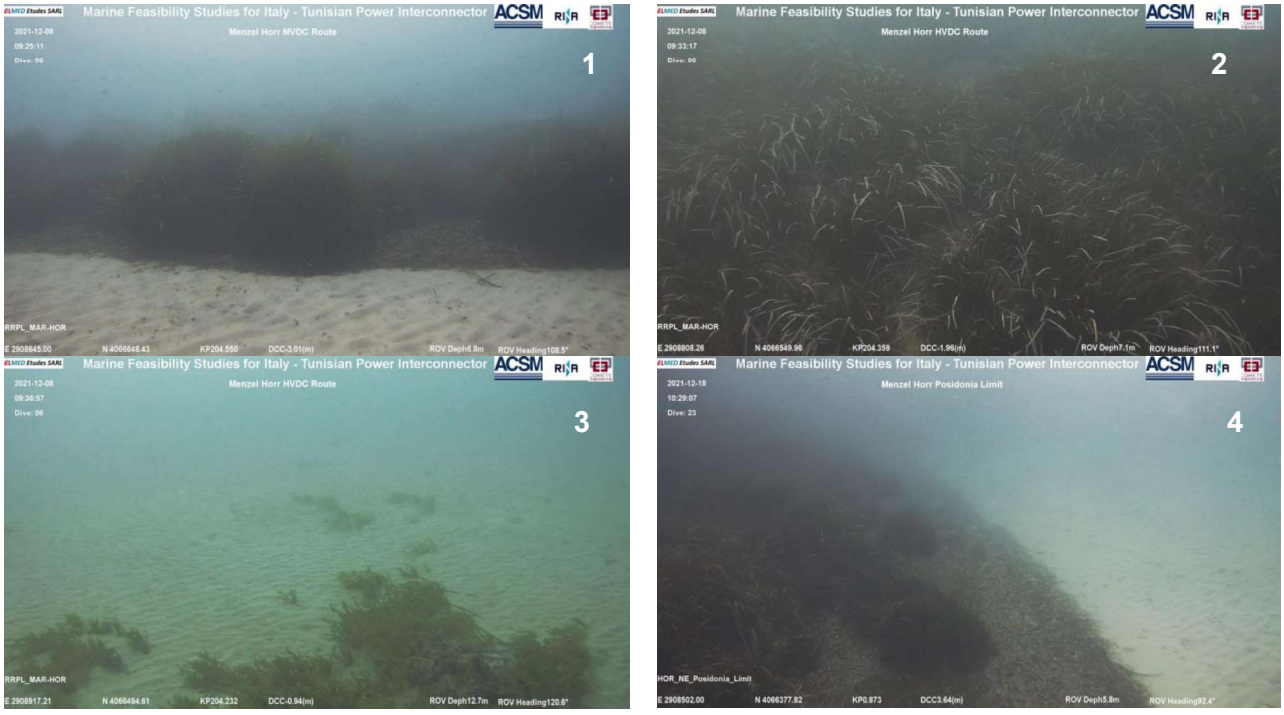

Figure 5.12: Posidonia distribution along the route

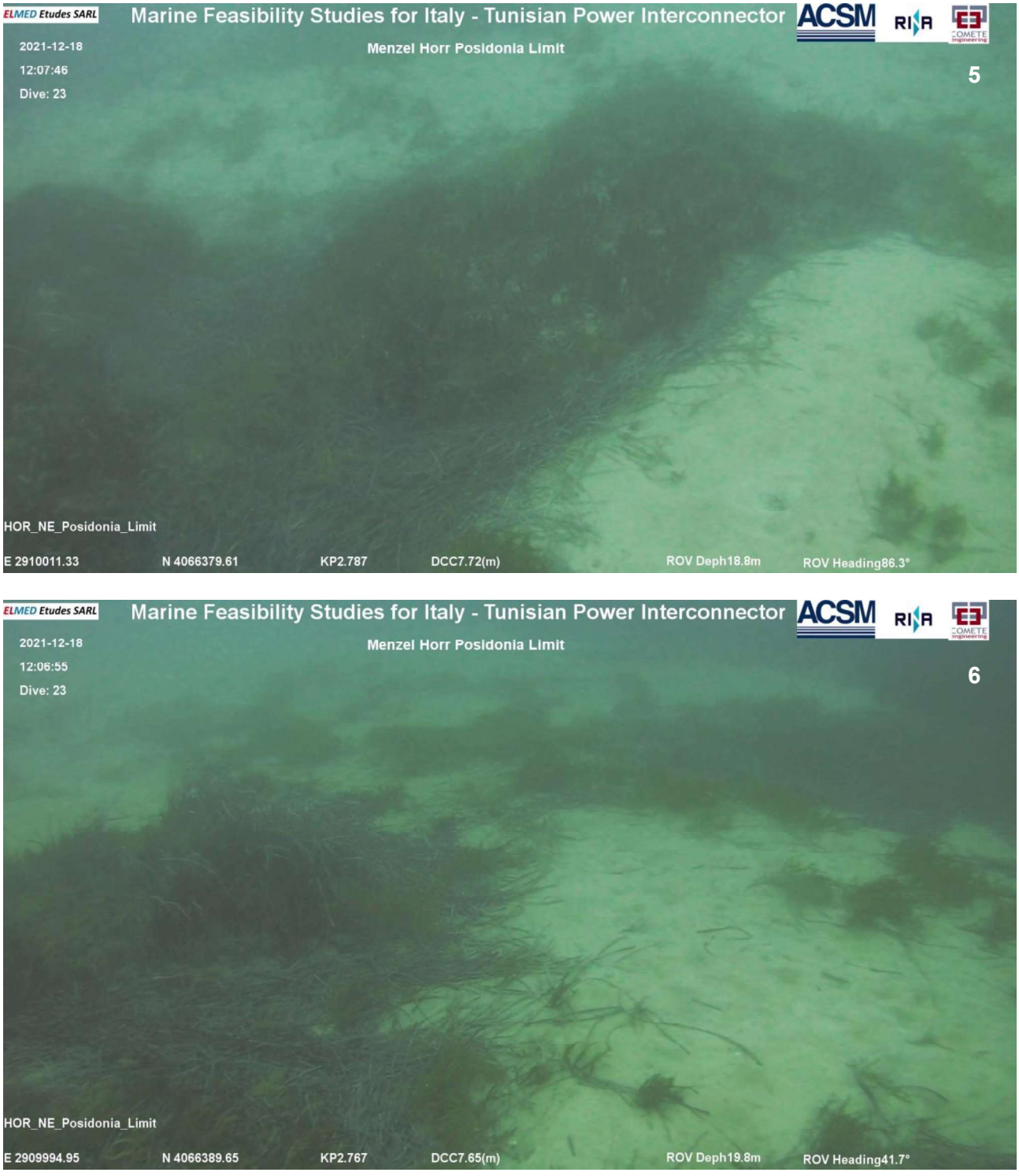

Figure 5.13: Posidonia matte and leaves being replaced by Caulerpa in the eastern part of the corridor

Biogenic concretions, often covered by sediments, were detected from the start of the Nearshore survey area at KP 199.449 up to approximately KP 203.936. Similarly to Kelibia survey area, the nature of these “rock” patches seems to be biogenic from the ROV Visual Inspection images, showing local growth of pre-coralligenous and coralligenous assemblages (Figure 5.14), hosting gorgonians and the finger-shaped sea-pen (*Veretillum cynomorium*), (Figure 5.15). This indicates locally hard seabed patches between large extensions of fine to coarse sand covered with *Caulerpa sp.* (probably C. *taxifolia*) (Figure 5.16).

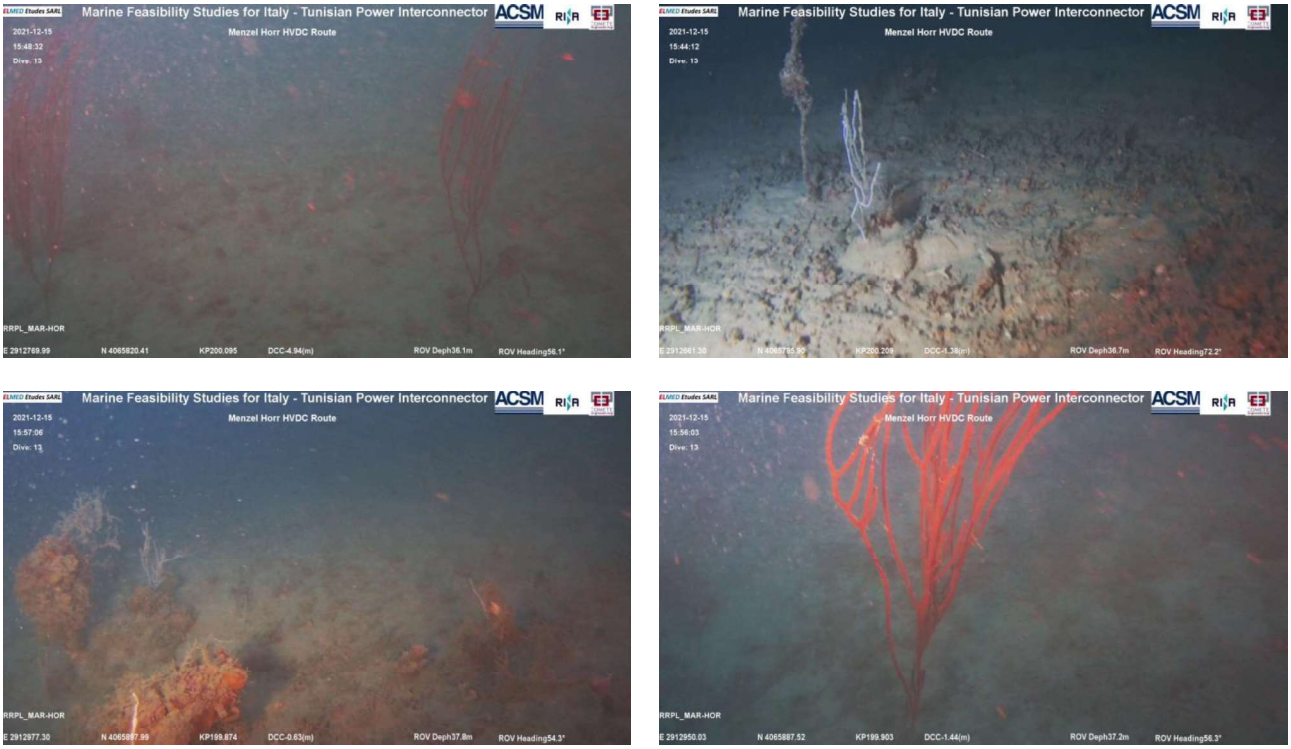

Figure 5.14: Biogenic concretion examples within the Menzel Horr survey area

Figure 5.15: Octocorallia examples within the Menzel Horr survey area

Figure 5.16: Sandy seabed with *Caulerpa sp* examples within the Menzel Horr survey area

The large number of scars found within the Menzel Horr area indicates an intense fishing and anchoring activity (Figure 5.17). It is to be highlighted that this part of the Tunisian coast is often used by all sort of vessels as a shelter area in case of rough weather conditions in the Sicily Channel thus new anchor scars may be found at any time.

No other anthropic activities evidence have been detected.

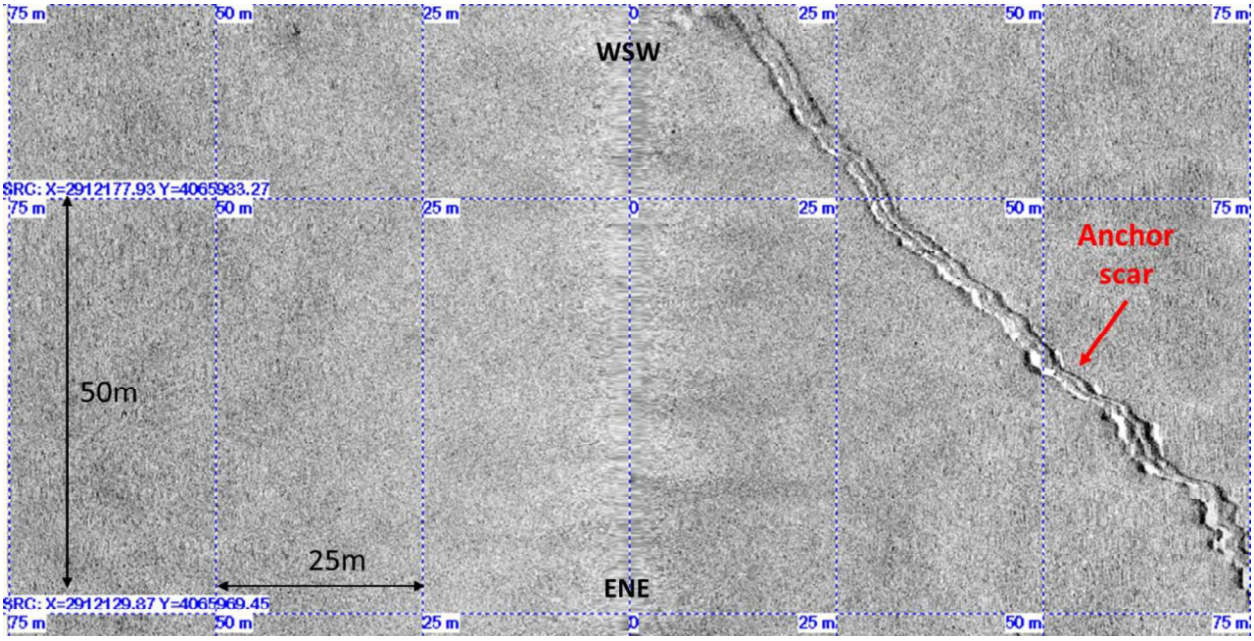

Figure 5.17: Example of anchor scar within Menzel Horr survey area (KP 201.141)

5.4.1.2.2 Electrode cable

Menzel Horr MVDC survey area shows a Posidonia oceanica meadow in its nearshore area. Starting from shore, Posidonia extends from 3.2m of water depth (WD) at KP 0.592 to its lower limit at 23.1m WD at KP 2.325 on the route. Posidonia meadow spreads largely to the Eastern part of the survey corridor. Along this eastern area, most of the Posidonia meadow is being replaced by *Caulerpa sp*, the ROV Visual Inspection detecting almost dead *matte* and Posidonia leaves.

A small patch of Posidonia is present on the western part at about 100m of the route. Between this small patch and the main meadow, a narrow area 150m wide free of Posidonia and covered with fine to coarse loose sand is detected.

The limits of the Posidonia meadow are highlighted in yellow in Figure 5.18 and the locations of the images performed during the ROV visual inspection are indicated as 1,2, 3 and 4.

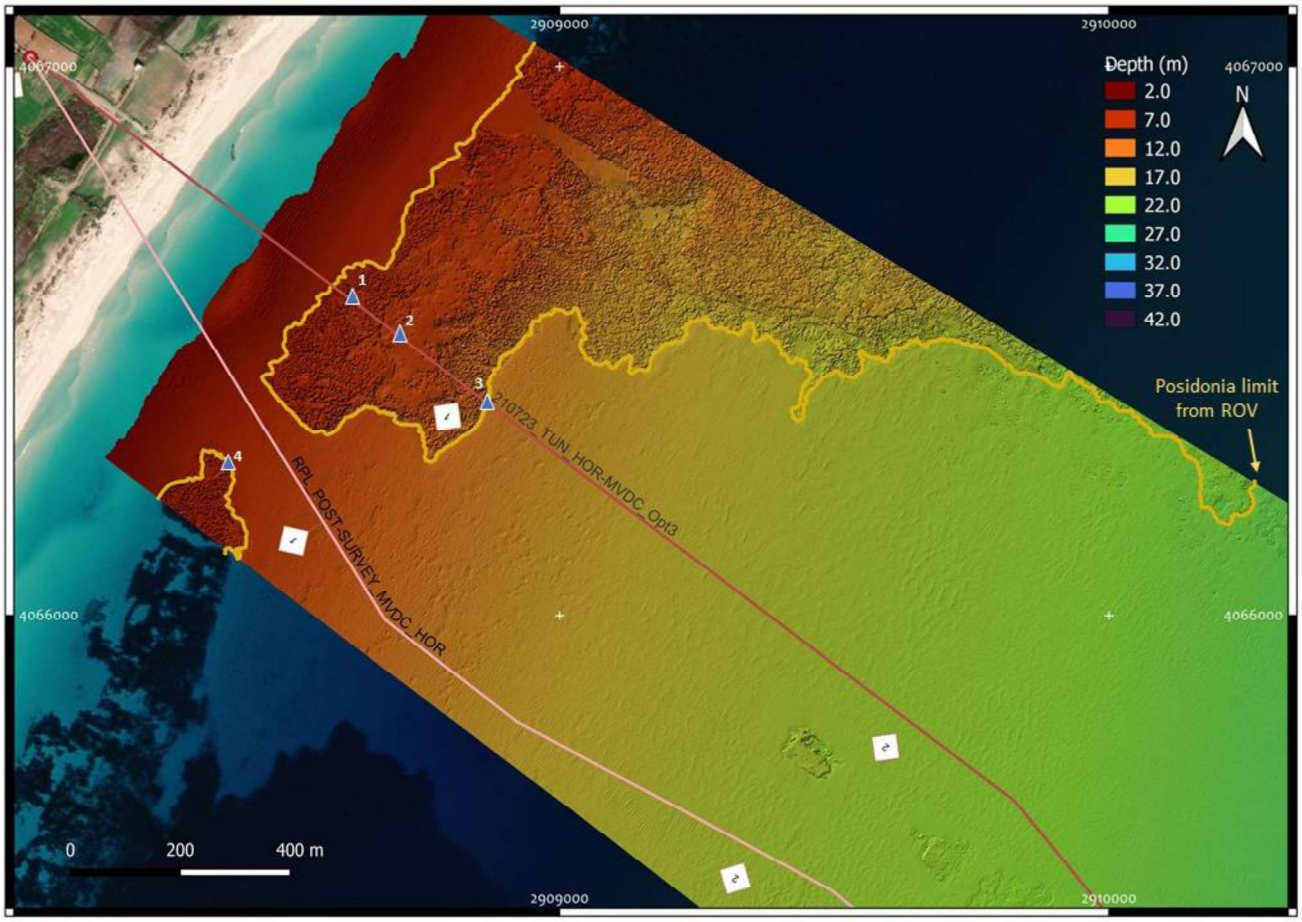

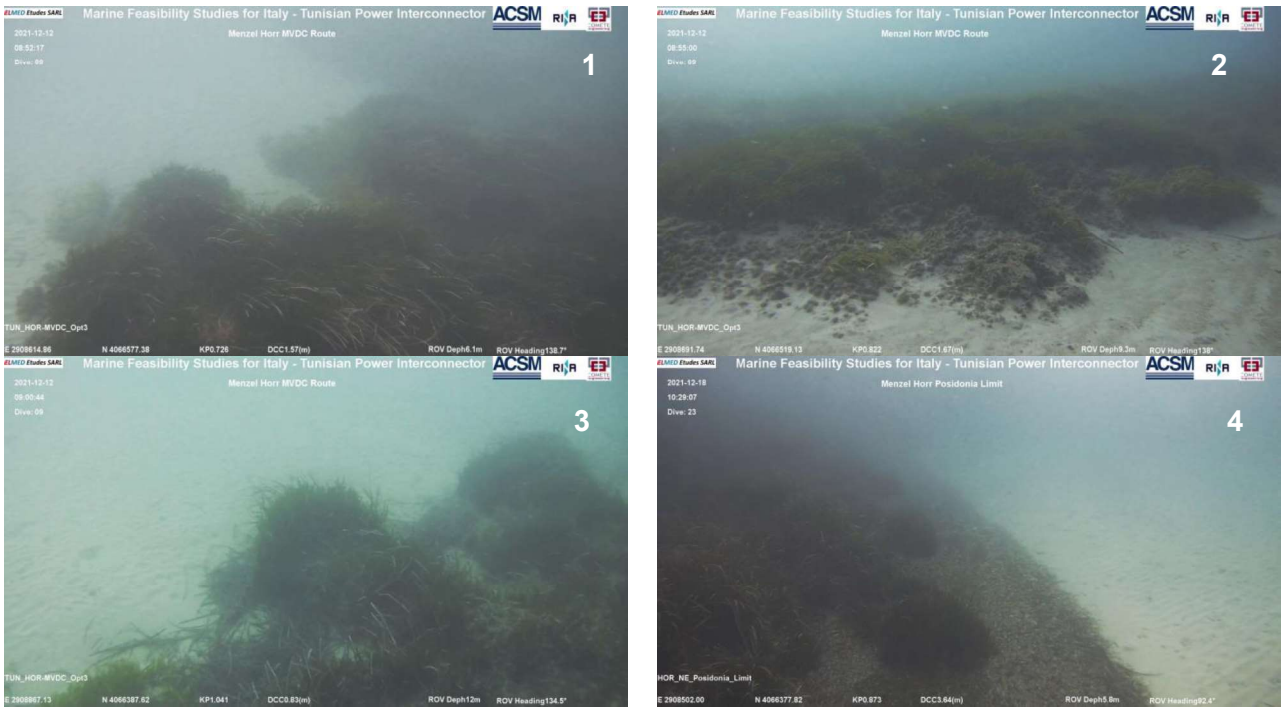

Figure 5.18: Posidonia distribution along the 210723_TUN_HOR-MVDC_Opt3

From KP 0.796 up to KP 1.548 the seabed is covered with fine to coarse sand with *Caulerpa sp* and what it looks to be probably dead *matte* of seagrass, maybe Posidonia. This area is characterized by occasional dead Posidonia leaves within fine to coarse sand and Caulerpa (probably C. *taxifolia*) (Figure 5.19a). From KP 1.548 onwards Caulerpa sp. extends all along the route with varying density (Figure 5.19b).

Figure 5.19: Sandy seabed with *Caulerpa sp* examples within the Menzel Horr MVDC survey area

Biogenic concretions were detected from KP 2.0 up to the end of the survey route, mostly between KP 4.0 and KP 6.608 and from KP 9 up to the end of the Menzel Horr MVDC area at KP 11.925. Similarly to Menzel

Horr HVDC survey area, the nature of these “rock” patches seems to be biogenic from the ROV Visual Inspection images, showing local growth of pre-coralligenous assemblages (Figure 5.20), and finger-shaped sea-pen (*Veretillum cynomorium*), within *Caulerpa* sp. assemblages on fine to coarse sandy seabed (Figure 5.21).

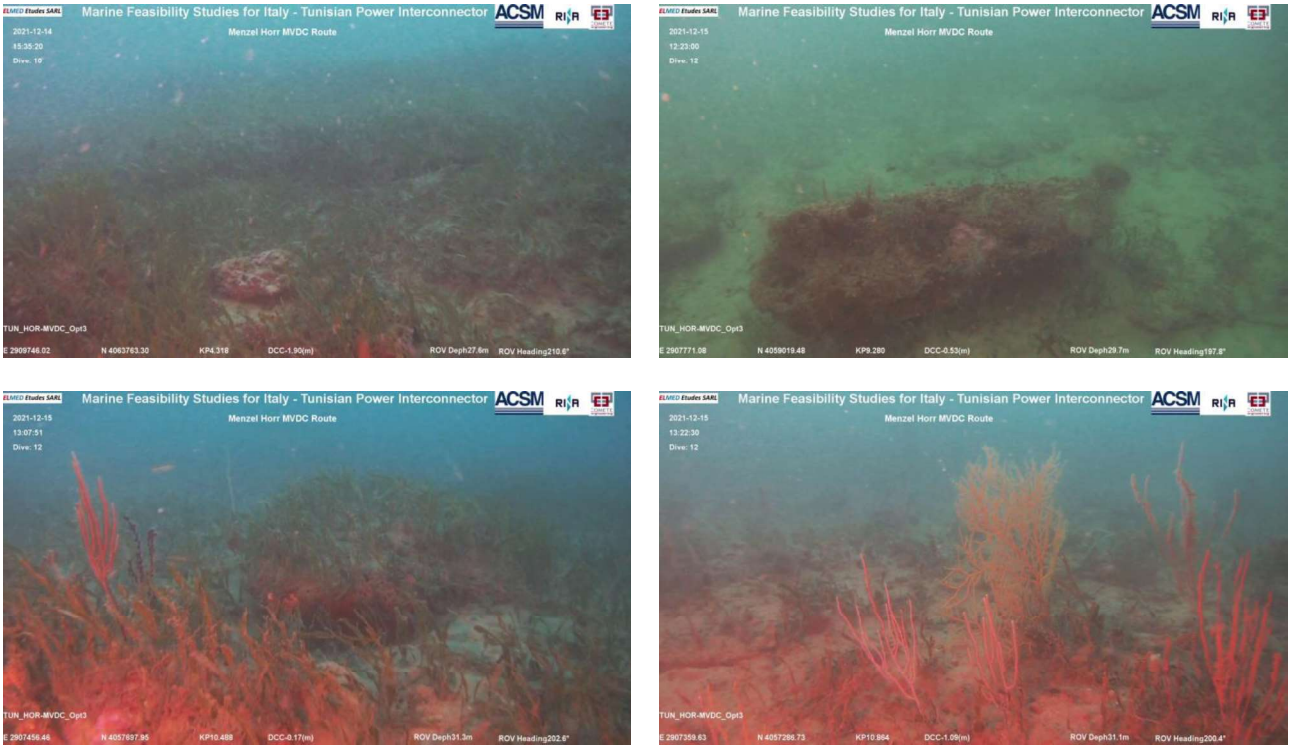

Figure 5.20: Biogenic concretion examples within the Menzel Horr MVDC survey area

Figure 5.21: Octocorallia examples between Caulerpa in the Menzel Horr MVDC survey area

Some scars have been found within the Menzel Horr-Opt3 MVDC area, indicating an important fishing and anchoring activity. It is to be highlighted that this part of the Tunisian coast is often used by all sort of vessels as a shelter area in case of rough weather conditions in the Sicily Channel thus new anchor scars may be found at any time.

No other anthropic activities evidence have been detected.

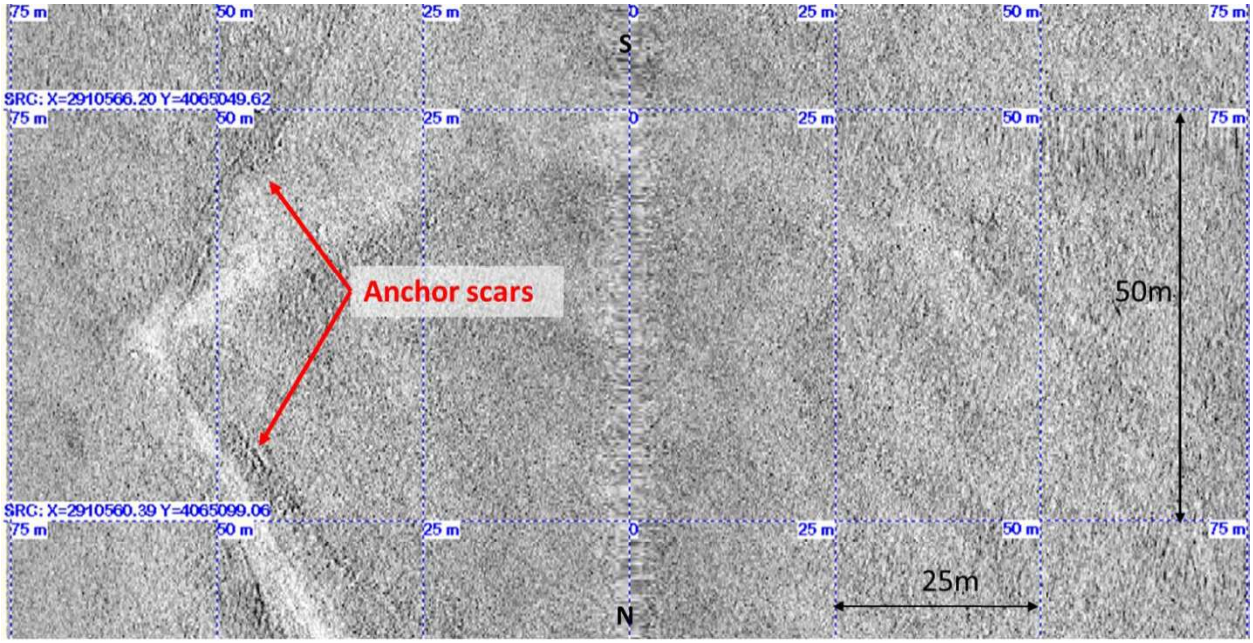

Figure 5.22: Example of scars within Menzel Horr MVDC survey area (KP 3.043)

5.4.2 Offshore survey

A bathymetric, morphological, and geophysical survey along a 3 km wide corridor from 40 m water depth at the Italian side to 40 m water depth at the Tunisian side was undertaken along a 500m wide corridor. A target visual analysis was also carried out. The cable corridor was divided into 10 blocks (Figure 3) and results are reported hereafter for blocks in Tunisian waters.

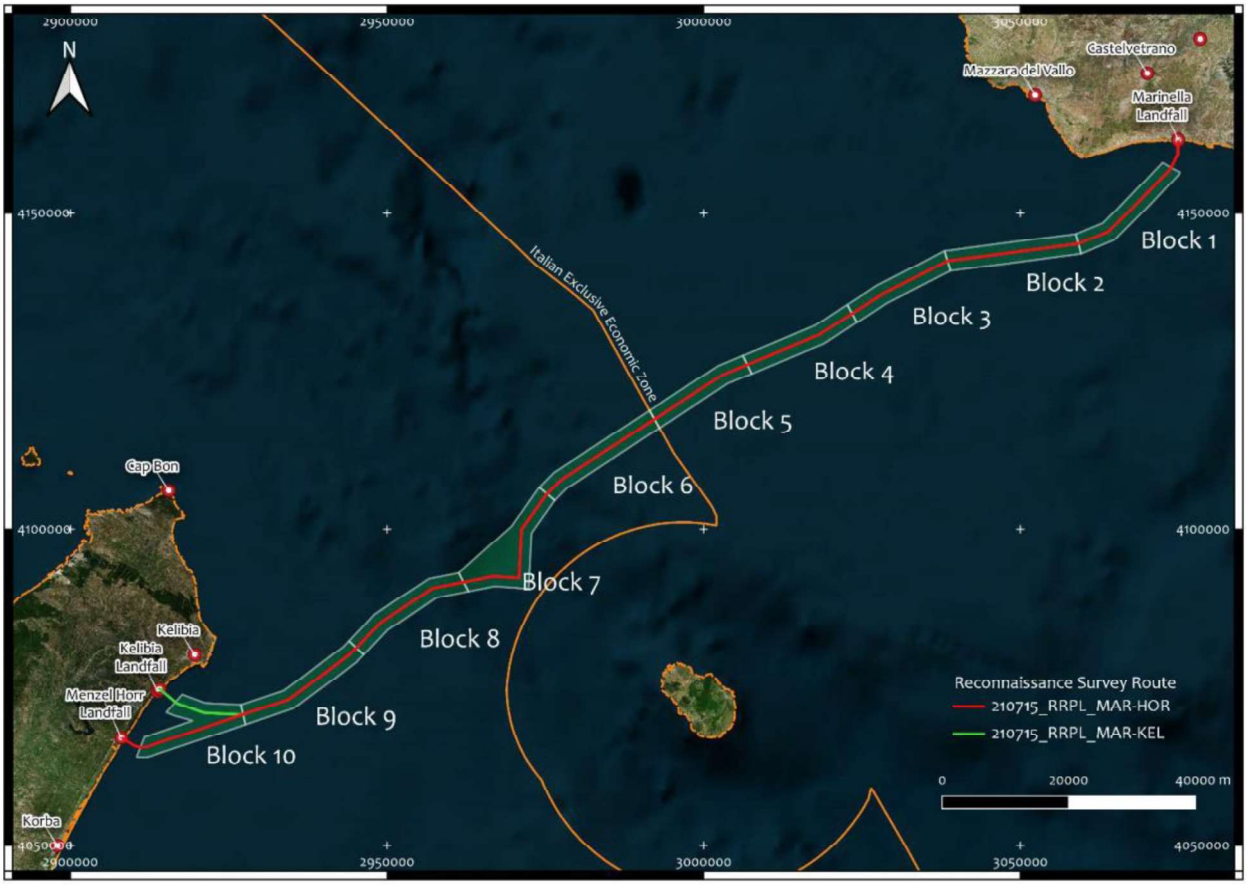

Figure 5.23: Offshore survey plan

Block 6

In Block 6, the water depth varies between 127.1m and 442.5m. All the area is characterized by an irregular trend with upwards and downwards sections and with the remarkable presence of a channel with slope values that in some cases exceeding 10°. Beyond the channel, water depth remains constant around 400m. In the remainder of Block, slope values never exceed 3°. This block is also characterized by sub cropping hardpan seafloor and coarse sediment, as continuation from Block 5. Shallow geology shows a progressive deepening reaching a 6m thickness for sandy sediments. Within the coarse sediment area, numerous depressions are detected. Occasionally gas seepages are detected suggesting a relation between the depressions and a local gas release. Abundant trawling scars were recorded.

Block 7

Block 7 is the deepest part of the whole corridor. The bathymetry increases quickly from 394.0m up to 800.0m on the abyssal plain called “Pantelleria Valley”. Following the survey route, water depth decreases rapidly to about 600m passing through two significant steep ridges probably due to the presence of a rocky outcrop. The whole Block 7 is characterized by the presence of significant slope values of more than 20°, except for the abyssal plain part where the slope does not exceed 2°. The seabed is mainly characterized by fine sediment, likely clay reaching a thickness of up to 15m. An intensive fishing area is observed, and an area of debris is detected. This area is around 90m long and 120m wide representing a historical site of interest, most likely representing a shipwreck. Moderate trawling scars were recorded.

Block 8

In the first half of Block 8, water depth increases quickly from 525.9m to about 270m over a stretch of 3km. The first half of Block 8 presents significant slope values related to the presence of rocky outcrops with slope values exceeding 15°. More specifically, the ridge between Block 8 and Block 9 recorded slope values exceeding 20°. Slope values though in the second part of this block do not exceed 2°. The northern part of

Block 8 is characterized by fine sediment while coarse sediment is identified between the outcropping rocks. These outcrops appear to be biogenic calcareous origin. An intensive fishing area is recorded at the end of the block. Moderate trawling scars were recorded.

Block 9

Water depth increases gently from 202.9m up to 84.4m with slope values less than 2° except for a very small step with a maximum slope of 3°. Surficial geology is characterized by fine sediments and extensive presence of scars suggesting intense fishing activity. Small depressions are observed along the northern sector of the block, arranged in groups with possible gas seepage. Sediment thickness is identified between 2m and 7m along the block. Abundant trawling scars were recorded.

Block 10

Block 10 is characterized by the deviation of the two survey routes, one towards the Kelibia landfall and the other towards Menzel Horr landfall. For both routes, the bathymetry decreases gently from a maximum 84.4m to a minimum of 35.6m with slope values never exceeding 4°. Surficial geology is shows intense scar presence suggesting intense fishing activity. The seabed is characterized as coarse sediment with a sub cropping area and scattered boulders. Shallow geology shows a sub-parallel stratification likely dominated by fine sediment stacking. Small and localized depressions are recorded with no evidence of rising gas seepage. Abundant trawling scars were recorded with some reaching 0.4m in depth and 1000m in length.